Issue 1 2019 | Volume 15

The Journal on Advanced Studies in Theoretical and Experimental Physics, including Related Themes from Mathematics

PROGRESS IN PHYSICS

"All scientists shall have the right to present their scientific research results, in whole or in part, at relevant scientific conferences, and to publish the same in printed scientific journals, electronic archives, and any other media." — Declaration of Academic Freedom, Article 8

ISSN 1555-5534

The Journal on Advanced Studies in Theoretical and Experimental Physics, including Related Themes from Mathematics

PROGRESS IN PHYSICS

A quarterly issue scientific journal, registered with the Library of Congress (DC, USA). This journal is peer reviewed and included in the abstracting and indexing coverage of: Mathematical Reviews and MathSciNet (AMS, USA), DOAJ of Lund University (Sweden), Scientific Commons of the University of St. Gallen (Switzerland), Open-J-Gate (India), Referativnyi Zhurnal VINITI (Russia), etc.

Electronic version of this journal:
http://www.ptep-online.com

Postal Address

Department of Mathematics and Science,
University of New Mexico,
705 Gurley Ave., Gallup, NM 87301, USA

ISSN: 1555-5534 (print)
ISSN: 1555-5615 (online)

Standard Address Number: 297-5092
Printed in the United States of America

January 2019 **Vol. 15, Issue 1**

CONTENTS

Information for Authors

Progress in Physics has been created for rapid publications on advanced studies in theoretical and experimental physics, including related themes from mathematics and astronomy. All submitted papers should be professional, in good English, containing a brief review of a problem and obtained results.

All submissions should be designed in LaTeX format using *Progress in Physics* template. This template can be downloaded from *Progress in Physics* home page http://www.ptep-online.com

Preliminary, authors may submit papers in PDF format. If the paper is accepted, authors can manage LaTeXtyping. Do not send MS Word documents, please: we do not use this software, so unable to read this file format. Incorrectly formatted papers (i.e. not LaTeXwith the template) will not be accepted for publication. Those authors who are unable to prepare their submissions in LaTeXformat can apply to a third-party payable service for LaTeX typing. Our personnel work voluntarily. Authors must assist by conforming to this policy, to make the publication process as easy and fast as possible.

Abstract and the necessary information about author(s) should be included into the papers. To submit a paper, mail the file(s) to the Editor-in-Chief.

All submitted papers should be as brief as possible. Short articles are preferable. Large papers can also be considered. Letters related to the publications in the journal or to the events among the science community can be applied to the section *Letters to Progress in Physics*.

All that has been accepted for the online issue of *Progress in Physics* is printed in the paper version of the journal. To order printed issues, contact the Editors.

Authors retain their rights to use their papers published in *Progress in Physics* as a whole or any part of it in any other publications and in any way they see fit. This copyright agreement shall remain valid even if the authors transfer copyright of their published papers to another party.

Electronic copies of all papers published in *Progress in Physics* are available for free download, copying, and re-distribution, according to the copyright agreement printed on the titlepage of each issue of the journal. This copyright agreement follows the *Budapest Open Initiative* and the *Creative Commons Attribution-Noncommercial-No Derivative Works 2.5 License* declaring that electronic copies of such books and journals should always be accessed for reading, download, and copying for any person, and free of charge.

Consideration and review process does not require any payment from the side of the submitters. Nevertheless the authors of accepted papers are requested to pay the page charges. *Progress in Physics* is a non-profit/academic journal: money collected from the authors cover the cost of printing and distribution of the annual volumes of the journal along the major academic/university libraries of the world. (Look for the current author fee in the online version of *Progress in Physics*.)

Picometer Toroidal Structures Found in the Covalent Bond

Omar Yépez

Clariant Corporation, 2730 Technology Forest Blvd, The Woodlands, TX 77381. E-mail: omar.yepez@clariant.com

The same topology observed for the atom's nuclei is identified in the covalent chemical bond. A linear correlation is found between the normalized bond longitudinal cross section area and its correspondent bond energy. The normalization number is a whole number. This number is interpreted as the Lewis electron pair. A new electron distribution for different diatomic molecules follows. Same number of electrons present different bond energies, occupying different areas. Therefore, it is inferred that the chemical energy is a consequence of the mass defect or gain due to the mass fusion of valence electrons participating in the bond.

1 Introduction

The topological analysis of the electron density has provided useful information about the bonding in a molecule. However, not much progress has been made to reveal the fundamental features of chemical bonding postulated by Lewis, i.e. the electron pair. According to Lewis structures there are bonding electron pairs in the valence shell of an atom in a molecule, and there are also nonbonding pairs or lone pairs in the valence shell of many of the atoms in a molecule. So far, it has not been seen any evidence of electron pairing in the topological analysis of the electron density. An increased concentration of electron density is observed between the two bonded atoms, which could be interpreted as the electron density equivalent of a Lewis bonding pair [1]. Nevertheless, there is no way to be sure about it. The same occurs about the existence of lone pairs. This same reference arrives to the conclusion that electron pairs are not always present in molecules, and even when they are, they are not as localized as the approximate models may suggest [2].

Therefore, a method to measure the number of electrons that participate in the bond will definitely probe or not the existence of Lewis electron pairs.

In 1996 the shapes of the deuteron at the femtometer scale were reported. The deuteron presents three different shapes: a torus, a sphere inside another sphere and two separated spheres [3]. These are the same shapes observed in every single molecule's Laplacian of the electron density but at the picometer scale. It is inferred that those are the shapes of the electron while it is participating in the chemical bond. Lack of identifying these shapes with the electron misleads the molecule's topological analysis.

This paper uses this new shapes in the analysis of different diatomic molecules and CO_2. Thanks to this, the topology of the chemical bond is properly identified. The longitudinal cross section area of the bond is correlated with its bond energy. Only when this area is divided by a whole number, a linear correlation between this bond area and its energy occurs. This whole number is most of the time an even number and thus, it is interpreted as the electron pair. Consequently, an electron distribution in the molecule is possible. First time model independent evidence of the Lewis electron pair is found.

1.1 Electron pair topology

Covalent bonds or lone pairs will be detected by using the structures observed in Fig. 1, namely: the two separated spheres (***ts***), the torus (***t***) and the sphere in a sphere (***ss***). Valence electrons participating in the σ bond (two electrons involved) occur by adopting the two separated sphere structure, ***ts***. Double (four electrons involved) and quadruple bonds (eight electrons involved) also use this structure. A lone pair occurs as a torus shape around quadruple bonds or as a ***ss*** structure around more electronegative atoms. As the electronegativity of the nucleus increases, non-bonding electrons tend to form a toroidal structure around its atom helium core. This occurs until the next noble gas structure is fulfilled.

2 Experimental

By cutting the silhouette of the two separated sphere structure, involving the bonded atoms, the bond longitudinal cross section areas (bond area) were determined from the contour map of the Laplacian of its charge density. An example of such silhouette (green lines) can be observed in Fig. 3 for the fluorine molecule. They were printed on paper, cut and weighted. The bond length was used to calibrate the longitudinal cross section area measured in each bond. Then, these areas were correlated with their respective bond energies.

The contour map of the Laplacian of the charge density for fluorine, F_2 and dicarbon, C_2 molecules were found in [4], oxygen O_2 was found coordinated to a molibdenum atom in [5]. Nitrogen, N_2 is from [7]. Carbon monoxide, CO from [8]. Cyanide CN^- from [11]. Nitrogen monoxide, NO from [9] and carbon dioxide CO_2 was found in [10].

3 Results

Fig. 2 shows a straightforward correlation between the bond area divided by a number n and the bond energy of each bond. This number n is a whole number and it is interpreted as the

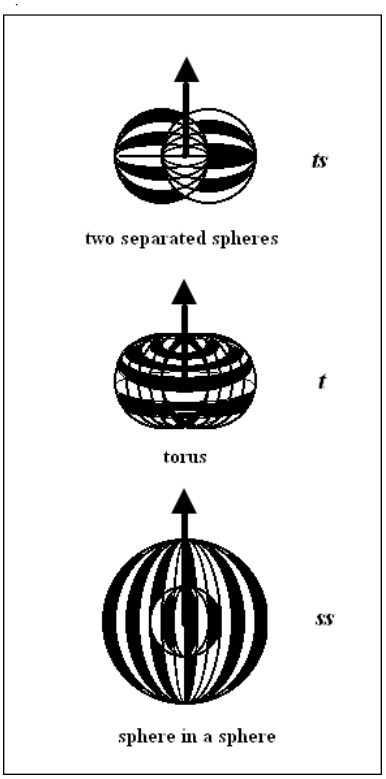

Fig. 1: Observables structures of the electron. This is after [3].

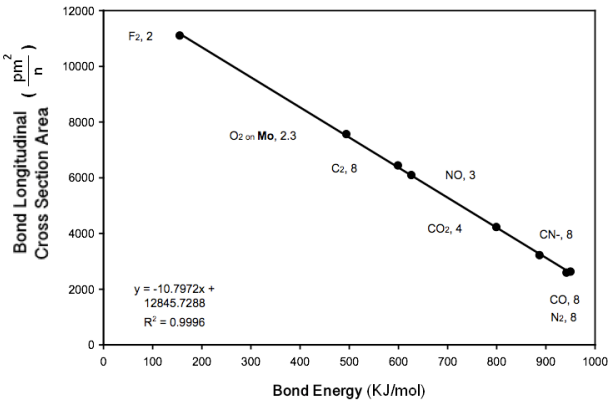

Fig. 2: Correlation between bond longitudinal cross section area and its energy for different diatomic molecules and CO_2.

number of electrons involved in the bond. It has to be stressed that the $y-$axis location for each experimental point is very sensitive to the number n. Fractions of this number makes the r^2 get lower than 0.999. It is clear that as the normalized bond area diminishes, the bond energy increases.

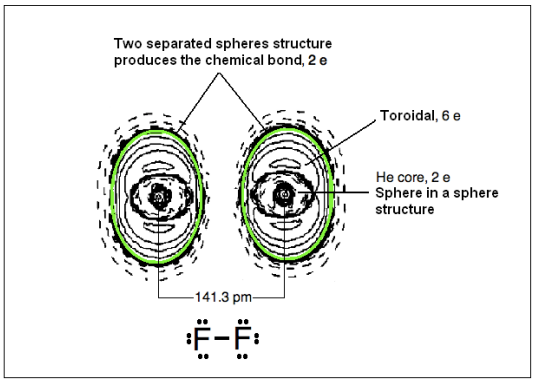

Fig. 3: Fluorine molecule. There is no discernible structures between the atoms. The different electron's structures are indicated. The green line shows where the bond was cut. The original figure is from [4]. Used under Creative Common License.

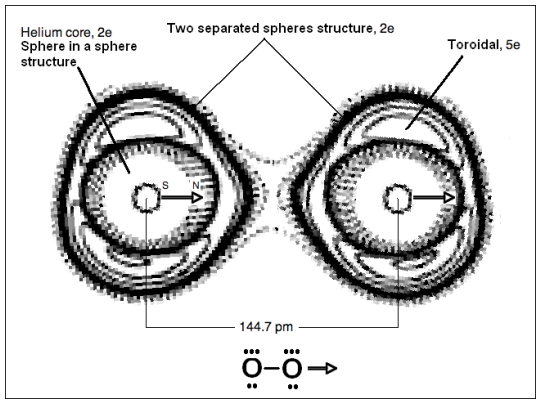

Fig. 4: Oxygen molecule coordinated by a Mo atom. The different electron's structures are indicated. The magnetic moments are shown with the arrow with North and South poles. The original figure is from [5]. Used with permission of the editors.

3.1 Homonuclear diatomic molecules

Fluorine, F_2. Fig. 3 shows the fluorine molecule. The sphere in a sphere structure is clearly observed at the center of each F atom. This is due to the helium core and account for two electrons. The next six electrons are in the toroidal structure around each helium core. As observed in Fig. 2, the F–F bond has two electrons. The two bonding electrons belong to both nuclei in a ***ts*** structure. Due to this bonding, there is no discernible structure between the F atoms. Therefore, one can still put a stroke between these two atoms, understanding that there is a bond through this structure. Hence F–F is all right. The dots around each F atom just denotes the pairing of each atom's 6 toroidal electrons. This is the usual Lewis structure.

Oxygen, O_2. Fig. 4 shows that the oxygen molecule highly resembles the fluorine one. The n number was not a whole

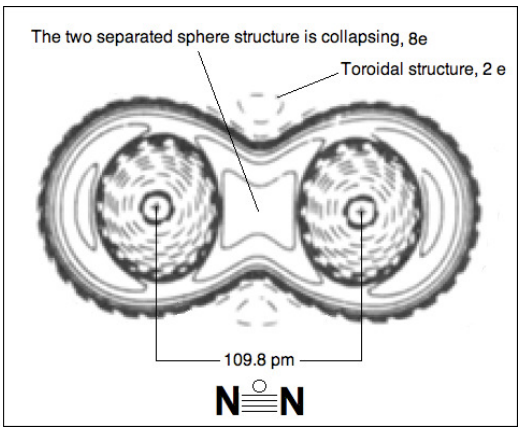

Fig. 5: Nitrogen molecule. The original figure is from [7]. Used with permission of the editors.

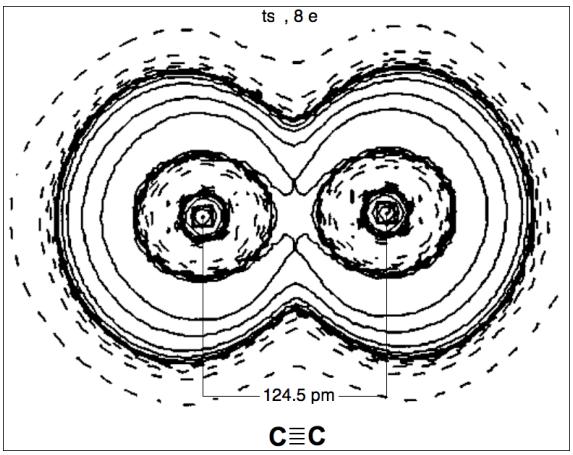

Fig. 6: Dicarbon molecule.The original figure is from [4]. Used under Creative Commons License.

number giving 2.3. The uncoupled electrons in each oxygen atom will produce a magnetic attraction in the line of the bonding. Probably, this may distort the molecule in a way to make it digress from the experimental trend observed. However, the resemblance to the fluorine molecule and the closeness of the n number to 2, strongly suggests that the number of electrons involve in the O–O bond is 2.

As a consequence, the toroidal structure on the oxygen's helium core, previously observed in F_2, necessarily have 5 electrons each. This odd number means two uncoupled magnetic momenta. One in each oxygen atom. They will align as indicated in the figure. This will create a net magnetic moment in the molecule, i.e. the oxygen molecule is paramagnetic.

The magnetic attraction is rendering a shorter bond area in this molecule. Probably, this is why this molecule is away from the general trend observed in Fig. 2. Dividing between a larger n number is just compensating this magnetic attraction. In other words, to have an $n = 2$ in this molecule, the energy of the O–O bond should be 410 kJ/mol and not the experimental 494 KJ/mol. f There have not been any consensus about how the oxygen's Lewis structure should be written. The molecule's paramagnetism does not help. This is because an uncoupled electron structure has to be written, somehow contradicting Lewis pairing hypothesis. O–O, O=O and O÷O has been proposed. From these structures, the more pertinent is O÷O because the dots are the two uncoupled electrons observed in Fig. 4. The Lewis structure printed in Fig. 4 indicates the existence of odd pairing, which is supported by the molecule paramagnetism.

Nitrogen, N_2. As it is noticeable from Fig. 5, the nitrogen atoms are not separated. This is probably due to the lower electronegativity in comparison with fluorine and oxygen molecules. The well defined ***ts*** structure previously observed for fluorine and oxygen disappears, giving way to the same structure but with its spheres more collapsed; this is covering both nitrogen atoms' helium cores.

According to the results from Fig. 2, four of the five nitrogen valence electrons are compromised in the N–N bond. Since this molecule is diamagnetic, it is believed that the two remaining electrons join forming a toroidal lone pair structure around the N–N bond. This ring will occur in the midpoint between the bonding nitrogens. Structures like this have been observed, for example in the acetylene molecule [12]. As a consequence of this electron distribution, all nitrogen's five valence electrons are joined and this is why this molecule presents the highest bond energy in the series F, O, N, C.

The usual Lewis structure is a triple bond between the nitrogens and two lone pairs, one at each nitrogen atom. However, this molecule has one of the highest bond energies and also the smaller bond area measured from the pool of molecules tested. Therefore, it should not surprise that a very high number of valence electrons join for this bond. Furthermore, there is no structures in Fig. 5 to justify the presence of lone pairs on either N atoms. As it was observed in F–F or in O÷O. Hence, the Lewis structure pictured in Fig. 5 with four strokes and the lone pair making a ring (torus) around the middle of the N–N bond is a new Lewis structure.

Dicarbon, C_2. Fig. 6 presents an even less collapsed ***ts*** structure in comparison with N_2. This is due to less number of valence electrons to bond and to the lower electronegativity that carbon has. The C–C bond in dicarbon involves all valence electrons from each carbon, i.e. 8, and they are around each atom's helium core. The diamagnetism of this molecule reveals that all its bonded electrons are magnetically coupled. Again, no lone pair structures are noticeable in this molecule. Hence, the Lewis structure depicted in Fig. 6 is new.

Upon comparing these four molecules, one can arrive to the conclusion that the chemical σ bond is mostly performed

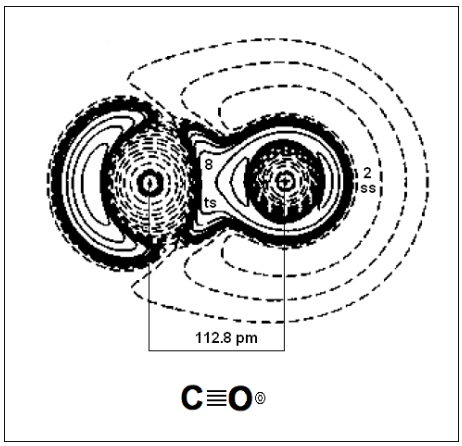

Fig. 7: Carbon monoxide. The two concentric semicircles in the Lewis structure represent an ***ss*** lone pair structure located on the oxygen atom. The original figure is from [8]. Used with permission of the editors.

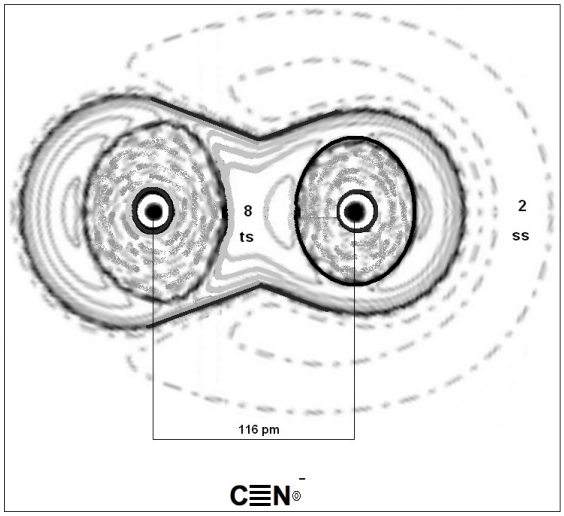

Fig. 8: Cyanide molecule.The two concentric semicircles in the Lewis structure represent an ***ss*** lone pair structure located on the nitrogen atom. The original figure is from [11]. Used with permission of the editors.

by this ***ts*** structure and the separation between the spheres depends on the atom's electronegativity. As the electronegativity of the bonded atoms diminishes, more electrons are involved in the bond.

3.2 Heteronuclear diatomic molecules

Carbon monoxide, CO. As observed in Fig. 2, the C–O bond involves 8 electrons. Accordingly, Fig. 7 presents the electron distribution in CO. From the 10 valence electrons to share: 4 from the carbon and 4 from the oxygen are joined around the helium core of each atom. The other 2 oxygen's valence electrons are in a lone pair. This is the ***ss*** structure over the oxygen's helium core.

This molecule is isoelectronic with N_2. However, the difference between the atoms' electronegativity makes the lone pair to form over the oxygen. In the case of N_2, there is no difference in electronegativity, and thus it is believed that its lone pair will be at the mid point between the N–N bond in a toroidal shape.

The current Lewis structure of CO is a triple bond between the carbon and the oxygen and one lone pair on each atom. Somehow trying to achieve the octet rule. The new Lewis structure is a quadruple bond for the C–O bond and one lone pair only on the oxygen in an ***ss*** structure. This last feature has been noted as two concentric circles in the new Lewis structure (see Fig. 7).

Finally, there is a controversy about the dissociation energy of CO. The values can be 881, 926, 949, 941 or 1070 KJ/mol coming from different kind of experiments [13]. In the case of Fig. 2, the value 926 KJ/mol from electron impact experiments or 949 KJ/mol from pre-dissociation data produced the best linear correlation with the other molecules of the group.

Cyanide, CN^-. As in the case of carbon monoxide, the C–N bond involves 8 electrons. Fig. 8 presents the electron distribution in the molecule: 4 valence electrons from carbon and 4 more from the nitrogen make this bond in an ***ts*** structure around the atoms' helium cores. The nitrogen however, remains with one uncoupled electron. Since this molecule is diamagnetic, an extra electron is needed to couple and cyanide finish with a negative charge. This charge is a ***ss*** lone pair, clearly observed on the nitrogen. This occurs on the nitrogen atom because it is more electronegative than carbon. The current Lewis structure is a triple bond between the carbon and the nitrogen and two lone pairs; one on each atom. This is to try to achieve the octet rule. Again, just like in the CO molecule, the new Lewis structure is a quadruple bond and the lone pair repeats on the more electronegative atom.

Nitrogen monoxide, NO. Fig. 9 presents the NO molecule. As observed in Fig. 2, the N–O bond involves three electrons. This will imply that one of those three electrons is not magnetically coupled with the other two and therefore, this molecule will be paramagnetic. In this join of three electrons, the nitrogen shares 1 and the oxygen shares 2. By this way, the nitrogen can couple the other 4 electrons as one toroidal structure around its helium core. The oxygen will arrange its other 4 electrons in the same manner. The current Lewis structure depicts an uncoupled electron on the nitrogen and a double bond between the nitrogen and the oxygen. The new Lewis structure leaves the odd electron in the N–O bond. Thus, this would be an example of a three electron bond and therefore, this bond is paramagnetic. Thus, the new Lewis structure draws a magnetic moment vector over the single N–

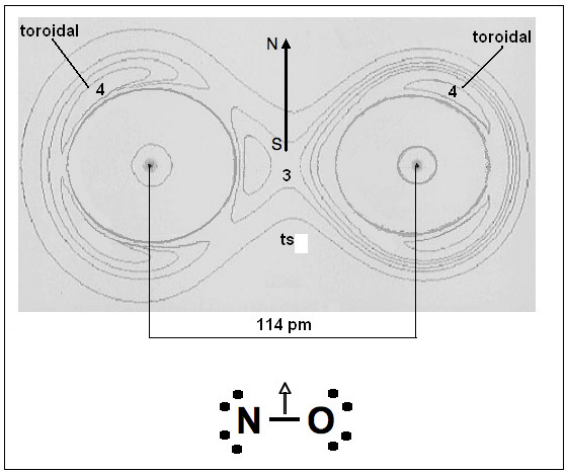

Fig. 9: Nitrogen monoxide molecule. It has a three electron σ bond. 4 electrons forms a toroidal structure around each atom's helium core. The original figure is from [9]. Used with permission of the editors.

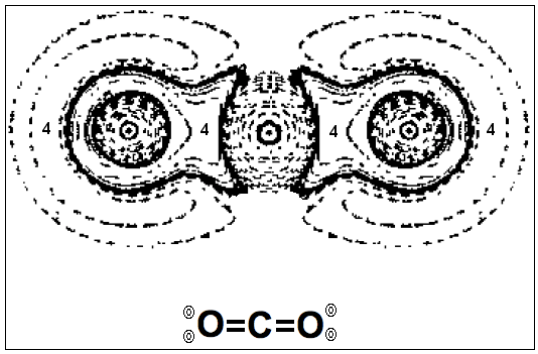

Fig. 10: Carbon dioxide, CO_2. The new Lewis structure specifies that the two lone pairs on the oxygen atoms are in an ***ss*** structure. The original figure is from [10]. Used with permission of the editors.

O bond. The two lone pair on each atom are also depicted.

Carbon dioxide CO_2. Fig. 10 shows that the 4 valence electrons of carbon are used at each side of the molecule to produce two C–O bonds with 4 electrons each. The remaining 4 electrons of the oxygen go to an ***ss*** lone pair over each oxygen atom. The current Lewis structure presents a double bond towards each oxygen atom and two lone pairs on each oxygen. The new Lewis structure just stresses that these lone pairs are in an ***ss*** structure.

4 Discussion

The three shapes observed in Fig. 1 are the "attractors" identified by Bader *et al* after the topological analysis of a large number of molecules [6]. Specifically, the core attractor can be identified as the ***ss*** shape; the bonding attractor as the ***ts*** shape and the non-bonding attractor as the toroidal shape. Given that the same shapes have been observed for the deuteron [3], it is inferred that these attractors are actually different shapes of the electron.

The results presented in Fig. 2 are paramount to understand the chemical bond. The bond area was found to be inverse proportional to the correspondent bond energy. Something similar has been observed before. It is common knowledge that as the number of bonds increases between two carbon atoms, the interatomic distance diminishes. By this way, a single bond is larger than a double bond and a double larger than a triple bond. Thus, it is not strange that another dimensional relationship does occur between the bond area and the bond energy. However, as observed in Fig. 2, the same number of bonding electrons, 8, produced the main chemical bond between the bonded atoms in: C_2, CN^- and CO, rendering different bond areas and bond energies. This means that those electrons are changing sizes in the bond and their longitudinal cross section area corresponds to different energies.

How all these electrons are together in a progressively smaller place? Electrostatic repulsion is non-existent in these arrangements. This is because, all these electron charges are neutralized by the counter charge from their atom nuclei. This will certainly help to have all of them in just one location. In a given molecule, most of the time an even number of electrons are found in the bond between two atoms. This is because the magnetic coupling between valence electrons magnetic momenta renders such even number and diamagnetism to the bond. Paramagnetism occurred in two cases O_2 and NO, to which, the electron distribution helped to locate where is the uncoupled electron producing it.

Another example of inverse proportion between the occupied longitudinal cross section area and the bond energy can be found in nuclear isotopes, where it is observed the general trend of reduction in the isotope radius as the number of neutrons increases in the isotope. Reference [14] presents such relationship for oxygen isotopes. This means more nuclear bonding energy to keep all those neutrons in the nucleus in a progressively smaller longitudinal cross section area. Just what was observed in Fig. 2 with electrons instead. Therefore, it is believed that no repulsive electric forces manifest in the chemical bond situation. More likely, the bonding electrons behavior is controlled by the properties of their masses, i.e. mass fusion.

Hence, before the bond can occur, valence electrons will naturally repel each other because of mass repulsion. Thus, an activation energy would be needed to overcome such repulsion. After that, the bond occurs as a consequence of valence electrons mass fusion. Consequently, this mass fusion defect or gain will translate to an energy release or increase respectively. This answers what in a molecule changes in mass to account for the chemical energy.

Received on October 6, 2018

References

1. Guillespie R. J. and Popelier P. L. A. Chemical Bonding and Molecular Geometry, from Lewis to Electron Densities. Oxford University Press, New York, 2001, Chapter 7.
2. Guillespie R. J. and Popelier P. L. A. Chemical Bonding and Molecular Geometry, from Lewis to Electron Densities. Oxford University Press, New York, 2001, p. 179.
3. Forest J. L., Pandharipande V. R., Pieper S. C., Wiringa R. B., Schiavilla R. and Arriaga A. *Phys. Rev. C*, 1996, v. 54, 646.
4. Chan W.-T. and HamiltonI. P. *J. Phys. Chem.*, 1998, v. 108, 2473.
5. Macchi P., Schultz A. J., Larsen F. K., and Iversen B. B. *J. Chem. Phys.*, 2001, v. 105, 9231.
6. Bader R. F. W. Atoms in Molecules, a Quantum Theory. Clarendon Press, Oxford, 1990, p. 294.
7. Bader R. F. W. *Chem. Rev.*, 1991, v. 91, 893.
8. Bader R. F. W., Johnson S., Tang T. H. and Popelier P. L. A. *J. Phys. Chem.*, 1996, v. 100, 15398.
9. Aray Y., Rodriguez J. and Lopez-Boada R. *J. Phys. Chem. A*, 1997, v. 101, 2178.
10. Bader R. F. W. and Keith T. A. *J. Chem. Phys.*, 1993, v. 99, 3683.
11. Daza M. C., Dobado J. A., Molina J. and Villaveces J. L. *Phys. Chem. Chem. Phys.*, 2000, v. 2, 4089.
12. Gadre S. R., Bhadane P. K. *Resonance*, 1999, v. 4, 14.
13. Pauling L. and Sheehan W. F. Jr. *Proc. N. A. S.*, 1949, v. 35, 359.
14. Lapoux V., Somà V., Barbieri C., Herbert H., Holt J. D. and Stroberg S. R. arXiv: nucl-ex/1605.07885v2.

Toward the Fields Origin

Jacques Consiglio

52, Chemin de Labarthe. 31600 Labastidette. France
E-mail: Jacques.Consiglio@gmail.com

Here I continue my analysis of particles mass and couplings, and show *why and how* the full SM particles spectrum exists and must exist; that it constitutes a mechanically coherent system of resonances, and *how* it is compatible with GR and cosmology.

1 Introduction

Here I show *why* the SM mass spectrum must exist, and *how* it comes to be what it is. This paper follows [1] where I use a mass equation to analyze the SM elementary particles mass spectrum, and [3] where I discuss cosmological density parameters and their history. It is structured as follows:

In Section 2, for the reader's convenience I first recall my main results related to particles mass; then I recall some of my results in cosmology.

In Section 3, I complement the analysis provided in [1] and show that the couplings and the resonances constitute a coherent system where each particle is a double sub-harmonic of the Planck mass.

Section 4 is the important one as it gives an origin to the SM particles; I show *why and how* the Planck mass imply the SM particles resonances, including also mass-less particles. It shows that this theory is about the very foundations of the physical world.

In Section 5, I show that the mass-resonance equation is compatible with cosmology and general relativity (GR). This is not trivial at all as it is based on the cube of a length, which seems in contradiction with the linear relation between wavelengths and energy. Doing so I show an effective symmetry of scale in GR and cosmology (which is already in [3]).

In Section 6, I discuss the fine structure constant; its interpretation in QED and its position in the field as depicted here.

When reading this paper, please keep in mind that each and every parameter of the standard theories which are analyzed here, when computed from the equations I give are well in the ranges given by CODATA (2014) and the Planck mission results [4], with no exception (the values needed to compute all quantities are provided).

2 Previous results, in very short

2.1 Particles resonances

In [1] and the references therein, I found a mass equation that comes in two slightly different instances; one for leptons and quarks:

$$m = \frac{X}{\left(\frac{1}{N\,P} + K\,D\right)^3} + \mu\,, \tag{1}$$

where N, P, K are integral numbers, X and μ are constant real parameters, and D is a real parameter which is particle group dependent; and one for massive bosons:

$$m = m_e \times \frac{\left(\frac{1}{N_e P_e} + K_e D_e\right)^3}{k\,\pi\left(\frac{1}{N_b P_b} + K_b D_b\right)^3}, \tag{2}$$

with index e for the electron and index b for a boson. The little k introduced at the denominator is computed using the following equation, which is deduced from their resonances geometry:

$$k^3\,\pi/144 = 266\,D_b\,(\pi/k)^{1/3}. \tag{3}$$

The numerical values for X and μ are of little interest here, but the relations between the different D is critical. At first, I evaluate D_e, X, and μ fitting the equation to the leptons masses.

$$X = 8.1451213299073\,\text{KeV}.$$

$$\mu = 241.676619539\,\text{eV}.$$

The fit is optimal in the sense that I take the smallest possible N, P, and K. Then for quarks I need to use the fine structure constant to modify the D:

$$D_q = D_e\,(1 + \alpha),$$

and finally, after modeling the field interactions related to the D and partly understanding the resonance substructure, I deduce for the Z and W bosons:

$$D_{WZ} = \frac{\alpha^2}{1\,+\,\alpha^2} + \frac{D_e}{2(1\,-\,\alpha^2)} - \frac{D_e^2}{6(1\,+\,\alpha^2)},$$

and for the H^0:

$$D_H = \frac{\alpha^2}{1\,+\,\alpha^2} + \frac{D_e}{2(1\,-\,\alpha^2)} - \frac{D_e^2}{1\,+\,\alpha^2}.$$

This set of parameters corresponds to the fundamental field because all particles masses are computed with X, μ, D_e, and α, which are constants. The form of the resonance is particle group dependent (leptons, quarks and massive bosons), and the coefficients of the resonances are particle dependent.

Empirical fit targeting minimal N and P gives the resonances in Tables 1, 2, and 3 where very simple patterns appear; stunningly for quarks and bosons only one resonance parameter is variable (N for quarks, and K for bosons).

Table 1: Electron, muon, tau in MeV/c^2.

-	P = N	K	Computed	Measured
e	2	2	0.510 998 9461	0.510 998 9461(31)
μ	5	3	105.658 3752	105.658 3745(24)
τ	9	5	1 776.84	1 776.82(16)

Table 2: Quarks resonances in MeV/c^2.

-	P	N	K	Computed	Estimate
u	3	2	−6	1.93	1.7 - 3.1
d	3	19/7	−6	5.00	4.1 - 5.7
s	3	7	−6	106.4	80 - 130
c	3	14	−6	1,255	1,180 - 1,340
b	3	19	−6	4,285	4,130 - 4,370
t	3	38	−6	172,380	172,040 ±190 ± 750

Please note that the up quark resonance is $2 = 38/19 = 14/7$, and that of the down is $19/7 = 38/14$; in both cases we have two resonances giving the same mass. This will be useful later and quite stunning. Note also that the single variable resonance parameter of quarks, which is N, depends on 2, 7, and 19. It is the same for bosons in Table 3, but with K.

Table 3: Bosons resonances in MeV/c^2.

-	P = N	K	Computed	Measured
$W^{\pm}$	12	−2	80, 384.9	80, 385 ± 15
Z^0	12	−7	91, 187.56	91, 187.6 ± 2.1
H^0	12	−19	125, 206	125.090 ± 240

Last, the three bosons widths are computed from resonance geometry and substructure in coherence with the Ds. They come as a difference in mass with a hypothetical particle where their K is shifted as follows:

$$K \to K + 1 + 1/24, \tag{4}$$

in the case of the W and Z, and for the H^0:

$$K \to K + 1/144/6\,. \tag{5}$$

The three Tables above correspond to the fundamental field, but there is also an adjacent field, where leptons also ring as shown in Table 4. It comes with the constraint P=K instead of P=N in Table 1. It uses different parameters (index α):

$$X_\alpha = 8.02160795579\,\mathrm{keV/c^2}, \tag{6}$$

$$\mu_\alpha = \mu\left(\frac{\pi}{2} + \frac{\pi}{137} + \left(\frac{2\pi}{137}\right)^2\right). \tag{7}$$

Table 4: Second view on electron, muon, tau in MeV/c^2.

-	P=K	N	Computed	Measured
e	2	2	0.510 998 9461	0.510 998 9461(31)
μ	3	8	105.658 3752	105.658 3745(24)
τ	4	16	1 776.84	1 776.82(16)

Expressions giving D_e, D_α, and α are given in the next subsection.

Now looking at the different resonances in the Tables 1, 2, 3, and 4, and keeping all distinct numbers except fractions we get two sums which will play a singular role; firstly with the Ns and Ps, we compute the sum of all integral resonances in the space domain:

$$\Sigma_{N,P} = 2+3+4+5+7+8+9+12+14+16+19+38 = 137\,. \tag{8}$$

Then the sum of all possible shifts in K, increasing or reducing the resonance lengths. The term $266 = 2{\times}7{\times}19$ is related to the bosons'little k and is the product of their Ks.

$$\Sigma_K = (2\times 7\times 19) + 2+3+4+5-6 = 274\,. \tag{9}$$

Finding 137 here is not only reminiscent of the fine structure constant; the sum can be exponentiated in order to separate the 12 terms into distinct independent oscillators. Then it also suggests that the SM mass spectrum is defined by N and P being sub-harmonic components of a high mass, logically the Planck mass and, conversely in K, that a second sub-harmonic system exist which is orthogonal. For simplicity I shall denote this "dual sub-harmonic".

2.2 Couplings

Based on the idea of sub-harmonics, I have deduced the reduced Planck mass resonance in [1], but the deduction is incomplete as I do not find an exact value for the lesser term of its specific coupling D_p. Now I use the following value:

$$D_p = \frac{1}{\sqrt{137^2 - 19\pi^2 + \dfrac{4\pi}{19}}}\,. \tag{10}$$

The first reason is that, if compared to the calculus of the fine structure constant in [2], the lesser term in (10) represents a spin 2 current - i.e. not a particle - and secondly the computed Planck mass is perfectly centered in error bars:

$$M_p = \sqrt{\frac{\hbar\, c}{8\pi\, G}} = \frac{X}{\left(D_p^4 + \dfrac{D_e}{266^2}\right)^3}\,. \tag{11}$$

Last, the expression (10) (together with (12) hereafter) will later be shown exact at least up to 15 decimal places. Other couplings have the same form as (10) which was generalized

after computing α firstly from the leptons resonance and then from the Bohr model in [1], and [2].

They are:

$$D_e = \frac{1}{\sqrt{(4\times(274+19))^2 + 7\pi^2 - \dfrac{19\pi}{19-1}}}\,, \tag{12}$$

$$D_\alpha = \frac{1}{\sqrt{(16\times(274+3))^2 + 2\times(274+19+1)\pi^2 - \dfrac{19}{4\pi}}}\,, \tag{13}$$

where $\frac{19}{4\pi}$ is best guess. And of course:

$$\alpha = \frac{1}{\sqrt{137^2 + \pi^2 - \dfrac{1}{137.5}\times\dfrac{1}{2}\times\left(1+\dfrac{1}{4}\right)}}\,, \tag{14}$$

where the lesser terms may be incomplete, but lead to a value in agreement with CODATA (2014).

2.3 Energy and cosmology

Based on the results in the previous subsection it becomes relevant to suppose that no freedom exist in the field parameters. It naturally raise the question of cosmological data; in particular the densities of matter, dark matter and the elusive dark energy. In [3], assuming that the universe has permanent critical density, like it has now, and that its observable radius R_U recesses at the speed of light, I have shown that the cosmological term Λ is not constant but:

$$\Lambda \approx \frac{2\pi}{3\,R_U^2}\,, \tag{15}$$

where $R_U = c\,T$, with T the universe age; and secondly that the dark and visible energies obey the following proportionality relation, at any epoch:

$$\rho_D = 2\pi^2\,\rho_V = \frac{2\pi^2}{2\pi^2+1}\,\rho_T = \frac{11}{8}\,\rho_{DE} = \frac{11}{3}\,\rho_{DM}\,, \tag{16}$$

where:

— ρ_V, is the "visible" energy density,

— ρ_{DE}, is the dark energy density,

— ρ_{DM}, is the (cold) dark matter density,

— ρ_T, is the total energy density, $\rho_T = \rho_{DM} + \rho_{DE} + \rho_V$ and

— $\rho_D = \rho_{DM} + \rho_{DE}$ is the total dark fields density.

Those two relation imply that all energy densities related to mass evolve like $1/R_U^2$; it will be used as argument in the following sections. Several other results come from the same hypothesis:

— MOND is GR weak field approximation in a universe where energy and space-time expand linearly together,

— The MOND parameter value is $a_0 = H\,c/2\pi$,

— Discrepancy between the Hubble parameter measured locally (SN1A) and measured from events close to the event horizon (CMB and BAO), by a factor $\approx 1 + 1/2\pi^2$.

— The discrepancy creates the illusion of accelerated expansion.

— The reduction of wavelengths also creates the illusion of an initial inflation, since when $t \to 0$ wavelengths become infinitely large.

Where all quantities are calculable, computed, epoch dependent, and agree with experimental data (except for the inflation factor which I could not compute).

3 Couplings and particles mass

In this section I first discuss correlations between coupling coefficients; then between couplings and particles resonances.

3.1 Melting resonances and gearings

The template for a coupling coefficient is:

$$D = \frac{1}{\sqrt{A^2 + B\,\pi^2 + C}}\,.$$

where each term on the right-hand side represent a length, and one of the coefficients B and C is negative. They are evaluated by simple division for D_e (12) and D_α (13) after their values are fit to experimental data (leptons masses). Note that α (14) is computed differently but the same method would hold, and D_p (10) is first logically deduced, and then verified by computing the Planck mass from (11).

Examination of the four coupling formulas shows identical and look-alike coefficients in distinct places; the same component appears sometimes as a straight line (in A), sometimes in the rotation (in B), and sometimes in C which, at least in α, is the inverse of a rotation length from which the term π^2 at the denominator is removed. Then each coupling represents a specific piece or view of a unique movement, where (part of) the movement has a numerically isolated effect; and this requires identification. Firstly:

— The term $275 = (137 + 1/2)\times 1/2$ in α (14) represents the same "physical object" as in 275 + 19 in D_α (13). I shall not give a definition of "physical object".

— This same term 275 + 19 in D_α represents the same "physical object" as 274 + 19 in D_e (12).

— The increment $274 \to 275$ is found to come from the round trip of the electron around the proton when computing α in [2].

Here the same object represented by 274 can be seen as a piece of rotation (when multiplied by π^2), a part of a simple length, and of an inverted length. Therefore it is irrelevant to believe in distinct "forces". The coupling system above is a single movement, a unique clockwork and each coupling is a length seen from a specific perspective.

Secondly, the same term 137 is in α (14) and D_p (10). It also represents a single "physical object".

— So 274 and 137 are the bottom line of the couplings - but we have 19 associated to 274 as a kind of excess.

— The excess may be understood as a mutual interaction between D_p and D_e; the former requiring 19 rotations of negative length (like a shortcut), meaning that the length 137 is reduced by the excess in 274 + 19 - and/or conversely.

Thirdly, by extension, all the terms 19, 19π, and $-19\pi^2$ also refer to a "single object".

Finally, the gearing components are three cube differences 1, 7, and 19 in α (14), D_e (12), and D_p (10) respectively, that is to say in the fundamental field; D_α is not fundamental and the exception to this rule.

This being said, the term $19 - 1$ at the denominator in D_e (12) is of high interest because like for the $1/275$ in α it must be understood as a rotation where the $1/\pi^2$ is removed, hence we should read $19\pi^2 - 1\pi^2$. Therefore, by the same identifications, it means that the term π^2 in α (14) is subtracted from $19\pi^2$ in D_p (10). Together with the terms 137 in the same formulas, this is more than a connection between the fundamental field and electromagnetism. It can be said that the coupling D_e has the role of "flushing" π^2, and then α out of the fundamental field - hence a single movement.

On the practical grounds of testability and technology, those two coefficients are very important outputs; because anything that we can do with electromagnetic forces has a corresponding effect in the fundamental field where, obviously, D_p is a very strong share of the unified super-force. We discuss the geometry of couplings that include a gearing, that is to say a simple clockwork which it is necessarily reversible. So I'll bet that the fundamental field, which is not gravity and actually much stronger than electromagnetism, can be manipulated... with electrons.

3.2 Resonances and couplings

The coherence between the coupling coefficients and the particles resonances is very impressive, to begin with the rotation terms in D_e and D_p, namely $-19\pi^2$ and $7\pi^2$:

— Quarks masses as computed in Table 2 depend on a single variable number N, which values are in {2, 19/7, 7, 14, 19, 38} and therefore only combine 2, 7, and 19.

— The ratio of the resonance term N is 2 between the charm and strange on the one hand, and the top and bottom on the other hand. It is interesting that it is also the ratios of their electric charge.

— Bosons resonances also depend only on 2, 7, and 19 for K but also for N = P = 12 = 19-7.

— A high term $266 = 2\times7\times19$ appears twice; to compute the bosons' little k and to compute the Planck mass. We logically assume that it is the simplest expression of the unified super-force.

— Finally, even though this is a little less direct, the leptons resonances in Table 1 can be written 5 = 7-2 for the muon, and 9 = 7+2 for the tau - thus combining a radial resonance 2 of the electron with the rotation term of D_e.

The second aspect is given in the equations (8) and (9) with the sums $\Sigma_{N,P} = 137$ and $\Sigma_K = 274$. It probably means that the SM field is complete and that there is no other particles to discover (except of course if more resonances exist with the same numbers). As mentioned before, my interpretation is that the SM massive particles spectrum is a set of dual sub-harmonics of the Planck mass. But interestingly, for two reasons, the Planck mass is not a particle:

— Firstly, $D_p^4 < D_e/266^2$, where the opposite relation (>) is verified by all particles, as required by the equation.

— Secondly, it combines two couplings instead of one and the resonances (N, P).

I may even give a third reason, which is that in quantum theory it should be the natural unit of mass where the gravitational coupling is 1, which has no reason to be a particle.

4 On the SM fields origin

At this point using the sums $\Sigma_{N,P} = 137$ and $\Sigma_K = 274$, I have deduced the equations (10) and (11) and computed the Planck mass under the assumption that it depends a minima on its sub-harmonics. But there should rather be a physical reason for the sub-harmonics to depend on the Planck mass, otherwise the construction seems absurd. Hence the next question: Can we find a *physical* origin to the SM particles spectrum in the Planck mass equations without knowing the dual sub-harmonic system and its components (i.e. the sums to 137 and 274)? To solve this question we shall assume the Planck mass equation (11) and the values of D_e and D_p with infinite precision.

Here the theoretical situation is unique and rather fantastic, because everything in the field now depend on two quantities: D_p and D_e. In effect, the adjacent field and α are flushed out of the fundamental field defined by those two quantities. In principle we have reached the bottom and the only way to create a resonance is by combining D_p and D_e; as said this unique and fantastic. But how do we get the SM spectrum? and why should we get it?

The Planck mass in (11) includes two ringing lengths D_p^4 and $D_e/266^2$. It is a resonant system from which we know very little but: a) a resonance implies perfectly balanced oscillating "forces" and b) since this is GR we can guess that either M_p defines the light cone or, at the opposite, that the light cone defines it. So assume that the ringing lengths are the effects of a single "force" that rests on the light cone; it splits in two components which are necessarily space (3D) and time (1D) and correspond to the coefficients D_p^4 and $D_e/266^2$ respectively. Those are orthogonal and simple projections, proportional to the sine and cosine of the "force" amplitude, so we have a physical angle ϕ:

$$\phi = \arctan\left(\frac{D_e}{266^2 \times D_p^4}\right) = 1.33509... \approx \frac{4}{3}\,. \qquad (17)$$

But now by construction of the equation we compare a simple 3-volume associated to D_p^4 to a length associated to $D_e/266^2$.

Since the Planck mass equation uses D_e and $K > 0$, it rings like a lepton of spin 1/2, and then a change in phase π of this resonance is associated to one unit of volume $4\pi/3$; and since this is the Planck mass, this change in phase also defines the units of time and length. Hence comparing the effect of the "force" (the change in phase) to the volume to which the "force" applies (the unit of volume) we get a ratio:

$$\psi = \frac{\left(\frac{4\pi}{3}\right)}{\pi} = \frac{4}{3} \tag{18}$$

which is *almost equal* to ϕ in (17) where the volume corresponds to D_p^4 and the change in phase to the length $D_e/266^2$. This ratio is expressed in unit of m^3/rad, and it links the phase of quantum theory to the volume of the mass equation. But *almost equal* means a difference where a perfect match is mandatory: now the difference $\phi - \psi$ is significant! We need a physical correction to (17) that gives exactly 4/3 and does not modify the Planck mass. And since we have reached the bottom, there is nothing else remaining but D_p and $D_e/266^2$ to implement the correction. Hence:

1) All we can do is add in (17) more currents of type D_p interfering with $D_e/266^2$, giving a suite of $h_i\, D_p^i\, D_e/266^2$, with h_i a harmonic coefficient.

2) The field is entirely defined by the particles resonances, including all charges, masses, etc, then each h_i should be a known term that we can recognize.

3) The suite of h_i should also include the mass-less field, and all resonances that we do not know of.

Then from the point 1) above, and in coherence with the two others, the correction has a very simple form:

$$4/3 = \arctan\left(\frac{D_e \sum_{i=0}^{\infty} h_i\, D_p^i}{266^2 \times D_p^4}\right), \tag{19}$$

with $h_0 = +1$ for the Planck mass.

Now we want to solve this equation, and for this we have a few criteria enabling to proceed by successive approximation on i growing ($i = 1$, then $i = 2$, etc...):

a) As a must, since $D_p \approx 1/137$, we expect a gain at order i of roughly two decimals compared to the order $i - 1$.

b) As a guideline, the result should be natural and then the effect of the correction at order i should be in the range of the optimum - but not equal. The optimum at order i being the value of h_i where the equality is verified with $h_j = 0$ for $j > i$.

c) As a result, each h_i should represent resonance(s). Here we can safely recognize what we know.

On this basis, the interesting part is for $0 < i < 8$:

— $h_1 = -1$,

— $h_2 = -7$,

— $h_3 = +25$,

— $h_4 = -81$,

— $h_5 = +(7 + 14 + 19 + 38 + \frac{38}{19} + \frac{14}{7} + \frac{38}{14} + \frac{19}{7}) \times 2\pi$,

— $h_6 = -556 = -(137 \times 4 + 8)$,

— $h_7 = -216 = -144 \times \frac{3}{2}$,

As we shall see this suite includes the entire SM particles spectrum.

The relative distance of each h_i to the optimum is given in Table 5 for each step.

Table 5: Optimum vs h_i value.

Order	Value	Δ vs optimum
h_1	1	$< 6\%$
h_2	7	$< 2.5\%$
h_3	25	$< 2.5\%$
h_4	81	$< 5\%$
h_5	≈ 549.33	$< 0.8\%$
h_6	556	$< 0.3\%$
h_7	216	$< 0.3\%$

The difference with 4/3 is now $\approx 3 \times 10^{-16}$, which is in the expected range for i=7, and each h_i is close to the optimum. The connection of this series to the particles resonances in Tables 1, 2, and 3 and to the SM spectrum is almost trivial:

a) At first we find the Muon and Tau products NP (25 and 81) from Table 1, for i = 3 and i = 4 respectively. One could wonder why we are not closer to the optimum; but recall the constraint N=P for these resonances (see [1]). In both cases, we have the closest square to the optimum.

b) Then at i=5 the sum of all quarks circular resonances multiplied by 2π (- meaning that each number here represents a resonance length or its inverse). It includes, and then confirms, the fractional resonance as guessed in [1] and recalled in section 2.1 following Table 2. Here the optimum is ≈ 554, but considering the factor 2π, the relevant part is less than 1 point away from its optimum.

c) For i=7 we find the product NP=144 of the bosons double circular resonances, but multiplied by 3 (for 3 bosons) and divided by 2 (possibly because it should be divided by 2π, but those masses are already divided by π in (2)).

d) It leads to understanding the other terms as it must include also the SM mass-less particles as resonances of coefficient 1 *, to which the mass equation does not apply:

— $h_1 = -1$, the photon,

— $h_2 = -7 = -(4 + 3)$, by similarity with h_3, h_4, and quarks'sum h_5, it splits into the electron NP=4 plus 3 mass-less neutrinos,

— $h_6 = -(137 \times 4 + 8)$, the expected UFO, 137 with 4 resonances, plus 8 mass-less gluons.

Finally, we have found all the resonances in N and P of the Tables 1, 2, and 3 (except for 3), but we also find $K \approx i$:

— $h_2 \rightarrow$ electron, $K = 2$ (Tables 1 and 4).

— $h_3 \rightarrow$ muon, $K = 3$ (Tables 1 and 4).

*Like a photon can be seen to ring 1 to 1 in E and B in Maxwell theory

— $h_4 \rightarrow$ tau, $K = 4$ (Table 4) and $K = 5$ (Table 1).

— $h_5 \rightarrow$ quarks, $K = -6$ (Table 2).

— $h_6 \rightarrow$ no known massive particles.

— $h_7 \rightarrow 2 \times 7 \times 19$, bosons' K in {-2, -7, -19} (Table 3), but also from $1/266^2$.

Here we have a perfect ordering and some interesting aspects emerge:

a) We notice that with h_4 the tau is exceptional; firstly it takes two K (one in the fundamental field and one in the adjacent field) and coincidentally, it is here that the D_p^i at the numerator of (19) cancels the D_p^4 at the denominator.

b) Identically, it is with the next coefficient, when $i > 4$, that the Ks become negative (quarks and bosons). So we have a clear border which is between h_4 and h_5.

c) This is also where the fine structure constant appears in the Ds for quarks and bosons.

d) The second exception is the bosons $266 = 2 \times 7 \times 19$ used in Σ_K; it is coherent with the term $1/266^2$.

So we see *why and how* the SM spectrum is there; it shows that this theory is not another parametric model. Here the Planck mass, space-time, and the SM spectrum are neither independent nor separable, but three aspects of the same unity. Incidentally, it also shows that the expressions giving D_p and D_e are exact at least up to the 15^{th} decimal.

But now, this leads to a few obvious deductions, some of which can be tested:

1) Three neutrino, no more,

2) Three charged lepton, no more,

3) Neutrinos ranks with the electron in h_2, which means something very odd in the field symmetry (or symmetries),

4) No quark of higher mass (than the top),

5) Quarks mixing disagree with the standard concept as we have 8 physical resonances but only 6 masses,

6) No additional boson (i.e. a single Higgs, no Z'),

7) One new resonance, 137, ranking with gluons in h_6.

The resonance 137 corresponds to $\Sigma_{N,P} = 137$ as the full massive matter field resonance; but locally, it could also be a kind of mass-less monopole à la Lochak [5] carrying the matter field signature. It comes in 4 instances, like this monopole, and it is consistent with the fourth power of D_p in (11).

5 Scale symmetry and compatibility with GR

The mass equation depends linearly on the inverse of a volume at the denominator (initially a volume at the numerator); then if we simply apply the metric variations in the gravitational field to this volume, the equation is obviously incompatible with Einstein's theory of general relativity. But GR assumes that particles *have* mass, which we know is wrong; and also, on the basis of the previous section, we can mean that this incompatibility is certainly due to the incompleteness of GR and even SR - think of the Planck mass relations to a) the light cone, b) the units of length/time and volume, and c) the SM particles spectrum. So let us come back to the origin of the equation as shown in [1] and find *how* it can be compatible with GR already.

I start in 1 dimension and consider 2 identical propagating waves crossing each other, giving:

$$m = X N^2 , \tag{20}$$

with N an integral number representing the number of oscillations crossing each other within a generic length "1", and X a constant of unit kg.m^{-1}. So the N^2 represents a length (or $1/N^2$ an inverted length). But for a resonance to exist we need a mirror which is not part of the resonance but has energy:

$$m = X N^2 + \mu , \tag{21}$$

Then I add the quantized length K D, repeated each time two oscillations cross:

$$m = \frac{X}{\frac{1}{N^2} + KD} + \mu , \tag{22}$$

with K an integral number and D a constant of unit m^{-1}. Finally, in 3 dimensions I take the cube and get the inverse of a volume at the denominator:

$$m = \frac{X}{\left(\frac{1}{NP} + KD\right)^3} + \mu , \tag{23}$$

where the unit of X changes to kg.m^{-3}, and $N^2 \rightarrow NP$, where N and P are two integral that may be different since we now also have a rotational degree of freedom. Hence this equation is incompatible with GR by construction. But now in [3], I found the equations (15) and (16) which imply that all relevant densities evolve like $\Lambda \sim 1/R_U^2$; *and then the density X follows the same law*, that is:

$$X = \frac{const.}{R_U^2} . \tag{24}$$

Here there is no absolute length and the only reference length to consider is R_U; the hypothetical length "1" introduced in (20) is then $\sim R_U$, the volume at the numerator of (1) and (2) is $\sim R_U^3$, and then mass is proportional to $R_U^3/R_U^2 = R_U$. Provided the universe does not create particles permanently, this is the hypothesis in [3]; so the equation is a fit with my results in cosmology.

In addition it is now evident *how* the mass equation is compatible with GR, because if we vary the position of a particle in the gravitational field, its wavelength also varies and it will "see" R_U in reverse proportions to this variation: the lesser (resp. the higher) a particle energy in the gravitational field, the longer (resp. the shorter) is wavelength for a given observer, the lesser (resp. the higher) the universe age ($R_U = c\,T$) it "see". Hence a beautiful symmetry of scale which applies only to massive particles and shows the universality of the result: at any place and any epoch, a particle rest mass is proportional to the universe age it locally sense with Λ or dark energy.

6 The fine structure constant

Firstly what is it? In QED, it is the probability for an electron to absorb or emit a virtual photon. But here it is computed in [3] as a relative length that depends on the electron resonance, its spin, and $\Sigma_{N,P} = 137$. As per (14) it includes:

- An amplitude 2/137, where 137 is the sum of all massive particles resonances except the up and down quark. Then the electron is 2/137 parts of the field.

- Spin 1/2 gives π^2, half a turn for one unit of 137, but also $275 = (137 + 1/2) \times 2$, where the spin appears as the factor 2 to get a full turn 2π; the term 1/2 is geometrical.

- An additional component 1/4 which corresponds firstly to the muon resonance 8 in Table 4 (giving $(137 + 1/2) \times 8$), but also I believe to the compositeness of the electron (in the form of 2 distinct currents).

So α is firstly how much the electron gears the field, how much it contributes to the field resonance; its share of the job; and not the opposite like in QED. This interaction is permanent, and not a probability. So, with respect to QED and its methods of calculus, what difference does it make? Absolutely none as long as symmetry remains. The field can even fluctuate, randomly or not.

Secondly, where is it? The answer is not obvious since we have only two harmonics of Table 4 in the expression (14) giving α, and nothing about it in Table 1. But we also have the sum $\Sigma_{N,P} = 137$ and the equation (7) linking μ and μ_α which is also based on π and 137. This link does not use X or X_α, so we can guess that α is in their difference. Since it is unit-less let us compute:

$$\frac{X + X_\alpha}{X - X_\alpha} \approx 131\,, \tag{25}$$

which we find in the expected range. Trying to invert the angle μ/μ_α in (7) to complement the clockwork, I eventually found an expression that holds at about $5\,10^{-9}$ with:

$$\frac{2\pi\,(X + X_\alpha)}{X\,(1-\alpha) - X_\alpha\,(1+\alpha)} = 137^2 - 137\,\pi + \frac{2}{137.5}\left(1 + \frac{1}{4}\right), \tag{26}$$

which is symmetrical in X, X_α, and α. From the reasoning in the previous sections and the form of this expression, it looks like this quantity represents the remainder of D_p^2 once α has been flushed out of the fundamental field.

7 Conclusion

I think I have shown that talking *free* parameters is blunt lie. I think I have also shown that piling up ad-hoc quantum fields to match anything is not such a great idea. Here the field is unique and its parameters are structurally coherent from α to Z^0 (necessarily including all other useful letters in between, even though I miss a few). It has the beauty of self definition, of self generation, and above all that of the necessarily unique: here there is only one, not even two. No two things of different nature; no particles "in" space. No vibrating thingy but only paths and dimensions - and then structures appear naturally by geometrical necessity; only structures from constraint, no freedom. How could it be less?

8 Addendum: what next?

Since the fit in section 4 is not perfect and despite the fact that the sets of {N, P} and {K} seem complete from the sums $\Sigma_{N,P}$ and Σ_K, we may try to continue the sequence of h_i and guess more resonances requiring more particles. I shall discuss two cases; I first assume that the SM is complete and as a second case I assume a graviton.

Assume the SM complete; then, following the suite of h_i in section 4 it was easy to fit down to a residual error of 3.88×10^{-43} (which is ridiculous) without introducing new quantities/resonances but only some mixes, inversions, widths, and a few numbers in π. I had to stop here because the h_i are decreasing rapidly down to $h_{17} \approx 0.00052$, which is much smaller than $D_p \approx 0.00734$.

Here is what I first found with possible correspondence:

— $h_8 = 156 = -(137 + 19) = -(144 + 12)$, no comment,

— $h_9 = -(38 + 19 - 1)$, t + b - 1 (Table 2),

— $h_{10} = -(\pi^2)$, geometry,

— $h_{11} = -(12 - 7/12)$, bosons N (Table 3) + 7/12 (new?),

— $h_{12} = -((7 + 1)/(14 + 1))$, (s + 1)/(c + 1) (Table 2),

— $h_{13} = -(3/4)$, inverse of 4/3,

— $h_{14} = -(1 + 1/24)$, W and Z bosons width (4),

— $h_{15} = -(1/7 + 4/(274 + 19 + 1))$, inverse of the rotation of D_e and that of D_α times 8,

— $h_{16} = -(1/(144 \times 6) + 1/((274 + 19) \times (16)))$, Higgs boson width (5) + inverse of D_e main coefficient times 4,

— $h_{17} = -(\pi^2/137^2)$, geometry, maybe from μ/μ_α (7).

It shows that I cannot predict any observable in this manner. But on the other hand, each expression above is so obviously related to a number used elsewhere that I wonder if the series may be right. The Table 6 gives the value or range of each harmonic coefficient and its distance to the optimum at each step. Now not only each harmonic stays close to the optimum, but the h_i seems to quickly converge to zero.

Table 6: Optimum vs h_i value.

Order	Value	Δ vs optimum (%)
h_8	156	< 0.5%
h_9	56	< 0.2%
h_{10}	≈ 9.87	< 0.9%
h_{11}	≈ 11.4	< 0.04%
h_{12}	≈ 0.533	< 1.1%
h_{13}	≈ 0.750	< 1.1%
h_{14}	≈ 1.042	< 0.12%
h_{15}	≈ 0.156	< 0.01%
h_{16}	≈ 0.00137	< 0.3%
h_{17}	≈ 0.000526	< 0.7%

Now assume a graviton; it requires to add a resonance "1", and the first place that makes sense is to add a massless boson in h_7 with: $h_7 = -217 = -(144 \times \frac{3}{2} + 1)$, and it can represent either the graviton or the photon (if misplaced in h_1); the residual error at order 7 is $< 4\,10^{-17}$ (instead of $3\,10^{-16}$) and its distance to the optimum is $< 0.06\%$. Then $h_8 \approx -(2\pi^2 + \frac{1}{\pi})$, with a residual error $< 7.5\,10^{-20}$ and a distance $< 0.2\%$ to the optimum. The terms in h_8 address 4-geometry with $2\pi^2$ the surface of a 4-sphere of radius unity, and the inverse of a change in phase π.

Submitted October 11, 2018

References

1. Consiglio J., On Quantization and the Resonance Paths. *Progress in Physics*, 2016, v. 12(3), 259–275.
2. Consiglio J., Take Fifteen Minutes to Compute the Fine Structure Constant. *Progress in Physics*, 2016, v. 12(4), 305–306.
3. Consiglio J., Are Energy and Space-time Expanding Together? *Progress in Physics*, 2017, v. 13(3), 156–160.
4. The Plank Collaboration. Planck 2015 results. I. Overview of products and scientific results. arXiv: 1502.01582.
5. Georges Lochak. The symmetry between Electricity and Magnetism and the equation of a leptonic Monopole. 2007, http://arxiv.org/abs/0801.2752

On the Cosmological Significance of Euler's Number

Hartmut Müller

E-mail: hm@interscalar.com

The paper derives and exemplifies the stabilizing significance of Euler's number in particle physics, biophysics, geophysics, astrophysics and cosmology.

Introduction

Natural systems are highly complex and at the same time they impress us with their lasting stability. For instance, the solar system hosts at least 800 thousand orbiting each other bodies. If numerous bodies are gravitationally bound to one another, classic models predict long-term highly unstable states [1, 2]. Indeed, considering the destructive potential of resonance, how this huge system can be stable?

In the following we will see that the difference between rational, irrational algebraic and transcendental numbers is not only a mathematical task. It is also an essential aspect of stability in complex systems.

Actually, if the ratio of any two orbital periods would be a rational number, periodic gravity interaction would progressively rock the orbital movements and ultimately cause a resonance disaster that could destabilize the solar system. Therefore, lasting stability in complex dynamic systems is possible only if whole number frequency ratios can be avoided.

Obviously, irrational numbers cannot be represented as a ratio of whole numbers and consequently, they should not cause destabilizing resonance interaction [3, 4].

Though, algebraic irrational numbers like $\sqrt{2}$ do not compellingly prevent resonance, because they can be transformed into rational numbers by multiplication. In the case of $\sqrt{2}$ as a frequency ratio, every even harmonic is integer, because $\sqrt{2} \cdot \sqrt{2} = 2$.

However, there is a type of irrational numbers called transcendental which are not roots of whole or rational numbers. They cannot be transformed into rational or whole numbers by multiplication and consequently, they do not provide resonance interaction.

Actually, frequencies of real periodical processes are not constant. Their temporal change is described by accelerations, the derivatives of the frequencies. Naturally, accelerations are not constant either.

Surprisingly, there is only one transcendental number that inhibits resonance also regarding accelerations and any other derivatives: it is Euler's number $e = 2.71828\ldots$, because it is the basis of the natural exponential function e^x, the only function that is the derivative of itself.

In this way, the number continuum provides the solution for lasting stability in systems of any degree of complexity. The solution is given a priori: frequency ratios equal to Euler's number, its integer powers or roots are always transcendental [5] and inhibit destructive resonance interaction regarding all derivatives of the interconnected periodic processes. Therefore, we expect that periodic processes in stable systems show frequency ratios close to integer powers of Euler's number or its roots. Consequently, the logarithms of the frequency ratios should be close to integer 0, 1, 2, 3, 4, ... or rational values $\frac{1}{2}, \frac{1}{3}, \frac{1}{4}, \ldots$

In the following we will exemplify our hypothesis in particle physics, biophysics, geophysics, astrophysics and cosmology. We start with the solar system.

Euler's number stabilizes the solar system

Let us analyze the ratios of the orbital periods of some planets. Saturn's sidereal orbital period [6] equals 10759.22 days, that of Uranus is 30688.5 days. The natural logarithm of the ratio of their orbital periods is close to 1:

$$\ln\left(\frac{30688.5}{10759.22}\right) = 1.05.$$

Jupiter's sidereal orbital period equals 4332.59 days, that of the planetoid Ceres is 1681.63 days. The natural logarithm of the ratio of their orbital periods is also close to 1:

$$\ln\left(\frac{4332.59}{1681.63}\right) = 0.95.$$

Not only neighboring orbits show Euler ratios, but far apart from each other orbits do this as well. Pluto's sidereal orbital period is 90560 days, that of Venus is 224.701 days. The natural logarithm of the ratio of their orbital periods equals 6:

$$\ln\left(\frac{90560}{224.701}\right) = 6.00.$$

In [7] we have analyzed the orbital periods of the largest bodies in the solar system including the moon systems of Jupiter, Saturn, Uranus and Neptune, as well as the exoplanetary systems Trappist 1 and Kepler 20. In the result we can assume that the stability of all these orbital systems is given by the transcendence of Euler's number and its roots.

Euler's number stabilizes biological rhythms

Biological processes are of highest complexity and their lasting stability is of vital importance. Therefore, we expect that established periodical biological processes show Euler frequency ratios. In fact, at resting state, the majority of adults

prefer to breath [8] with an average frequency of 15 inhale-exhale sequences per minute, while their heart rate [9] is close to 67 beats per minute. The natural logarithm of the ratio of these frequencies equals $1+\frac{1}{2}$:

$$\ln\left(\frac{67}{15}\right) = 1.50.$$

Mammals including human show electrical brain activity [10] of the Theta type in the frequency range between 3 and 7 Hz, of Alpha type between 8 and 13 Hz and Beta type between 14 and 34 Hz. Below 3 Hz the brain activity is of the Delta type, and above 34 Hz the brain activity changes to Gamma.

The frequencies 3 Hz, 8 Hz, 13 Hz and 34 Hz define the boundaries. The logarithms of their ratios are close to integer and half values:

$$\ln\left(\frac{8}{3}\right) = 0.98, \qquad \ln\left(\frac{13}{8}\right) = 0.49, \qquad \ln\left(\frac{34}{13}\right) = 0.96.$$

In [11] we have analyzed various biological frequency ranges and assume that their stability is given by the transcendence of Euler's number and its roots.

Euler's number stabilizes the atom

The most stable systems we know are of atomic scale. Proton and electron form stable atoms, the structural elements of matter. The lifespans of the proton and electron surpass everything that is measurable, exceeding 10^{30} years. No scientist ever witnessed the decay of a proton or an electron. What is the secret of their eternal stability?

In standard particle physics, the electron is stable because it is the least massive particle with non-zero electric charge. Its decay would violate charge conservation. Indeed, this answer only readdresses the question. Why then is the elementary electric charge so stable?

In theoretical physics, the proton is stable, because it is the lightest baryon and the baryon number is conserved. Indeed, also this answer only readdresses the question. Why then is the proton the lightest baryon? To answer this question, the standard model introduces quarks which violate the integer quantization of the elementary electric charge.

Now let us proof our hypothesis of Euler's number as universal stabilizer and analyze the proton-to-electron ratio 1836.152674 that is considered as fundamental physical constant [12]. It has the same value for the natural frequencies, oscillation periods, wavelengths, rest energies and rest masses of the proton and electron. In fact, the natural logarithm is close to seven and a half:

$$\ln(1836.152674) = 7.51.$$

This result suggests the assumption that the stability of the proton and electron comes from the number continuum, more specifically, from the transcendence of Euler's number, its integer powers and roots. In [13] we have analyzed the mass distribution of hadrons, mesons, leptons, the W/Z and Higgs bosons and proposed fractal scaling by Euler's number and its roots as model of particle mass generation [14]. In this model, the W-boson mass 80385 MeV/c^2 and the Z-boson mass 91188 MeV/c^2 appear as the 12 times scaled up electron rest mass 0.511 MeV/c^2:

$$\ln\left(\frac{80385}{0.511}\right) = 11.97, \qquad \ln\left(\frac{91188}{0.511}\right) = 12.09.$$

In [15] Andreas Ries did apply fractal scaling by Euler's number to the analysis of particle masses and in [16] he demonstrated that this method allows for the prediction of the most abundant isotopes.

Global scaling based on Euler's number

Our hypothesis about Euler's number as universal stabilizer allows us to calculate Pluto's orbital period from that of Venus multiplying 6 times by Euler's number:

$$\textit{Venus orbital period} \cdot e^6 = \textit{Pluto orbital period}.$$

Each time we multiply by Euler's number, we get an orbital period of a planet in the following sequence: Mars, Ceres, Jupiter, Saturn, Uranus and Pluto. Dividing by Euler's number, we get close to the orbital period of Mercury. Earth's orbital period we get multiplying by the square root of Euler's number. The same is valid for Neptune relative to Uranus.

Euler's number and its roots are universal scaling factors that inhibit resonance and in this way, stabilize periodical processes bound in a chain system. Pluto's orbital period can be seen as the 6 times scaled up by Euler's number orbital period of Venus or as the 3 times scaled up by Euler's number orbital period of Jupiter.

In the same way, the oscillation period of the electron can be seen as the $7 + \frac{1}{2}$ times scaled up oscillation period of the proton. Here it is important to understand that only scaling by Euler's number and its roots inhibits resonance interaction and provides lasting stability of the interconnected processes.

Now we could ask the question: Starting with the electron oscillation period, if we continue to scale up always multiplying by Euler's number, will we meet the orbital period, for instance, of Jupiter?

Actually, it is true. If we multiply the electron natural oscillation period 66 times by Euler's number, we meet exactly the orbital period of Jupiter:

$$\textit{electron oscillation period} \cdot e^{66} = \textit{Jupiter orbital period}.$$

The oscillation period of the electron has a duration of $2\pi \cdot 1.288089 \cdot 10^{-21} s = 8.0933 \cdot 10^{-21}$ s. Jupiter' orbital period takes 4332.59 days = $3.7331 \cdot 10^8$ s. In fact, the natural logarithm of the ratio of Jupiter' orbital period to the electron oscillation period equals 66:

$$\ln\left(\frac{3.7331 \cdot 10^8\ \text{s}}{8.0933 \cdot 10^{-21}\ \text{s}}\right) = 66.00.$$

PROPERTY	ELECTRON	PROTON
rest energy E	0.5109989461(31) MeV	938.2720813(58) MeV
rest mass $m = E/c^2$	$9.10938356(11) \cdot 10^{-31}$ kg	$1.672621898(21) \cdot 10^{-27}$ kg
blackbody temperature $T = E/k$	$5.9298446 \cdot 10^{9}$ K	$1.08881 \cdot 10^{13}$ K
angular frequency $\omega = E/\hbar$	$7.763441 \cdot 10^{20}$ Hz	$1.425486 \cdot 10^{24}$ Hz
angular oscillation period $\tau = 1/\omega$	$1.288089 \cdot 10^{-21}$ s	$7.01515 \cdot 10^{-25}$ s
angular wavelength $\lambda = c/\omega$	$3.8615926764(18) \cdot 10^{-13}$ m	$2.103089 \cdot 10^{-16}$ m

Table 1: The basic set of physical properties of the electron and proton (c is the speed of light in a vacuum, $\hbar$ is the reduced Planck constant, k is the Boltzmann constant). Data taken from Particle Data Group [12]. Frequencies, oscillation periods, temperatures and the proton wavelength are calculated.

Forming atoms and molecules, proton and electron are substantial components of biological organisms as well. Through scaling, Euler's number stabilizes biological processes down to the subatomic scales of the electron and proton. Dividing the angular frequency of the electron 48 times by Euler's number, we get the average adult human heart rate:

$$electron\ angular\ frequency\ /\ e^{48} = adult\ human\ heart\ rate.$$

In fact, the natural logarithm of the ratio of the average adult human heart rate 67/min to the electron angular frequency (tab. 1) equals -48:

$$\ln\left(\frac{67/60}{7.763441 \cdot 10^{20}}\right) = -48.00.$$

In a similar way, dividing the angular frequency of the proton 57 times by Euler's number, we get the average adult human respiratory rate:

$$proton\ angular\ frequency\ /\ e^{57} = adult\ respiratory\ rate.$$

In fact, the natural logarithm of the ratio of the average adult human resting respiratory rate 15/min to the proton angular frequency (tab. 1) equals -57:

$$\ln\left(\frac{15/60}{1.425486 \cdot 10^{24}}\right) = -57.00.$$

Through scaling by Euler's number, systemically important processes of very different scales avoid resonance. In [17] we have shown how the metric characteristics of biological systems are embedded in the solar system and prevented from destructive proton and electron resonance through scaling by Euler's number.

The exceptional stability of the electron and proton predestinates them as the forming elements of baryonic matter and makes them omnipresent in the universe. Therefore, the prevention of complex systems from electron or proton resonance is an essential condition of their lasting stability.

This uniqueness of the electron and proton predispose their physical characteristics (tab. 1) to be treated as natural metrology, completely compatible with Planck units. Originally proposed in 1899 by Max Planck, they are also known as natural units, because they origin only from properties of nature and not from any human construct. Natural units are based only on the properties of space-time.

Max Planck wrote [18] that these units, "regardless of any particular bodies or substances, retain their importance for all times and for all cultures, including alien and non-human, and can therefore be called natural units of measurement".

If now we express Jupiter's body mass in electron masses, we can see how Euler's number prevents Jupiter from destructive electron resonance. In fact, the logarithm of the Jupiter-to-electron mass ratio is close to the integer 132:

$$\ln\left(\frac{1.8986 \cdot 10^{27}\,\mathrm{kg}}{9.10938 \cdot 10^{-31}\,\mathrm{kg}}\right) = 131.98.$$

As we have seen already, the natural logarithm of the ratio of Jupiter's orbital period to the electron oscillation period equals 66 that is 132/2.

The same is valid for Venus. The natural logarithm of the ratio of Venus' orbital period 224.701 days = $1.9361 \cdot 10^7$ s to the electron oscillation period is close to the integer 63:

$$\ln\left(\frac{1.9361 \cdot 10^{7}\,\mathrm{s}}{8.0933 \cdot 10^{-21}\,\mathrm{s}}\right) = 63.04.$$

At the same time, the logarithm of the Venus-to-electron mass ratio is close to the integer 126 that is $2 \cdot 63$:

$$\ln\left(\frac{4.8675 \cdot 10^{24}\,\mathrm{kg}}{9.10938 \cdot 10^{-31}\,\mathrm{kg}}\right) = 126.01.$$

For Jupiter and Venus, now we can write down an equation that connects the body mass M with the orbital period T:

$$\left(\frac{T}{\tau_{\,electron}}\right)^2 = \frac{M}{m_{\,electron}}.$$

In [19, 20] we have shown that mass-orbital scaling arises as a consequence of macroscopic quantization in chain systems of harmonic quantum oscillators and can be understood as fractal equivalent of the Hooke's law. Saturn's moon system demonstrates square root mass-orbital scaling for one and the same body, like in the case of Jupiter and Venus. The moon systems of Jupiter and Uranus show, that mass-orbital scaling can be valid also for couples of different bodies. This may mean that the orbital period of a given body is not always a function of its own mass, but depends on the mass distribution in the whole system.

In [21] we have shown how global scaling by Euler's number determines the masses, sizes, orbital and rotation periods, orbital velocities and surface gravity accelerations of the largest bodies in the solar system.

Not only the bodies of Jupiter and Venus are prevented from destructive electron resonance, but the Sun as well. In fact, the logarithm of the Sun-to-electron mass ratio is close to the integer 139:

$$\ln\left(\frac{1.9884 \cdot 10^{30}\,\mathrm{kg}}{9.10938 \cdot 10^{-31}\,\mathrm{kg}}\right) = 138.94.$$

In this way, the body mass of Jupiter is the 7 times scaled down by Euler's number body mass of the Sun. The body masses of Neptune and Uranus appear as the 3 times scaled down by Euler's number body mass of Jupiter.

Scaling down by Euler's number another 3 times, we get the body mass of Venus. Again scaling down by Euler's number 2 times, we get the body mass of Mars. Scaling down by Euler's number 4 times, we get the body mass of Pluto, then dividing always by Euler's number we get the body masses of Haumea and Charon.

In [22] we did show that global scaling by Euler's number can be seen as stabilizing mechanism of planetary atmospheres that determines their stratification. In [23,24] we have applied scaling by Euler's number in engineering and developed methods of resonance inhibition and stabilization in ballistics, aerodynamics and mechanics.

Euler's number stabilizes the universe

Having analysed the solar system, now we venture into more distant regions of the Milky Way. However, we have to consider that distance measurement by parallax triangulation is precise enough only up to 500 light years. With the increase of the distances, indirect methods are applied blurring the difference between facts and model claims.

Currently there is no precise measurement of the distance to the Galactic Center, but 26,000 light years = $2.46 \cdot 10^{20}$ m seems an accepted estimation [25]. The natural logarithm of this distance divided by the proton wavelength (tab. 1) is close to the integer 83:

$$\ln\left(\frac{R_{\mathrm{GC-Sun}}}{\lambda_{\mathrm{proton}}}\right) = \ln\left(\frac{2.46 \cdot 10^{20}\,\mathrm{m}}{2.103089 \cdot 10^{-16}\,\mathrm{m}}\right) = 83.05.$$

If the current measurement is correct, it would mean that the solar system orbits the Galactic Center at a distance that avoids resonance interaction with it. Good for us.

The Andromeda galaxy M31 seems to be at a distance of 2.5 million ly = $2.365 \cdot 10^{22}$ m [26] away from the Milky Way (MW). The natural logarithm of this distance divided by the electron wavelength (tab. 1) is close to the integer 80:

$$\ln\left(\frac{R_{\mathrm{MW-M31}}}{\lambda_{\mathrm{electron}}}\right) = \ln\left(\frac{2.365 \cdot 10^{22}\,\mathrm{m}}{3.861593 \cdot 10^{-13}\,\mathrm{m}}\right) = 80.10.$$

For reaching the island of stability that corresponds with the integer logarithm 80, the M31-to-MW distance has to decrease by 240,000 ly down to 2.26 million light years:

$$\lambda_{\mathrm{electron}} \cdot e^{80} = 2.26 \cdot 10^{6}\ \mathrm{ly}.$$

They seem to do exactly this. M31 is approaching (more precisely, 2.5 million years ago was approaching) the Milky Way at about 100 kilometers per second, as indicated by blueshift measurements [27]. If this velocity is constant, the current distance to M31 should be already 1,000 light years shorter than the 2.5 million years old distance we can measure today.

Standard model calculations expect that both galaxies will collide in a few billion years [27]. Considering the stabilizing function of Euler's number, we expect that after reaching the integer logarithm 80, the approach will be finished and the distance between both galaxies will be stabilized at 2.26 million light years. In this way, the consideration of Euler's number as resonance inhibitor and universal stabilizer can modify predictions completely.

The cosmic microwave background radiation (CMBR) is traditionally interpreted as a remnant from an early stage of the observable universe when stars and planets didn't exist yet, and the universe was denser and much hotter. Admittedly, there are alternative models [28] in development proposing explanations for the CMBR which do not implicate standard cosmological scenarios. However, traditionally CMBR data is considered as critical to cosmology since any proposed model of the universe must explain this radiation.

If this cosmic background process is stable, its average temperature 2.725 Kelvin [29] should correspond with an integer power of Euler's number. In fact, the CMBR-to-proton blackbody temperature ratio is close to the logarithm -29:

$$\ln\left(\frac{\mathrm{T}_{\mathrm{CMBR}}}{\mathrm{T}_{\mathrm{proton}}}\right) = \ln\left(\frac{2.725\ \mathrm{K}}{1.08881 \cdot 10^{13}\ \mathrm{K}}\right) = -29.01.$$

In this way, the cosmic background seems to be stable, and the current temperature of the CMBR is not accidental.

We assume that global scaling by Euler's number stabilizes the whole universe [30], from the atoms up to the galaxies and the intergalactic space. In this case, any linear (non-logarithmic) observation of very large-scale structures will

discover a scaling-up-effect that appears as exponential expansion of the universe. At the same time, any linear observation of very small-scale structures will discover a scaling-down-effect that appears as exponential compression down to an apparent spacetime singularity.

Conclusion

The consideration of Euler's number as resonance inhibitor and universal stabilizer adds a new aspect to our comprehension of the evolution of the universe, explaining not only the stability of the solar orbital system, but also the stability of its trajectory through the galaxy.

On the example of the M31-MW approach we demonstrated how the consideration of Euler's number as stabilizer can modify predictions completely. Applying global scaling by Euler's number to planetary systems, we can identify stabilized astrophysical processes and predict the evolution of systems that are still in formation.

We have shown that the current cosmic background temperature is not accidental and manifests the cosmological significance of Euler's number as well.

Stabilizing the proton-to-electron ratio, Euler's number provides the formation of atoms. Euler's number stabilizes biological frequency ranges down to the subatomic scale and embeds them in the dynamics of the solar system.

Finally, the apparent expansion of the universe could turn out to be a compelling consequence of the stabilizing role of Euler's number and its integer powers.

Acknowledgements

The author is grateful to Viktor Panchelyuga, Dmitri Rabounski, Yuri Vladimirov, Dmitri Pavlov, Oleg Kalinin, Alexey Petrukhin and Leili Khosravi for valuable discussions.

Submitted on November 29, 2018

References

1. Heggie D. C. The Classical Gravitational N-Body Problem. arXiv: astro-ph/0503600v2, 11 Aug 2005.
2. Hayes B. The 100-Billion-Body Problem. American Scientist, v. 103, no. 2, 2015.
3. Dombrowski K. Rational Numbers Distribution and Resonance. *Progress in Physics*, 2005, v. 1, no. 1, 65–67.
4. Panchelyuga V.A., Panchelyuga M. S. Resonance and Fractals on the Real Numbers Set. *Progress in Physics*, 2012, v. 8, no. 4, 48–53.
5. Hilbert D. Über die Transcendenz der Zahlen e und π. *Mathematische Annalen*, 1983, v. 43, 216–219.
6. Astrodynamic Constants. JPL Solar System Dynamics. ssd.jpl.nasa.gov (2018).
7. Müller H. Global Scaling of Planetary Systems. *Progress in Physics*, 2018, v. 14, 99–105.
8. Ganong's Review of Medical Physiology (23rd ed.), p. 600.
9. Spodick D. H. Survey of selected cardiologists for an operational definition of normal sinus heart rate. *The American J. of Cardiology*, 1993, vol. 72 (5), 487–488.
10. Tesche C. D., Karhu J. Theta oscillations index human hippocampal activation during a working memory task. *PNAS*, vol. 97, no. 2, 2000.
11. Müller H. Chain Systems of Harmonic Quantum Oscillators as a Fractal Model of Matter and Global Scaling in Biophysics. *Progress in Physics*, 2017, v. 13, 231–233.
12. M. Tanabashi et al. (Particle Data Group), Phys. Rev. D 98, 030001 (2018), www.pdg.lbl.gov
13. Müller H. Fractal Scaling Models of Natural Oscillations in Chain Systems and the Mass Distribution of Particles. *Progress in Physics*, 2010, v. 6, 61–66.
14. Müller H. Emergence of Particle Masses in Fractal Scaling Models of Matter. *Progress in Physics*, 2012, v. 8, 44–47.
15. Ries A. Qualitative Prediction of Isotope Abundances with the Bipolar Model of Oscillations in a Chain System. *Progress in Physics*, 2015, v. 11, 183–186.
16. Ries A. Bipolar Model of Oscillations in a Chain System for Elementary Particle Masses. *Progress in Physics*, 2012, vol. 4, 20–28.
17. Müller H. Astrobiological Aspects of Global Scaling. *Progress in Physics*, 2018, v. 14, 3–6.
18. Max Planck. Über Irreversible Strahlungsvorgänge. *Sitzungsbericht der Königlich Preußischen Akademie der Wissenschaften*, 1899, vol. 1, 479–480.
19. Müller H. Scaling of Moon Masses and Orbital Periods in the systems of Saturn, Jupiter and Uranus. *Progress in Physics*, 2015, v. 11, 165–166.
20. Müller H. Scaling of body masses and orbital periods in the Solar system as consequence of gravity interaction elasticity. // Abstracts of the XII. International Conference on Gravitation, Astrophysics and Cosmology, dedicated to the centenary of Einstein's General Relativity theory. Moscow, PFUR, 2015.
21. Müller H. Scale-Invariant Models of Natural Oscillations in Chain Systems and their Cosmological Significance. *Progress in Physics*, 2017, v. 13, 187–197.
22. Müller H. Global Scaling of Planetary Atmospheres. *Progress in Physics*, 2018, v. 14, 66–70.
23. Müller H. The general theory of stability and objective evolutionary trends of technology. Applications of developmental and construction laws of technology in CAD. Volgograd, VPI, (1987).
24. Müller H. Superstability as a developmental law of technology. Technology laws and their Applications. Volgograd-Sofia, (1989).
25. Groom D. E. et al. Astrophysical constants. *European Physical Journal C*, vol. 15, 1, 2000, www.pdg.lbl.gov
26. Ribas I. et al. First Determination of the Distance and Fundamental Properties of an Eclipsing Binary in The Andromeda Galaxy. arXiv:astro-ph/0511045v1, 2005.
27. Cowen R. Andromeda on collision course with the Milky Way. *Nature.com*, 31 May 2012.
28. Lopez-Corredoira M. Non-standard models and the sociology of cosmology. Science Direct, *Studies in History and Philosophy of Modern Physics*, vol. 46, Part A, May 2014, pp. 86–96.
29. Fixsen D. J. The Temperature of the Cosmic Microwave Background. *The Astrophysical Journal*, vol. 707 (2), 916–920. arXiv:0911.1955, 2009.
30. Müller H. Global Scaling. The Fundamentals of Interscalar Cosmology. *New Heritage Publishers*, Brooklyn, New York, USA, (2018).

Retraction of "Outline of a Kinematic Light Experiment"

Christian M. Wackler

While re-examining the experimental proposal outlined in *Progress in Physics*, 2018, vol. 14, issue 3, pages 152–158, I became aware of a fatal flaw in its theory. A uniformly rotating disk and a light source pulsing at a constant rate cannot serve to determine whether the speed of light depends on the motion of the radiation source. Therefore, I retract the paper. Apologies are expressed to all readers. However, as the preliminary considerations developed in the article remain valid, it is much to be hoped that physicists will tackle the all-important light speed question experimentally.

Editor's comment:

In response to Wackler's retraction, his original article was removed from the journal's online archives. However, the print version of Progress in Physics still contains the original article, since the author solicited retraction after printing.

Submitted on December 15, 2018

Optical Absorption in GaAs/AlGaAs Quantum Well due to Intersubband Transitions

Suleiman B. Adamu[1], Inuwa A. Faragai[2], and Usman Ibrahim[3]

[1,3] Department of Physics, Sule Lamido University Kafin Hausa, P.M.B 048, Jigawa State, Nigeria.
E-mail: Sulbash@gmail.com

[2]Department of Physics, Kano State University of Science and Technology, Wudil, Kano.
E-mail: Ialiyufaragai@yahoo.co.uk

Intersubband transition in quantum wells have strong potential for device application and are challenging field of fundamental studies. In this paper, intersubband optical absorption in GaAs/AlGaAs quantum well is investigated. Using a simple numerical approach and mathematical modeling applied to the first two conduction subbands, simplified expression for the optical absorption is obtained. The results obtained shows that the dephasing and other scattering mechanism have impact on absorption peaks and can only be tolerated to certain limits.

1 Introduction

Since the early years of quantum well studies, intersubband transitions in quantum well (QW) structures have attracted much attention. Both theoretical and experimental investigation were carried out by different researchers [1].

Rybalko et al. [2] proposed new approach to study light absorption in tunnel-coupled GaAs/AlGaAs quantum wells for electro-optic. In addition, Refs. [3] report the investigation of the effect of intersubband optical transitions of the magnetic field and tilt angle. Many physical effects of a semiconductor in quantum well structures have been exploited, such as infrared photodetectors [4, 5]. Furthermore, intersubband transitions in a multiple quantum well (MQW) structures were reported in Refs. [6–8]. Numerical investigation for absorption spectra induced by an ultrafast infrared pulse on the double quantum well structure were studied by Wu [9].

In this paper, we will derive the equation of optical absorption in GaAs/AlGaAs quantum well, by the modified version of Lorentzian approximation that is well proven itself in describing of electronics properties of these semiconductors. The equation obtained will be numerically solved and discussed.

2 Model Equation

We consider an intersubband transition in a P-conduction band $n_{12} = 1, 2$, interacting with photon energy governed by

$$E_n = \frac{n\hbar^2}{2m_e^*}\left(\frac{\pi}{L}\right)^2, \tag{1}$$

where m_e^* is the electron effective mass in the conduction band, L is the length of the quantum well, $\hbar$ is the reduced Planks constant and the transition energy ΔE between the two subbands is obtained from $E_{12} = E_2 - E_1$.
After projection of the photon energy along the dipole moment, the optical absorption coefficient as in Ref. [10] can be written as

$$\alpha(\hbar\omega) = \frac{2\pi\omega}{n_r V c\epsilon_0}\sum_{\vec{k_t}} \mathrm{g}\left(E_b - E_a - \hbar\omega\right)\left|\hat{e}\,\vec{\mu}_{ba}\right|^2 (f_b - f_a), \tag{2}$$

where ω is the frequency of the photon energy, n_r is the refractive index, c is the velocity of light, $\mathrm{g}\left(E_b - E_a - \hbar\omega\right)$ is the line shape function, e the electronic charge, μ_{ba} is the intersubband dipole moment, V is the volume of the entire material, ϵ_0 is the permittivity of the material, f_b and f_a are the carrier densities populating subbands a and b, respectively. We consider numerically calculated transition adjusted to a simple Lorentzian approximation given by

$$\mathrm{g}\left(\Delta E\right) = \frac{1}{\pi}\frac{(\Gamma/2)}{\Delta E^2 + (\Gamma/2)^2}, \tag{3}$$

where Γ is the linewidth. Therefore the modified Lorentzian approximation in terms of photon energy can be written as

$$\mathrm{g}(\Delta E - \hbar\omega) = \frac{1}{\pi}\sum_{1\neq 2}\frac{(\Gamma/2)}{(\Delta E - \hbar\omega)^2 + (\Gamma/2)^2}, \tag{4}$$

where ΔE and $\hbar\omega$ are the transition photons energy between subband $(1, 2)$ and the adjusted frequency, respectively.
However, transition $(2, 1)$ occurs at the top conduction subband corresponds to the highest subband, after photon emission with electrons being annihilated from subband $a = 1$ to $b = 2$. Therefore, setting $(\Delta E - \hbar\omega) = 0$, in (4) one gets

$$\mathrm{g} = \frac{1}{\pi}\frac{1}{(\Gamma/2)}, \tag{5}$$

where Γ is the resulting Lorentzian broadening term, which we refer as dephasing energy in the subbands. Furthermore, the dipole moment is obtained by normalization of the enveloped wavefunction along the quantum well growth direction z, which is due to the electron excitation by the light

beam this can be expressed in the form

$$\mu_{21} = e \int_0^{L_z} \psi_2(z)\, z\, \psi_1(z) dz, \tag{6}$$

where

$$\psi_1(z) = \sqrt{\frac{2}{L_z}} sin\left(\frac{\pi}{L_z} z\right) \tag{7}$$

and

$$\psi_2(z) = \sqrt{\frac{2}{L_z}} sin\left(\frac{2\pi}{L_z} z\right). \tag{8}$$

However, to solve for the intersubband dipole moment we substituted (7) and (8) into (6), we get

$$\mu_{21} = \frac{2e}{L_z} \int_0^{L_z} sin\left(\frac{2\pi}{L_z} z\right) z\, sin\left(\frac{\pi}{L_z} z\right) dz. \tag{9}$$

Integrating eq. (9) simplifies to

$$\mu_{21} = -\frac{16}{9\pi^2} e L_z. \tag{10}$$

Equation (10) is the resulting dipole moment of the quantum well. We will now analyze the absorption coefficient due to intersubband transition in quantum well of GaAs/AlGaAs. Equation (10) lead to the absorption related to absorption coefficient of the intersubband governed by

$$\alpha(\hbar\omega) = \frac{\pi\omega}{n_r\, c\, \epsilon_0} \mathrm{g}\left(\Delta E - \hbar\omega\right) |\mu_{21}|^2 \left(N_2 - N_1\right), \tag{11}$$

where N_1 and N_2 are the population densities of the 1st and 2nd subbands, respectively.

However, when $N_2 = 0$, in which $E_1 < E_F < E_2$ in subband 1, then one finds

$$\alpha(\hbar\omega) = \frac{\pi\omega}{n_r\, c\, \epsilon_0} \mathrm{g}\left(\Delta E - \hbar\omega\right) |\mu_{21}|^2 N_1, \tag{12}$$

which is proportional to doping concentration. Furthermore, with $E_2 < E_F$ in subband 2, then

$$N_1 = \frac{m_e^* k_B T}{\pi\hbar^2 L_z} \ln\left[1 + e^{\left(\frac{E_F - E_1}{k_B T}\right)}\right], \tag{13}$$

where k_B is Boltzmann's constant, T is the temperature and E_F is the Fermi energy. Equation (13), can be simplified to

$$N_1 \approx \frac{m_e^*}{\pi\hbar^2 L_z} \left(E_F - E_1\right), \tag{14}$$

and subsequently,

$$N_2 \approx \frac{m_e^*}{\pi\hbar^2 L_z} \left(E_F - E_2\right). \tag{15}$$

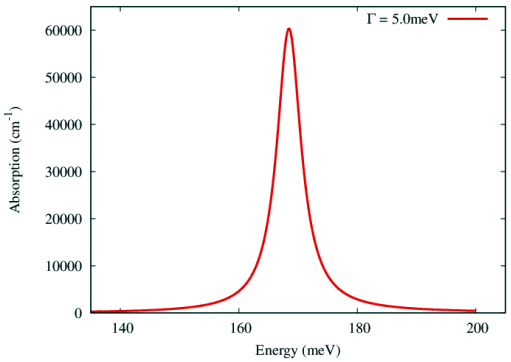

Fig. 1: Absorption spectra as a function of the incident photon energy in GaAs/AlGaAs dephasing energy $\Gamma = 5.0meV$.

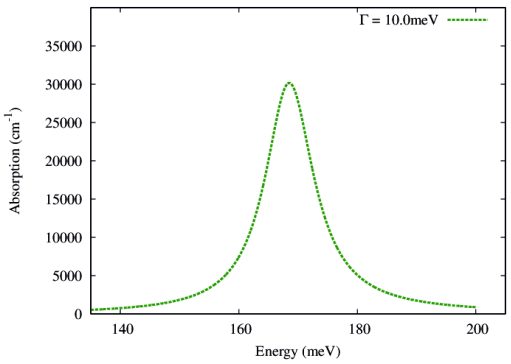

Fig. 2: Absorption coefficient against photon energy with dephasing energy $\Gamma = 10.0$ meV.

Finally, the optical absorption coefficient can be written as

$$\alpha(\hbar\omega) = \frac{\pi\omega}{n_r c \epsilon_0} \mathrm{g}\left(\Delta E - \hbar\omega\right) \left(\frac{16}{9\pi^2} e L_z\right)^2 \tag{16}$$

which is independent of doping concentration. The peak absorption is obtain where $\Delta E = \hbar\omega$ and can be expressed as

$$\alpha_{max}\left(\hbar\omega\right) = \frac{\omega}{n_r c \epsilon_0} \frac{1}{(\Gamma/2)} \left(\frac{16}{9\pi^2} e L_z\right)^2 N. \tag{17}$$

3 Results and Discussion

The result obtained for the absorption coefficient in the quantum well structure is computed and plotted using Equation (16) for 10 Å quantum well width and different dephasing energy. In figure 1, we plotted the optical absorption spectra as a function of photons energy with dephasing energy $\Gamma = 5.0$ meV. Figure 2 - 4 show absorption spectra with dephasing energies $\Gamma = 10.0$, 15.0 and 20.0 meV, respectively. In our result, one could clearly see that the absorption peaks decreases as the different dephasing energies are increase as shown in figure 5.

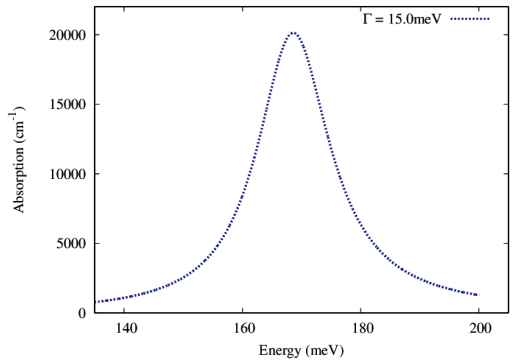

Fig. 3: Absorption coefficient against photon energy with dephasing energy $\Gamma = 15.0$ meV.

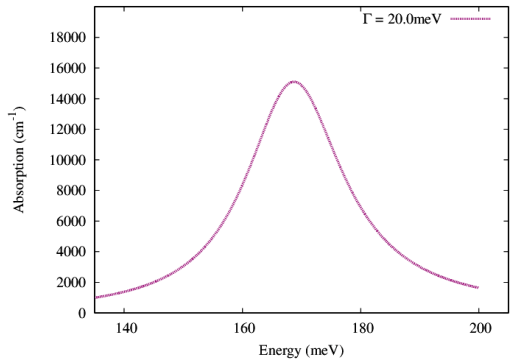

Fig. 4: Absorption coefficient as a function of the photon energy with dephasing energy $\Gamma = 20.0$ meV.

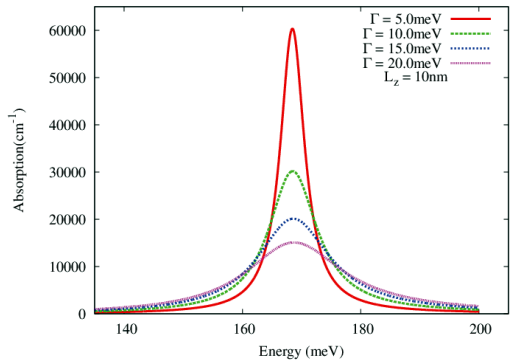

Fig. 5: Absorption coefficient as a function of the photon energy with various dephasing energy $\Gamma = 5.0, 10.0, 15.0$ and 20.0 meV and $L_z = 10$ nm.

4 Conclusion

On conclusion, we have showed the impacts of dephasing mechanism in the study of intersubbands optical absorption in GaAs/AlGaAs quantum well. Simulation results for transitions between the first two conductions subbands clearly revealed that, the optical absorption decreases with increasing the dephasing as indicated in figure 5. This effects can be controlled by adjusting the carries densities populating the lower subband or controlling the quantum well width, which will be presented in our next publications.

Acknowledgements

We are indebted to Abdullahi Mikailu for his time and assistance.

Submitted on December 23, 2018

References

1. Liu H. C., Levine B. F., Andersson J. Y. Quantum Well intersubband Transition Physics and Devices. Kluwer Academic Publishers, 1994.
2. Rybalko D. A., Ya Vinnichenko M., Vorobjev L. E., Firsov D. A., Balagula R. M., Yu Panevin V., Kulagina M. M., Vasil'iev A. P. Intersubband light absorption in tunnel-coupled GaAs/AlGaAs quantum wells for electro-optic studies, *Journal of Physics: Conference Series*, 2014, v. 541, 012081.
3. Kasapoglu E., Sari H., Sökmen I. Intersubband optical absorption in a quantum well under a tilted magnetic field. *Superlattices and Microstructures*, 2001, v. 29(1), 25–37.
4. F.D.P. Alves, G. Karunasiri, N. Hanson, M. Byloos, H.C. Liu, A. Bezinger, M. Buchanan, NIR, MWIR and LWIR quantum well infrared photodetector using interband and intersubband transitions, *Infrared Phys. Technol.*, 2007, v. 50, 182–186.
5. B.F. Levine, Quantum-well infrared photodetectors, *J. Appl. Phys.*, 1993, v. 74 (R1).
6. Gevorgyan A. H., Mamikonyan N. E., Kostanyan A. A., Kazaryan E. M. Intersubband optical absorption in GaAs parabolic quantum well due to scattering by ionized impurity centers, acoustical and optical phonons *Physica E: Low-dimensional Systems and Nanostructures*, 2018, v. 103, 246–251.
7. Shumilov A. A., Ya Vinnichenko M., Balagula R. M., Makhov I. S., Firsov D. A., Vorobjev L. E. Intersubband light absorption in double GaAs/AlGaAs quantum wells under lateral electric field, *Journal of Physics: Conference Series*, 2016, v. 690, 012017.
8. Vorobjev L. E., Danilov S. N., Titkov I. E., Firsov D. A., Shalygin V. A., Zhukov A. E., Kovsh A. R., Ustinov V. M., Ya Aleshkin V., Andreev B. A., Andronov A. A., Demidov E. V. Optical absorption and birefringence in GaAs/AlAs MQW structures due to intersubband electron transitions, *Nanotechnology*, 2000, v. 11, 218–220.
9. WU Bin-He. Transient Intersubband Optical Absorption in Double Quantum Well Structure. *Commun. Theor. Phys. (Beijing, China)*, 2005, v. 43(4), 759–764.
10. Ming, C Wu. EE 232 Lightwave Devices Lecture 9: Intersubband Absorption in Quantum Wells. University of California, Berkeley, Electrical Engineering and Computer Sciences Dept., 2008, 9–12.

The Cosmological Significance of Superluminality

Hartmut Müller

E-mail: hm@interscalar.com

The paper derives the constancy and the value of the speed of light from stability conditions in chain systems of harmonic quantum oscillators. It is also shown that these stability conditions lead to scale-invariant superluminal velocity quantization. The cosmological significance of superluminality is discussed.

Introduction

I remember well that day in 1997 when my teenage son was asking me: "Why is the speed of light so slow?"

In fact, 299792458 m/s is a very finite velocity, and it is not too high regarding even the solar system. In interstellar and intergalactic scales, it becomes obvious how disappointingly slow it really is.

One year later, reading on the pioneering research of Günter Nimtz [1], my heart started to beat faster. Already in 1992, Enders and Nimtz demonstrated that photonic tunneling proceeds at superluminal signal velocities. The signal velocity is the velocity of the transmitted cause, i.e. of the information. As they reported, no signal reshaping took place during tunneling and all frequency components were equally transmitted. Later superluminal amplitude modulated (AM) and frequency modulated (FM) microwave experiments were carried out using different photonic barriers. Mozart's 40th symphony was FM tunneled at a speed of $4.7c$ without any significant distortion [2].

Superluminal propagation of infrared pulses through periodic fiber Bragg gratings was experimentally demonstrated [3]. Velocities of nearly $3c$ were observed [4] in the propagation of electric pulses along coaxial lines having spatially periodic impedances.

Nevertheless, superluminal tunneling is still under discussion. However, while Nimtz argues with facts (measurements) for superluminal signal transmission, his opponents counter with purely theoretical approaches. One of the main counterarguments is the alleged violation of causality [5, 6].

Causality requires the existence of a maximum speed of physical interaction, but could it be that 299792458 m/s is already high enough? This is very unlikely, if we consider the unity of the universe up to scales of billions light years.

By the way, in astronomic calculations, gravitation is traditionally considered as being instantaneous. First Laplace [7] demonstrated that gravitation does not propagate with the speed of light c. Modern estimations [8] confirm a lower limit of $2 \cdot 10^{10}\, c$. Exceeding 299792458 m/s has nothing to do with time travel, grandfather paradox or any other violation of causality. This would be relevant in the case of an infinitely high velocity, but 299792458 m/s is finite.

Furthermore, the value 299792458 m/s does not follow from any established theory, and consequently, none of those theories had to be changed if the speed of light would be even 55 times higher than 299792458 m/s.

What exactly makes possible to exceed 299792458 m/s? The point is that the tunneling time does not depend on the barrier length. This was theoretically described by Thomas E. Hartman [9] in 1962. Thirty years later, the Hartman effect was demonstrated experimentally with evanescent microwaves by Enders and Nimtz [10]. Numerous studies [11] have shown that the tunneling time equals approximately the reciprocal frequency of the carrier wave, independently of the length and the type of barrier (periodic lattice structures, double prisms, undersized wave guides).

Probably, not only photons and phonons can tunnel, but also electrons [12, 13], protons [14] and atoms [15] can do it.

Is superluminality just a laboratory artefact? It is very unlikely that laboratory experiments can exceed the complexity of astrophysical phenomena. Indeed, there are superluminal processes observed in deep space.

Already in December 1901, Jacobus Kapteyn [16] reported on apparent superluminal motion in the ejecta of the nova GK Persei [17], which was discovered in February 1901 by Thomas Anderson. Superluminal motion is observed in radio galaxies, BL Lac objects, quasars, blazars and recently also in some galactic sources called microquasars [18–21]. Superluminal motion has been observed [22] in the jet of M87. Many of the jets are evidently not close to our line-of-sight. Therefore, their superluminal behavior cannot be dismissed easily as an illusion.

Within the special relativity theory, the speed of light is postulated (not derived) to be constant. Up to now, there have not been sufficiently convincing explanations why the speed of light should be constant and why it should have the value which it has.

As proposed Albrecht and Magueijo [23], the speed of light might vary with the age of the universe and it might not have been constant in early stages. They suggest that a variable speed of light might solve the horizon, flatness and cosmological constant problems. Christoph Köhn [24] proposed a 5D space parametrized with two time coordinates to explain the constancy of the speed of light in the observable universe. For very small length scales of the present universe, or for the very early universe, the model speed of light is not constant, but depends on space-time. This is consistent with

current conclusions from loop quantum gravity models [25] and the string theory [26].

In the following we will show that the constancy and the value of the speed of light can be derived from stability conditions in fractal chain systems of harmonic quantum oscillators. Furthermore, we will demonstrate that the same stability conditions lead to scale-invariant superluminal velocity quantization.

Methods

The most stable systems we know are of atomic scale. Proton and electron form stable atoms, the structural elements of matter. The lifespans of the proton and electron surpass everything that is measurable, exceeding 10^{30} years. No scientist ever witnessed the decay of a proton or an electron. Therefore, the proton-to-electron ratio 1836.152674 is considered as fundamental physical constant [27]. Well, but what is the secret of this eternal stability?

Up to now, there have not been sufficiently convincing explanations why the electron and the proton should be stable and why the proton-to-electron ratio should have exactly the value which it has. In standard particle physics, the electron is stable because it is the least massive particle with nonzero electric charge. Its decay would violate charge conservation [28]. Indeed, this answer only readdresses the question. Why then is the elementary electric charge so stable?

In a similar explanation, the proton is stable, because it is the lightest baryon and the baryon number is conserved [29]. Indeed, also this answer only readdresses the question. Why then is the proton the lightest baryon? To answer this question, the standard model introduces quarks which violate the integer quantization of the elementary electric charge that is needed to explain the stability of the electron.

In [30] we introduced fractal chain systems of harmonic quantum oscillators as model of matter and did show that frequency ratios equal to Euler's number $e = 2.718\ldots$, its integer powers and roots inhibit destructive internal resonance interaction and in this way, provide lasting stability [31].

Already Dombrowski [32] did show that irrational numbers inhibit destabilizing resonance interaction, because they cannot be represented as ratios of whole numbers. Though, algebraic irrational numbers like $\sqrt{2}$ do not compellingly prevent resonance, because they can be transformed into rational numbers by multiplication.

Surprisingly, only Euler's number inhibits resonance also regarding all derivatives of the bound periodic processes, because it is the basis of the real exponential function e^x, the only function that is the derivative of itself. Furthermore, Euler's number, its integer powers and roots are always transcendental [33] and therefore, they provide the solution for lasting stability in chain systems of any degree of complexity.

Many physical characteristics of harmonic quantum oscillators are connected with their frequency by the fundamental constants – the speed of light and the Planck constant. Therefore, within our model, Euler's number, its integer powers and roots define also the ratios of wavelengths, velocities, impulses, accelerations and energies which inhibit resonance interaction, and in this way, support lasting stability of the chain system.

This is why we expect that stable quantum systems show ratios of their physical quantities close to integer powers of Euler's number and its roots. Consequently, the natural logarithms of the ratios should be close to integer 0, 1, 2, 3, 4, ... or rational values $\frac{1}{2}, \frac{1}{3}, \frac{1}{4}, \ldots$ In fact, the natural logarithm of the proton-to-electron ratio is close to seven and a half:

$$\ln(1836.152674) = 7.515427\ldots \simeq 6 + \frac{3}{2}.$$

Already in the eighties the scaling exponent 3/2 was found in the distribution of particle masses by Valery Kolombet [34]. Applying hyperscaling [30] by Euler's number (tetration), we get the next approximation of the logarithm of the proton-to-electron ratio:

$$6 + \frac{e^e}{10} = 7.515426\ldots$$

This result supports our assumption that the stability of the proton and electron comes from the transcendence of Euler's number, its integer powers and roots. In this way, the proton mass appears as scaled up by Euler's number and its roots electron mass.

In [35] we have analyzed the mass distribution of hadrons, mesons, leptons, the W/Z and Higgs bosons and proposed fractal scaling by Euler's number and its roots as model of particle mass generation [36]. In this model, the W-boson mass 80385 MeV/c^2 and the Z-boson mass 91188 MeV/c^2 appear as the 12 times scaled up by Euler's number electron rest mass 0.511 MeV/c^2:

$$\ln\left(\frac{80385}{0.511}\right) = 11.97, \qquad \ln\left(\frac{91188}{0.511}\right) = 12.09.$$

Andreas Ries [37] did apply fractal scaling by Euler's number to the analysis of atomic masses and demonstrated that this method allows for the prediction of the most abundant isotopes.

In comparison to dimensionless constants like the proton-to-electron ratio, conversion constants define dimensional ratios. For instance, the Planck constant defines the energy one must invest to generate a harmonic quantum oscillation of a given frequency, and the speed of light defines the propagation space of such an oscillation.

Like one can measure distances in units of time, for example in light years, energy can be measured in units of frequency. Only the dimensions are different.

In this way, we can interpret the speed of light as fundamental space – time converter, the square of the speed of light as fundamental mass – energy converter and the Planck

DIMENSIONS	CONVERSION CONST.	VALUE
space – time	$\lambda / \tau = c$	299792458 m/s
energy – mass	$E / m = c^2$	$8.9875518 \cdot 10^{16}$ m^2/s^2
energy – time	$E \cdot \tau = \hbar$	$1.0545718 \cdot 10^{-34}$ Js
energy – space	$E \cdot s = \hbar \cdot c$	$3.1615267 \cdot 10^{-26}$ Jm
mass – space	$m \cdot s = \hbar / c$	$3.5176729 \cdot 10^{-43}$ kgm
mass – time	$m \cdot \tau = \hbar / c^2$	$1.1733694 \cdot 10^{-51}$ kgs

Table 1: Some fundamental conversion constants (c is the speed of light in a vacuum, $\hbar$ is the Planck constant). Data taken from Particle Data Group [27].

constant as fundamental time – energy converter. Some fundamental conversion constants are shown in table 1.

Table 1 is completely compatible with Planck units. Originally proposed in 1899 by Max Planck, they are also known as natural units, because they origin only from properties of nature and not from any human construct. Natural units are based only on the properties of space-time. Max Planck wrote [38] that these units, "regardless of any particular bodies or substances, retain their importance for all times and for all cultures, including alien and non-human, and can therefore be called natural units of measurement".

In [39] was demonstrated that the natural logarithm of the Planck-to-proton mass ratio equals 44. Consequently, one can define a dimensionless fundamental constant that equals to an integer power of Euler's number and contains the speed of light c, the Planck constant $\hbar$, the gravitational constant G and the proton rest mass m_p:

$$\frac{\hbar \cdot c}{G \cdot m_p^2} = e^{88}.$$

For the speed of light, now we can write:

$$c = c_0 \cdot e^{88},$$

where $c_0 = Gm_p^2/\hbar \simeq 1.8 \cdot 10^{-30}$ m/s can be interpreted as the velocity of free falling on each other proton masses at Planck length and Planck time. Assumed that the stability of any fundamental constant origins from Euler's number and its roots, we can generalize:

$$c_{n,m} = c \cdot e^{n/m},$$

where n, m are integer numbers. In general, the rational exponent is represented by finite continued fractions [30, 40]. The exponents n/m define a fractal set of stable velocities $c_{n,m}$ which are superluminal for $n > 0$.

In the following, we will verify the fractal set $c_{n,m}$ of stable subluminal and superluminal velocities on experimental and astrophysical data.

Results

Let us start with experimental data elaborated by Nimtz [1] in 1998, the barrier traversal time of a microwave packet through a multilayer structure inside a waveguide was measured. The center frequency has been 8.7 GHz. The tunneled signal traversed a 114.2 mm long barrier in 81 ps, whereas the signal spent 380 ps to cross the same air distance. Consequently, the group velocity of the tunneled signal was c (380/81) = $4.7c$ that is close to $c_{3,2} = c \cdot e^{3/2} = 4.5c$.

Already in 1995 a similar experiment was carried out by Aichmann et al. [41]. They modulated Mozart's 40th symphony on a microwave carrier. The modulation of the signal and thus the music traveled at the same superluminal velocity.

In another setup [42], amplitude modulated 9.15 GHz microwaves were generated by a synthesized sweeper, and a parabolic antenna transmitted parallel beams. The propagation time of the signal was measured across the air distance between transmitter and receiver and across the same distance but partially filled with a 28 cm long barrier of quarter wavelength slabs made of acrylic perspex. Each slab was 0.5 cm thick and the distance between two slabs was 0.85 cm. Two such structures were separated by an air distance of 18.9 cm forming a resonant tunneling structure. The signal tunneled the 28 cm long barrier in 125 ps that corresponds to a signal velocity of $7.5c$ that is close to $c_{2,1} = c \cdot e^2 = 7.3c$.

Mojahedi et al. [43] describe an experiment with single microwave pulses centered at 9.68 GHz. The signals tunneled through a one-dimensional photonic crystal with up to $2.5c$ that is close to $c_{1,1} = c \cdot e = 2.7c$. Hache et al. [4] studied the propagation of brief electric 10 MHz pulses along a coaxial line having a spatially periodic impedance. As well, signal velocities approximating $c_{1,1} = 2.7c$ were measured.

Remarkably, the same superluminal velocities were measured also by Hubble telescope observation. Superluminal motion at velocities close to $c_{1,1} = 2.7c$ was found [22] in two small features within the jet knot D about 200 pc from the nucleus of M87, the giant elliptical galaxy near the center of the Virgo Cluster. As well, the jet features DE and DW show velocities close to $c_{1,1} = 2.7c$, while the features DM, DE-W, HST-1α, HST-1γ, HST-1δ, HST-1ϵ and HST-2 show velocities close to $c_{3,2} = 4.5c$.

Other active galactic nuclei (AGN) show the same velocities of superluminal motion. Lister et al. [21] describe the parsec-scale kinematics of 200 different AGN jets based on 15 GHz VLBA data. Various components of the sources 0003+380, 0003-060, 0010+405 show velocities that approximate $c_{1,1} = 2.7c$ or $c_{3,2} = 4.5c$ or $c_{2,1} = 7.3c$.

Jorstad et al. [20] monitored the radio emissions in 42 gamma-ray bright blazars (31 quasars and 11 BL Lac objects) with the Very Long Baseline Array (VLBA) at 43, 22, 15 and 8.4 GHz and found superluminal motions with velocities approximating $c_{1,1} = 2.7c$ or $c_{3,2} = 4.5c$ or $c_{2,1} = 7.3c$ or $c_{5,2} = 12c$ or $c_{3,1} = 20c$ or $c_{7,2} = 33c$ respectively.

Now let us continue with astrophysical data of stable subluminal processes. In [30] we have analyzed the orbital velocities of large bodies in the solar system. For instance, the orbital velocity of Mercury oscillates between two points of Euler stability $c_{-17,2}$ = 61 km/s (perihelion) and $c_{-9,1}$ = 37 km/s (aphelion). The orbital verlocity of Venus is close to $c_{-9,1}$ = 37 km/s. Earth's orbital verlocity is close to $c_{-37,4}$ = 29 km/s. The orbital verlocity of Mars is between 21.97 and 26.50 km/s, approximating $c_{-19,2}$ = 22.4 km/s. Jupiter's orbital velocity is between 12.44 and 13.72 km/s, approximating $c_{-10,1}$ = 13.6 km/s. Saturn's orbital verlocity is between 9.09 and 10.18 km/s, approximating $c_{-31,3}$ = 9.8 km/s. The orbital verlocity of Uranus is between 6.49 and 7.11 km/s, approximating $c_{-32,3}$ = 7 km/s. Neptune's orbital verlocity is close to $c_{-11,1}$ = 5 km/s. Pluto's orbital verlocity oscillates between 6.10 and 3.71 km/s, approximating the same $c_{-11,1}$ = 5 km/s. By the way, the same velocities are typical for underground propagation of seismic P-waves [44].

Within our model, the quantized orbital velocities in the solar system are velocities of free fall, scaled up by Euler's number and its roots from the velocity of free falling on each other proton masses at Planck length and Planck time. The stability [45] of the orbital system origins from the transcendence of Euler's number, its integer powers and roots. In this way, Euler's number, its integer powers and roots define fractal sets of quantized subluminal and superluminal velocities established by stable periodical processes.

Conclusion

The worldwide-reproduced tunneling experiments show convincingly that the conditions required for superluminal signal transmission are not exotic. Therefore, it is possible to imagine that those conditions can emerge also in nature. For the same reason, the probability is quite high that conditions for superluminality can emerge in deep space, and this is already suggested by astrophysical observations.

Our model [30] of matter as fractal chain system of harmonic quantum oscillators suggests that stable processes establish subluminal or superluminal velocities corresponding to the speed of light scaled by integer powers of Euler's number and its roots. This circumstance could affect estimations of intergalactic distances and the meaning of the cosmic light horizon. Superluminal propagation of light and matter suggests the existence of cosmic superluminal horizons with a scale-invariant exponential distribution that follows the sequence of multiples of Euler's number.

In [31] we have discussed the cosmological significance of global scaling [46] and the stabilizing function of Euler's number regarding the apparent distances between the stars and galaxies.

The concept of process stability based on the avoidance of destructive resonance interaction provided by the transcendence of Euler's number and its roots, allowed us to derive the constancy and the value of the speed of light. Deriving the speed of light from the velocity of free falling on each other proton masses at Planck length and Planck time, perhaps we can reach a better understanding of gravitation and its sheer infinite velocity.

Acknowledgements

The author is grateful to Viktor Panchelyuga, Oleg Kalinin, Alexey Petrukhin and Leili Khosravi for valuable discussions.

Submitted on January 11, 2019

References

1. Nimtz G. Superluminal Signal Velocity. arXiv: physics/9812053v1 [physics.class-ph], (1998).
2. Nimtz G. *Prog. Quantum Electron.*, 2003, v. 27, 417.
3. Longhi S. et al. Measurement of superluminal optical tunneling times in double-barrier photonic band gaps. *Phys. Rev. E*, 2002, v. 65(4), 046610 // arXiv:physics/0201013.
4. Hache A., Poirier L. Long-range superluminal pulse propagation in a coaxial photonic crystal. *Applied Physics Letters*, 2002, v. 80(3), 518.
5. Nimtz G., Haibel A. Basics of Superluminal Signals. *Ann. Phys.* (Leipzig), 2002, v. 9(1), 1–5, arXiv: physics/0104063v1 [physics.class-ph] (2001).
6. Nimtz G. Superluminal Signal Velocity and Causality. *Foundations of Physics*, 2004, v. 34(12), 1889–1903.
7. Laplace P. Mechanique Celeste. 1825, pp. 642–645.
8. Van Flandern T. The Speed of Gravity – What the Experiments Say. *Physics Letters A*, 1998, v. 250, 1–11.
9. Hartman T. E. Tunneling of a wave packet. *Journal of Applied Physics*, 1962, v. 33(12), 3427.
10. Enders A., Nimtz G. Evanescent-mode propagation and quantum tunneling. *Physical Review E*, 1993, v. 48(1), 632–634.
11. Nimtz G. Tunneling Violates Special Relativity. arXiv: 1003.3944v1 [quant-ph], (2010).
12. Sekatskii S.K., Letokhov V. S. Electron tunneling time measurement by field-emission microscopy. *Phys. Rev. B*, 2001, v. 64, 233311.
13. Eckle P. et al. Attosecond Ionization and Tunneling Delay Time Measurements in Helium 2008. *Science*, 2008, v. 322, 1525.
14. Tuckerman M. E., Marx D. Heavy-Atom Skeleton Quantization and Proton Tunneling in Intermediate-Barrier Hydrogen Bonds. *Phys. Rev. Lett.*, 2001, v. 86(21), 4946–4949.
15. Lauhon L.J., Ho W. Direct Observation of the Quantum Tunneling of Single Hydrogen Atoms with a Scanning Tunneling Microscope. *Phys. Rev. Lett.*, 2000, v. 85, 4566.
16. Kapteyn J.C. Über die Bewegung der Nebel in der Umgebung von Nova Persei. *Astronomische Nachrichten*, 1901, v. 157(12), 201.
17. Shara M.M. et al. GK Per (Nova Persei 1901): HST Imagery and Spectroscopy of the Ejecta, and First Spectrum of the Jet-Like Feature. arXiv: 1204.3078v1 [astro-ph.SR] (2012).
18. Levinson A., Blandford R. On the Jets associated with galactic superluminal sources. arXiv: astro-ph/9506137v1, (1995).
19. Brunthaler A. et al. III Zw 2, the first superluminal jet in a Seyfert galaxy. arXiv: astro-ph/0004256v1, (2000).
20. Jorstad S.G. et al. Multiepoch Very Long Baseline Array Observations of Egret-Detected Quasars and BL Lacertae Objects: Superluminal Motion of Gamma-Ray Bright Blazars. *The Astrophysical Journal Supplement Series*, 2001, v. 134, 181–240.

21. Lister M.L. et al. MOJAVE X. Parsec-Scale Jet Orientation Variations and Superluminal Motion in AGN. arXiv: 1308.2713v1 [astro-ph.CO], (2013).
22. Biretta J.A., Sparks W.B., Macchetto F. Hubble Space Telescope Obesrvations of Superluminal Motion in the M87 Jet. *The Astrophysical Journal*, 1999, v. 520, 621–626.
23. Albrecht A., Magueijo J. A Time Varying Speed of Light as a Solution to Cosmological Puzzles. *Physical Review D*, 1999, v. 59(4), 043516.
24. Köhn C. The Planck length and the constancy of the speed of light in five dimensional space parametrized with two time coordinates. arXiv: 1612.01832v2 [physics.gen-ph], (2017).
25. Kiritsis E. Supergravity, D-brane Probes and thermal super Yang-Mills: a comparison. *Journal of High Energy Physics*, 1999, v. 9910(10).
26. Alexander S. On the varying speed of light in a brane-induced FRW Universe. *Journal of High Energy Physics*, 2000, v. 0011(17).
27. M. Tanabashi et al. (Particle Data Group), *Phys. Rev. D*, 2018, v. 98, 030001. www.pdg.lbl.gov
28. Steinberg R. I. et al. Experimental test of charge conservation and the stability of the electron. *Physical Review D*, 1999, v. 61(2), 2582–2586.
29. Nishino H. et al. Search for Proton Decay in a Large Water Cherenkov Detector. *Physical Review Letters*, 2009, v. 102(14), 141801, arXiv: 0903.0676.
30. Müller H. Scale-Invariant Models of Natural Oscillations in Chain Systems and their Cosmological Significance. *Progress in Physics*, 2017, v. 13, 187–197.
31. Müller H. On the Cosmological Significance of Euler's Number. *Progress in Physics*, 2019, v. 15, 17–21.
32. Dombrowski K. Rational Numbers Distribution and Resonance. *Progress in Physics*, 2005, v. 1, no. 1, 65–67.
33. Hilbert D. Über die Transcendenz der Zahlen e und π. *Mathematische Annalen*, 1983, v. 43, 216–219.
34. Kolombet V. Macroscopic fluctuations, masses of particles and discrete space-time, *Biofizika*, 1992, v. 36, 492–499.
35. Müller H. Fractal Scaling Models of Natural Oscillations in Chain Systems and the Mass Distribution of Particles. *Progress in Physics*, 2010, v. 6, 61–66.
36. Müller H. Emergence of Particle Masses in Fractal Scaling Models of Matter. *Progress in Physics*, 2012, v. 8, 44–47.
37. Ries A. Qualitative Prediction of Isotope Abundances with the Bipolar Model of Oscillations in a Chain System. *Progress in Physics*, 2015, v. 11, 183–186.
38. Max Planck. Über Irreversible Strahlungsvorgänge. *Sitzungsbericht der Königlich Preußischen Akademie der Wissenschaften*, 1899, vol. 1, 479–480.
39. Müller H. Gravity as Attractor Effect of Stability Nodes in Chain Systems of Harmonic Quantum Oscillators. *Progress in Physics*, 2018, v. 14(1), 19–23.
40. Panchelyuga V.A., Panchelyuga M.S. Resonance and Fractals on the Real Numbers Set. *Progress in Physics*, 2012, v. 8, no. 4, 48–53.
41. Aichmann H., Nimtz G., Spieker H. Verhandlungen der Deutschen Physikalischen Gesellschaft. v. 7, 1258, (1995).
42. Nimtz G. Superluminal Tunneling Devices. arXiv: physics/0204043v1 [physics.gen-ph], (2002).
43. Mojahedi M. et al. Time-domain detection of superluminal group velocity for single microwave pulses. *Phys. Rev. E*, 2000, v. 62(4), 5758–5766 .
44. Müller H. Quantum Gravity Aspects of Global Scaling and the Seismic Profile of the Earth. *Progress in Physics*, 2018, v. 14, 41–45.
45. Müller H. Global Scaling of Planetary Systems. *Progress in Physics*, 2018, v. 14, 99–105.
46. Müller H. Global Scaling. The Fundamentals of Interscalar Cosmology. *New Heritage Publishers*, Brooklyn, New York, USA, (2018).

Fermi Scale and Neutral Pion Decay

Paulo Roberto Silva

Departmento de Física (Retired Associate Professor), ICEx, Universidade Federal de Minas Gerais, Belo Horizonte, MG, Brazil.
E-mail: prsilvafis@gmail.com

A modified Fermi coupling of the weak interactions is proposed and in analogy with the Planck units, a Fermi scale is defined. We define a second Fermi length, a Fermi mass (related to the threshold energy for unitarity), and a Fermi time. The holographic principle (HP) is then applied to some two-dimensional objects, where the unit cell size is given by the second Fermi length. With the aid of non-linear Dirac equation, a formula is obtained relating the Fermi, the nucleon, and the electron masses. Another relationship is found, linking the second Fermi length to cosmological constant and Planck scales. Finally HP in 2-d is employed in a stationary condition for the free energy, as a means to evaluate the neutral pion decay time.

1 Introduction

Once fixed the separation of them, the gravitational interaction between two particles of equal masses goes with the product of the Newton's gravitational constant G times the mass squared. Analogously, the electrostatic interaction of two equal charges is given by the product of the K_e-constant, let us call it the Coulomb constant, times the electric charge squared.

In quantum mechanics (QM) or in quantum field theory (QFT), by considering for instance only the absolute value of the proton-electron attraction in the hydrogen atom, it is convenient to write

$$K_e e^2 = \alpha \hbar c. \tag{1}$$

In (1) we have: e the quantum of elementary electric charge, $\hbar$ the reduced Planck constant, c the speed of light in vacuum, and α is the electromagnetic coupling strength. Relation (1) can be translated to the gravitational interaction case and takes the form

$$GM^2 = \alpha_g \hbar c. \tag{2}$$

According to the QFT the couplings are running with the energy [1], and we may define an energy (mass) scale such that we have $\alpha_g = 1$ [2]. We call this mass the Planck mass, and using the value $\alpha_g = 1$ in (2), we obtain

$$M_{Pl} = \sqrt{\frac{\hbar c}{G}}\,. \tag{3}$$

The Compton length of a particle with the Planck mass gives the Planck length, and the Planck time can be also defined by using c. We have

$$L_{Pl} = \frac{\hbar}{M_{Pl}\, c} = \sqrt{\frac{\hbar G}{c^3}}\,, \tag{4}$$

$$t_{Pl} = \frac{L_{Pl}}{c} = \sqrt{\frac{\hbar G}{c^5}}\,. \tag{5}$$

An alternative way to obtain the Planck scale (units) is to compare the Compton length of a particle with its Schwarzschild radius [3]. As is posted in Wikipedia [4]:

"Originally proposed by the German physicist Max Planck, these units are also known as natural units because the origin of their definition comes only from properties of fundamental physics theories and not from interchangeable experimental parameters."

The idea of the Planck length as being the minimal length (related to a discreteness of the space-time?), was first proposed by C.A. Mead [5,6]. The difficulty to publish his results is commented by Mead [8] and also highlighted by Sabine Hossenfeld [9], in a more recent essay.

In reference [10], the Fermi coupling constant G_F was used as a means to estimate the muon decay time. The way of using G_F in those calculations resembles the employment of Newton gravitational constant G in the Newtonian mechanics. This has inspired the present author to look at the possibility of defining a Fermi scale (units) in an analogous way as the Planck's case (relations (3) to (5) of this work). Indeed in a recent paper [11], Roberto Onofrio conjectured that weak interactions could be a manifestation of gravity when investigated through high energy probes (short distances).

In section 2, we use estimates of G_F quoted in the literature, in order to evaluate numerically the principal Fermi units, namely the second Fermi length, the Fermi mass (the second Fermi energy), and the Fermi time. The second Fermi length is named this way, to avoid confusion with the usual Fermi length related to the electrical conductivity of metals, for instance.

In section 3, we use the Holographic Principle (HP) in two dimensions (2-d) plus a simple Dirac- like equation, besides a relation connecting the wave function to the entropy, as a means to obtain a closed relation encompassing the Fermi, the electron and the nucleon masses.

In section 4, the HP in 2-d is used again, relating the second Fermi length to a length related to the cosmological constant [12], the Planck length and the electromagnetic coupling α.

Section 5 provides an estimate of the neutral pion radius.

In section 6, the HP in 2-d is used to evaluate the neutral pion decay time.

Finally section 7 is reserved for the concluding remarks.

2 The Fermi scale (units)

In reference [10], the muon decay time was estimated starting from the relation

$$m_\mu c^2 = \frac{1}{R_W}\frac{G_F\, c^2}{h^2} m_\mu^2. \tag{6}$$

In (6) m_μ is the muon mass, G_F is the Fermi constant of the weak interactions and R_W is the weak radius of the muon. We observe from an inspection of (6) that it is possible to define a modified Fermi constant G_F^*, namely

$$G_F^* = \frac{G_F\, c^2}{h^2}. \tag{7}$$

It is convenient to write the "inverse transform" of (7) as

$$G_F = G_F^* \frac{h^2}{c^2}. \tag{8}$$

We will call (8): all-classic to quantum relativistic transmutation. The reason to do so is: G_F^* could in principle to exist in the realm of the classical mechanics, while G_F only makes sense in a quantum relativistic treatment. Observe that given a finite G_F^*, G_F vanishes if $h \to 0$, or if $c \to \infty$, and naturally when both things happen. As can be verified in (6) and (7) G_F^* behaves for the weak interactions as G works in the case of the Newton's gravitational theory. As weak interactions are non- linear interactions, it is possible to write a set of equations similar to Einstein equations, putting in those equations G_F^* in the place of G.

The Schwarzschild-like metric for these equations gives the Weak-Schwarzschild radius R_{WS}. Here we apply this recipe to a particle with the muon mass. We have

$$R_{WS} = \frac{2\, G_F^*\, m_\mu}{c^2} = 2\, R_W. \tag{9}$$

Substituting (7) into (9), we get

$$R_{WS} = \frac{2\, G_F\, m_\mu}{h^2}. \tag{10}$$

The establishment of a modified Fermi coupling, namely G_F^* (please see (7)) permit us immediately to define the Fermi scale (units) in analogous way we have proceed in the Planck scale case. Therefore taking in account relations (3) to (5) we can write

$$M_F = \sqrt{\frac{\hbar\, c}{G_F^*}}, \tag{11}$$

$$L_{SF} = \frac{\hbar}{M_F\, c} = \sqrt{\frac{\hbar\, G_F^*}{c^3}}, \tag{12}$$

$$t_F = \frac{L_{SF}}{c} = \sqrt{\frac{\hbar\, G_F^*}{c^5}}. \tag{13}$$

With respect to (11) we notice that as is discussed on page 526 of the book by Rohlf [13], in a modern description of the weak interactions, the weak coupling constant is running with the energy of the probe used to measure it. According to Rohlf [13], "The weak interaction rate cannot increase forever with increasing energy. At some very large energy, this would violate conservation of probability or unitarity. Unitarity is violated at the energy where the weak coupling becomes unity." In the present treatment this happens just at the energy scale given by the Fermi mass (M_F).

In order to estimate the quantities (11) to (13), related to the Fermi scale of length, let us take the value of G_F as quoted in the book by Rohlf (formula 18.33, page 509).

$$G_F = 8.96 \times 10^{-8}\ \text{GeV fm}^3. \tag{14}$$

By using (7), we have

$$G_F^* = 2.94 \times 10^{21}\ \text{Nm}^2/\text{kg}^2. \tag{15}$$

Substituting G_F^* given by (15) into relations (11) to (13), we find

$$M_F \cong 1.84\ \text{TeV/c}^2. \tag{16}$$

$$L_{SF} \cong 1.07 \times 10^{-19}\ \text{m}, \tag{17}$$

$$t_F \cong 3.57 \times 10^{-28}\ \text{s}. \tag{18}$$

3 Deducing the Fermi mass

In this section it is proposed that the Fermi mass can be deduced by considering the holographic principle (HP) in 2-d, plus a non-linear Dirac-like equation (NLDE). A formula relating an entropy estimate via HP in 2-d and the wave function evaluated in the NLDE is considered. We are inspired in the neutron weak decay given a proton, an electron and a neutrino.

Inspired in McMahon [14], the holographic principle in 2-d can be stated as

- The total information content of a 2-d universe, in this case a spherical surface of radius R_x, can be registered in the perimeter of one of its maximum circles.
- The boundary of this spherical surface, here the perimeter of its maximum circle, contains at most a single degree of freedom per unit cell length.

Making the requirement that the radius R_x coincides with the Compton wavelength of the nucleon λ_n and choosing the unit cell size as L_{SF}, we can write

$$S_1 = \frac{\pi\, \lambda_n}{L_{SF}}. \tag{19}$$

Meanwhile, let us consider the non-linear Dirac-like equation

$$\frac{\delta\phi}{\delta x} - \frac{1}{c}\frac{\delta\phi}{\delta t} = \frac{1}{\lambda_e}\phi - \frac{1}{\lambda_n}\phi^3. \tag{20}$$

In (20) λ_e stands for the Compton wavelength of the electron and the equation (20) is conceived within the structure of an abelian field theory. However in a paper dealing with the proton-electron mass ratio [15], a π-factor has appeared in an equation in order to take in account the curvature of the space due to the non-abelian character of the QCD. Therefore let us define

$$\phi = \pi\,\Psi. \tag{21}$$

Inserting (21) into (20), we look for the zero of the equation and we find

$$\Psi^2 = \frac{\lambda_n}{\pi^2\,\lambda_e}. \tag{22}$$

Now we combine the results of (19) and (22), but considering the possibility of an implicit spin-1 boson being at work. We write

$$3\,S_1\,\Psi^2 = 1. \tag{23}$$

The insertion of (19) and (22) into (23) gives

$$\lambda_n^2 = \frac{\pi}{3} L_{SF}\,\lambda_e. \tag{24}$$

Remembering that ($\hbar$ = c = 1)

$$\lambda_n = \frac{1}{m_n}, \quad \lambda_e = \frac{1}{m_e}, \quad L_{SF} = \frac{1}{M_F},$$

we finally obtain

$$3\,M_F\,m_e = \pi m_n^2. \tag{25}$$

Putting numbers in (25), we get

$$M_F \cong 1.8\ \mathrm{TeV/c^2}. \tag{26}$$

As we can see, the value here deduced for the Fermi mass, is very close to that obtained through of the use of the measured value of G_F displayed in (16).

4 Deducing the second Fermi length – II

In a previous section a modified Fermi coupling, G_F^*, was defined and we found that a Fermi scale could be constructed in analogy with the well-established Planck scale. Here we pursue another path towards the deducing o f the second Fermi length. The role played by relic neutrinos in cosmology and its possible connection with the cosmological constant problem [16,17], stimuli us to seek for a relationship between L_{SF} and R_Λ. Indeed according Cohen, Kaplan and Nelson [18], R_Λ may be thought as a geometric average between the ultraviolet (L_{Pl}) and the infrared (R_U) cut-offs of the gravitational interaction.

Meanwhile, although matter is globally electrically neutral, may be some connection to exist between charges fluctuations and the weak coupling. In this section we also intend to tie the Fermi scale L_{SF} to a new scale R_α, related to the electromagnetic coupling. Next we define R_α. We write

$$G\,M_\alpha^2 = \alpha^2\,\hbar\,c. \tag{27}$$

By taking $\hbar = c = 1$, we get from (27)

$$M_\alpha = \frac{\alpha}{\sqrt{G}}. \tag{28}$$

Based on (28) we take R_α as

$$R_\alpha = \frac{1}{M_\alpha} = \frac{L_{Pl}}{\alpha}. \tag{29}$$

Now let us consider a spherical surface universe of radius L_{SF}. We apply The HP in 2-d to it, which unit cell size of its maximum circle's perimeter is given by R_α, and we get the entropy S_2

$$S_2 = \frac{2\,\pi\,L_{SF}}{R_\alpha} = \frac{2\,\pi\,\alpha\,L_{SF}}{L_{Pl}}. \tag{30}$$

Turning to the relationship connecting the L_{SF} and the R_α scales, we may write the non-linear Dirac equation

$$\frac{\delta\Psi}{\delta x} - \frac{1}{c}\frac{\delta\Psi}{\delta t} = \frac{1}{R_\Lambda}\Psi - \frac{1}{L_{SF}}\Psi^3. \tag{31}$$

Looking at the zero of (31), we get

$$\Psi^2 = \frac{L_{SF}}{R_\Lambda}. \tag{32}$$

Now we make the requirement that

$$S_2\,\Psi^2 = 1 \tag{33}$$

and we find

$$L_{SF}^2 = \frac{R_\Lambda\,L_{Pl}}{2\,\pi\,\alpha}. \tag{34}$$

To numerically evaluate (34), we consider $R_\Lambda = \sqrt{L_{Pl}\,R_U}$ with $L_{Pl} = 1.6162 \times 10^{-35}$ m and $R_U = 0.8 \times 10^{26}$ m [19], which yields

$$L_{SF} \cong 1.12 \times 10^{-19}\ \mathrm{m}. \tag{35}$$

As can be verified, this value is close to that experimentally determined (please see equation (17)).

5 The pion radius

In a paper dealing with the quark confinement related to the metric fluctuations [20], we have estimated a string constant K given by

$$K = \frac{m_q^2\,c^3}{\alpha_s\,\hbar} = \frac{m_q^2}{\alpha_s}, \quad (\hbar = c = 1). \tag{36}$$

In (36) the symbols m_q and α_s, stand for the quark constituent mass and the strong coupling, respectively. Now let us take

$$K\,2\,R_\pi = m_\pi, \quad m_q = \frac{1}{2}m_\pi. \tag{37}$$

Combining the results of (36) and (37) and taking $\alpha_s \cong 1/3$ (please see ref. [21]), we obtain for the pion radius (being m_π the neutral pion mass)

$$R_\pi = \frac{2\,\alpha_s}{m_\pi} \cong \frac{2}{3\,m_\pi}. \tag{38}$$

Putting numbers in (38), we get

$$R_\pi \cong 0.98 \times 10^{-15} \text{ m} = 0.98 \text{ fm}. \tag{39}$$

6 Neutral pion lifetime from the holographic principle in 2-d

Let us consider the neutral pion decay, represented by the reaction

$$\pi^0 \to 2\,\gamma. \tag{40}$$

Taking in account the stationary condition for the free energy ($\Delta F = 0$), we get

$$\Delta U = T\,\Delta S. \tag{41}$$

Next we consider a 2-d universe, represented by a spherical surface of radius R_π and the entropy variation represented by the information contained on its maximum-circle perimeter, having a unit cell size equal to $2\,L_{SF}$. We can write

$$\Delta U = \frac{\alpha\,\hbar\,c}{R_\pi}, \quad \Delta S = \frac{\pi\,R_\pi}{L_{SF}}. \tag{42}$$

Besides this we consider

$$h\,\nu = \frac{h}{\tau} = T, \quad (k_B = 1). \tag{43}$$

Inserting the results of (42) and (43) into (41) and solving for τ, we obtain the neutral pion decay time given by

$$\tau = \frac{2\,\pi^2\,R_\pi^2}{\alpha\,c\,L_{SF}}. \tag{44}$$

Putting numbers in (44) we get

$$\tau_{estimated} = 0.81 \times 10^{-16} \text{ s}. \tag{45}$$

This value may be compared with [22]

$$\tau_{measured} = 0.84 \times 10^{-16} \text{ s}. \tag{46}$$

7 Concluding remarks

The estimate of the neutral pion decay time is usually obtained through the employment of the current algebra calculations. Partial conservation of the axial current (PCAC) prediction gives

$$\frac{h}{\tau} = \Gamma(\pi^0 \to 2\gamma) = \frac{\alpha^2\,m_\pi^3}{64\,\pi^3\,f_\pi^2}. \tag{47}$$

In the present paper, by using the concepts of the second Fermi length and the Hp in 2-d, we found a novel way to look at the neutral pion decay.

Meanwhile, Roberto Onofrio [11] conjectured that weak interactions should be considered as empirical evidences of quantum gravity at the Fermi scale. The "second" Fermi length estimated by Onofrio ($\sim 10^{-18}$ m) [11], is approximately one order of magnitude greater than that obtained in section 2 of this work. This comes from the fact that Onofrio used the expectation value of the Higgs field to fix the Fermi scale of energy, instead the unitary scale threshold we have used in the present work.

Submitted January 6, 2019

References

1. Kane G.L. Modern Elementary particle Physics, Addison-Wesley, (1994).
2. Silva P.R. arXiv: 0910.5747v1, (2009).
3. Roos M. Introduction to Cosmology, pp. 50, Wiley, 1995.
4. Wikipedia contributors, "Planck units", Wikipedia, The Free Encyclopedia, 18 Sep. 2015.
5. Mead C.A. *Phys. Rev. B*, 1964, v. 135, 849.
6. Mead C.A. *Phys. Rev.*, 1966, v. 143, 990.
7. Peres A., Rosen N. *Phys. Rev.*, 1960, v. 118, 335.
8. Mead C.A. *Physics Today*, 2001, v. 54(11), 15.
9. Hossenfeld S. `backreaction.blog.spot.com.br/2012/01/Planck_length_as_minimal_length.html`
10. Silva P.R. Weak Interactions Made Simple. viXra:1210.0014, (2012).
11. Onofrio R. On weak interactions as short-distance manifestations of gravity. arXiv:1412.4513v1[hep-ph], (Dec. 2014).
12. Silva P.R. arXiv: 0812.4007v1 [gr-qc], (Dec. 2008).
13. Rohlf J.W. Modern Physics from α to Z^0. Wiley, (1994).
14. McMahon D. String Theory Demystified. McGraw-Hill, (2009).
15. Silva P.R. Proton-electron mass ratio: a geometric inference. viXra:1312.0060, (2013).
16. Silva P.R. Weak Interaction and Cosmology. arXiv:0804.2683v1 [physics.gen-ph], (2008).
17. Silva P.R. *Braz. J. Phys.* 2008, v. 38, 587.
18. Cohen A., Kaplan D., Nelson A., *Phys. Rev. Lett.* 1989, v. 82, 4971.
19. Silva P.R. The Viscous Universe and the Viscous Electron, viXra:1507.0177, (2015).
20. Silva P.R. arXiv:0908.3282v1 [physics.gen-ph], (2009).
21. Silva P.R. *Int. J. Mod. Phys. A* 1997, v. 12, 1373.
22. Particle Data Group, *Phys. Lett.* 1988, v. 204B, 1.
23. Adler S.L. *Phys. Rev.* 1969, v. 177, 2426.
24. Bell J.S., Jackiw R. *Il Nuovo Cimento* 1969, v. 51, 47.

On the Incompatibility of the Dirac-like Field Operator with the Majorana Anzatz

Valeriy V. Dvoeglazov

UAF, Universidad Autónoma de Zacatecas Apartado Postal 636, Suc. 3, C. P. 98061, Zacatecas, Zac., México. E-mail: valeri@fisica.uaz.edu.mx

We investigate some subtle points of the Majorana(-like) theories. We show explicitly the incompatibility of the Majorana Anzatz with the Dirac-like field operator in the original Majorana theory in various spin bases.

1 Introduction.

Majorana proposed his theory of neutral particles [1], in fact, on the basis of the Dirac equation [2]. However, the quantum field theory has not yet been completed in 1937. The Dirac equation [2–4] is well known to describe the charged particles of the spin 1/2.

Usually, everybody uses the following definition of the field operator [5]:

$$\Psi(x) = \frac{1}{(2\pi)^3}\sum_h \int \frac{d^3\mathbf{p}}{2E_p}\Big[u_h(\mathbf{p})a_h(\mathbf{p})e^{-ip\cdot x} + v_h(\mathbf{p})b_h^\dagger(\mathbf{p})e^{+ip\cdot x}\Big], \tag{1}$$

as given *ab initio*. After actions of the Dirac operator at $\exp(\mp ip_\mu x^\mu)$ the 4-spinors ($u-$ and $v-$) satisfy the momentum-space equations: $(\hat{p} - m)u_h(p) = 0$ and $(\hat{p} + m)v_h(p) = 0$, respectively; the h is the polarization index; $\hat{p} = p^\alpha\gamma_\alpha$. It is easy to prove from the characteristic equations $Det(\hat{p} \mp m) = (p_0^2 - \mathbf{p}^2 - m^2)^2 = 0$ that the solutions should satisfy the energy-momentum relation $p_0 = \pm E_p = \pm\sqrt{\mathbf{p}^2 + m^2}$ with both signs of p_0.

However, the general method of construction of the field operator has been given in the Bogoliubov and Shirkov book [6]. In the case of the $(1/2, 0) \oplus (0, 1/2)$ representation we have:

$$\Psi(x) = \frac{1}{(2\pi)^3}\int d^4p\,\delta(p^2 - m^2)e^{-ip\cdot x}\Psi(p) = \frac{\sqrt{m}}{(2\pi)^3}\sum_{h=\pm 1/2}\int \frac{d^3\mathbf{p}}{2E_p}\theta(p_0)\Big[u_h(p)a_h(p)|_{p_0=E_p}e^{-i(E_pt-\mathbf{p}\cdot\mathbf{x})} + u_h(-p)a_h(-p)|_{p_0=E_p}e^{+i(E_pt-\mathbf{p}\cdot\mathbf{x})}\Big]. \tag{2}$$

$\theta(p_0)$ is the Heaviside function(al). During these calculations we did not yet assume, which equation did this field operator (namely, the $u-$ spinor) satisfy (apart from the Klein-Gordon equation), with negative- or positive- mass. The explicit introduction of the factor $\sqrt{m}$ is caused by the following consideration. The 4-spinor normalization is known [4] to be able being chosen to the unit:

$$\bar{u}_{(\mu)}(p)u_{(\lambda)}(p) = +\delta_{\mu\lambda}\,, \tag{3}$$
$$\bar{u}_{(\mu)}(p)u_{(\lambda)}(-p) = 0\,, \tag{4}$$
$$\bar{v}_{(\mu)}(p)v_{(\lambda)}(p) = -\delta_{\mu\lambda}\,, \tag{5}$$
$$\bar{v}_{(\mu)}(p)u_{(\lambda)}(p) = 0\,, \tag{6}$$

where μ and λ are the polarization indices. The action should be dimensionless in $c = \hbar = 1$. Thus, the Lagrangian density has the dimension $[energy]^4$, and the 4-spinor field, the dimension $[energy]^{3/2}$. From (3-6) we see that the momentum-space 4-spinors should be dimensionless in this formulation. The creation/ahhihilation operators should have the dimension $[energy]^{-1}$ if we want to keep the standard (anti) commutation relations (20-24). Therefore, a factor with the dimension $[energy]^{1/2}$ can be introduced explicitly in (2) for the sake of conveniency instead of that in the normalizations or in the anticommutation relations [5].

The creation/annihilation quantum-field operators are defined by their actions on the quantum-field states in the representation of the occupation numbers:

$$\begin{aligned} a_h^\dagger(E_p, \mathbf{p})|n>& = |n+1; \mathbf{p}, h>,\\ a_h(E_p, \mathbf{p})|n>& = |n-1; \mathbf{p}, h>,\end{aligned} \tag{7}$$

$$a_h(E_p, \mathbf{p})|0> = 0\,. \tag{8}$$

Their explicit forms and excellent discussion can be found in [7]. However, the action of $a_h(-p) \equiv a_h(-E_p, -\mathbf{p})$ on the quantum-field vacuum is different (according, in fact, to the consideration below). Namely, the QFT vacuum contains all negative-energy states according to the Dirac interpretation. So when acting $a_h(-E_p, -\mathbf{p})$ on the vacuum this operator changes it (destroys a "hole"). The result is *not* zero, as opposed to the action of $a_h(+E_p, \mathbf{p})$ on vacuum.*

In general we should transform $u_h(-p)$ to the $v(p)$ in order to follow the original Dirac idea, where antiparticles were treated as particles with negative energy. The procedure is the following one [8, 9]. In the Dirac case we should assume the

*The similar situation is encountered in quantum mechanics of harmonic oscillator, where the creation operator can be obtained after application of reflection operators to the annihilation operator, and vice versa. This is not surprising because quantum field theory has the oscillator representation too.

following relation in the field operator:

$$\sum_h v_h(p)b_h^\dagger(p) = \sum_h u_h(-p)a_h(-p)\,. \tag{9}$$

We need $\Lambda_{\mu\lambda}(\mathbf{p}) = \bar{v}_\mu(E_p,\mathbf{p})u_\lambda(-E_p,-\mathbf{p})$. By direct calculations, we find

$$-b_\mu^\dagger(p) = \sum_\lambda \Lambda_{\mu\lambda}(p)a_\lambda(-p)\,. \tag{10}$$

where $\Lambda_{\mu\lambda} = -i(\boldsymbol{\sigma}\cdot\mathbf{n})_{\mu\lambda}$, $\mathbf{n} \equiv \widehat{\mathbf{p}} = \mathbf{p}/|\mathbf{p}|$, and

$$b_\mu^\dagger(p) = +i\sum_\lambda (\boldsymbol{\sigma}\cdot\mathbf{n})_{\mu\lambda}a_\lambda(-p)\,. \tag{11}$$

Multiplying (9) by $\bar{u}_\mu(-E_p,-\mathbf{p})$ we obtain

$$a_\mu(-p) = -i\sum_\lambda (\boldsymbol{\sigma}\cdot\mathbf{n})_{\mu\lambda}b_\lambda^\dagger(p)\,. \tag{12}$$

The equations are self-consistent.

Next, we can introduce the helicity operator of the $(1/2,0)\oplus(0,1/2)$ representation:

$$\widehat{h} = \begin{pmatrix} \hat{h} & 0_{2\times2} \\ 0_{2\times2} & \hat{h} \end{pmatrix}. \tag{13}$$

where

$$\hat{h} = \frac{1}{2}\boldsymbol{\sigma}\cdot\widehat{\mathbf{p}} = \frac{1}{2}\begin{pmatrix} \cos\theta & \sin\theta e^{-i\phi} \\ \sin\theta e^{+i\phi} & -\cos\theta \end{pmatrix}, \tag{14}$$

which commutes with the Dirac Hamiltonian, thus developing the theory in the helicity basis. We can start from the Klein-Gordon equation, generalized for describing the spin-1/2 particles (i. e., two degrees of freedom), Ref. [3]; again $c = \hbar = 1$. If the 2-spinors are defined as in [10, 11] then we can construct the corresponding $u-$ and $v-$ 4-spinors in the helicity basis.

$$u_\uparrow = N_\uparrow^+\begin{pmatrix}\phi_\uparrow \\ \frac{E-p}{m}\phi_\uparrow\end{pmatrix} = \frac{1}{\sqrt{2}}\begin{pmatrix}\sqrt{\frac{E+p}{m}}\phi_\uparrow \\ \sqrt{\frac{m}{E+p}}\phi_\uparrow\end{pmatrix}, \tag{15}$$

$$u_\downarrow = N_\downarrow^+\begin{pmatrix}\phi_\downarrow \\ \frac{E+p}{m}\phi_\downarrow\end{pmatrix} = \frac{1}{\sqrt{2}}\begin{pmatrix}\sqrt{\frac{m}{E+p}}\phi_\downarrow \\ \sqrt{\frac{E+p}{m}}\phi_\downarrow\end{pmatrix}, \tag{16}$$

$$v_\uparrow = N_\uparrow^-\begin{pmatrix}\phi_\uparrow \\ -\frac{E-p}{m}\phi_\uparrow\end{pmatrix} = \frac{1}{\sqrt{2}}\begin{pmatrix}\sqrt{\frac{E+p}{m}}\phi_\uparrow \\ -\sqrt{\frac{m}{E+p}}\phi_\uparrow\end{pmatrix}, \tag{17}$$

$$v_\downarrow = N_\downarrow^-\begin{pmatrix}\phi_\downarrow \\ -\frac{E+p}{m}\phi_\downarrow\end{pmatrix} = \frac{1}{\sqrt{2}}\begin{pmatrix}\sqrt{\frac{m}{E+p}}\phi_\downarrow \\ -\sqrt{\frac{E+p}{m}}\phi_\downarrow\end{pmatrix}, \tag{18}$$

where the normalization to the unit was again used. Please note that as in Ref. [14] the $\gamma-$ matrices are the same as in the spinorial basis:

$$\gamma^0 = \begin{pmatrix}0_{2\times2} & 1_{2\times2} \\ 1_{2\times2} & 0_{2\times2}\end{pmatrix}, \quad \boldsymbol{\gamma}^j = \begin{pmatrix}0_{2\times2} & -\boldsymbol{\sigma}^i \\ \boldsymbol{\sigma}^i & 0_{2\times2}\end{pmatrix}. \tag{19}$$

Thus, in the helicity basis we also have $v_h(p) = \gamma_5 u_h(p)$ as usual. Next, both $u-$ and $v-$ spinors above are the eigenspinors of the helicity operator [14] because the 2-spinors ϕ_h are the eigenspinors of $\hat{h}$.*

We again define the field operator as in (2) except for the polarization index h, which now answers for the helicity (not for the third projection of the spin, see [14]). The commutation relations are assumed to be the standard ones [5,6,12,13], except for adjusting the dimensional factor(see the discussion above):

$$\left[a_\mu(\mathbf{p}), a_\lambda^\dagger(\mathbf{k})\right]_+ = 2E_p\delta^{(3)}(\mathbf{p}-\mathbf{k})\delta_{\mu\lambda}\,, \tag{20}$$

$$\left[a_\mu(\mathbf{p}), a_\lambda(\mathbf{k})\right]_+ = 0 = \left[a_\mu^\dagger(\mathbf{p}), a_\lambda^\dagger(\mathbf{k})\right]_+\,, \tag{21}$$

$$\left[a_\mu(\mathbf{p}), b_\lambda^\dagger(\mathbf{k})\right]_+ = 0 = \left[b_\mu(\mathbf{p}), a_\lambda^\dagger(\mathbf{k})\right]_+\,, \tag{22}$$

$$\left[b_\mu(\mathbf{p}), b_\lambda^\dagger(\mathbf{k})\right]_+ = 2E_p\delta^{(3)}(\mathbf{p}-\mathbf{k})\delta_{\mu\lambda}\,, \tag{23}$$

$$\left[b_\mu(\mathbf{p}), b_\lambda(\mathbf{k})\right]_+ = 0 = \left[b_\mu^\dagger(\mathbf{p}), b_\lambda^\dagger(\mathbf{k})\right]_+\,. \tag{24}$$

However, the attempt is now failed to obtain the previous result (11) for $\Lambda_{\mu\lambda}(p)$. In this helicity case

$$\bar{v}_\mu(p)u_\lambda(-p) = i\sigma^y_{\mu\lambda}\,. \tag{25}$$

Please remember that the changes of the spin bases are performed by the rotation in the spin-parity space.

2 Analysis of the Majorana Anzatz

It is well known that "*particle=antiparticle*" in the Majorana theory. So, in the language of the quantum field theory we should have

$$b_\mu(E_p,\mathbf{p}) = e^{i\varphi}a_\mu(E_p,\mathbf{p})\,. \tag{26}$$

Usually, different authors use $\varphi = 0, \pm\pi/2$ depending on the metrics and on the forms of the 4-spinors and commutation relations. It is related to the Kayser phase factor.

So, on using (11) and the above-mentioned postulate we come to:

$$a_\mu^\dagger(p) = +ie^{i\varphi}(\boldsymbol{\sigma}\cdot\mathbf{n})_{\mu\lambda}a_\lambda(-p)\,. \tag{27}$$

On the other hand, on using (12) we make the substitutions $E_p \to -E_p$, $\mathbf{p}\to-\mathbf{p}$ to obtain

$$a_\mu(p) = +i(\boldsymbol{\sigma}\cdot\mathbf{n})_{\mu\lambda}b_\lambda^\dagger(-p)\,. \tag{28}$$

The totally reflected (26) is $b_\mu(-E_p,-\mathbf{p}) = e^{i\varphi}a_\mu(-E_p,-\mathbf{p})$. Thus,

$$b_\mu^\dagger(-p) = e^{-i\varphi}a_\mu^\dagger(-p)\,. \tag{29}$$

Combining with (28), we come to

$$a_\mu(p) = +ie^{-i\varphi}(\boldsymbol{\sigma}\cdot\mathbf{n})_{\mu\lambda}a_\lambda^\dagger(-p)\,, \tag{30}$$

*However, when discussing the spin properties of $u(-p)$ and $v(-p)$ in the helicity basis one should clarify the notational issues. Due to $\phi_{\uparrow\downarrow}(-\mathbf{p}) = -i\phi_{\downarrow\uparrow}(\mathbf{p})$, $u_{\uparrow\downarrow}(-E_p,-\mathbf{p}) = \pm v_{\downarrow\uparrow}(E_p,\mathbf{p})$ we have $\widehat{h}u_{\uparrow\downarrow}(-E_p,-\mathbf{p}) = -\frac{1}{2}v_{\downarrow\uparrow}(E_p,\mathbf{p})$, and similarly for $v(-p)$ 4-spinors. However, the equation (25) below is valid within the used notation.

and

$$a^{\dagger}_{\mu}(p) = -ie^{i\varphi}(\boldsymbol{\sigma}^{*}\cdot\mathbf{n})_{\mu\lambda}a_{\lambda}(-p)\,. \qquad (31)$$

This contradicts with the equation (27) unless we have the preferred axis in every inertial system.

Next, we can use another Majorana anzatz $\Psi = \pm e^{i\alpha}\Psi^{c}$ with usual definitions

$$C = \begin{pmatrix} 0 & i\Theta \\ -i\Theta & 0 \end{pmatrix}\mathcal{K}\,, \quad \Theta = \begin{pmatrix} 0 & -1 \\ 1 & 0 \end{pmatrix} = -i\sigma^{y}\,. \qquad (32)$$

Thus, on using $Cu^{*}_{\uparrow}(\mathbf{p}) = iv_{\downarrow}(\mathbf{p})$, $Cu^{*}_{\downarrow}(\mathbf{p}) = -iv_{\uparrow}(\mathbf{p})$ we come to other relations between creation/annihilation operators

$$a^{\dagger}_{\uparrow}(\mathbf{p}) = \mp ie^{-i\alpha}b^{\dagger}_{\downarrow}(\mathbf{p})\,, \qquad (33)$$

$$a^{\dagger}_{\downarrow}(\mathbf{p}) = \pm ie^{-i\alpha}b^{\dagger}_{\uparrow}(\mathbf{p})\,, \qquad (34)$$

which may be used instead of (26). Due to the possible signs $\pm$ the number of the corresponding states is the same as in the Dirac case that permits us to have the complete system of the Fock states over the $(1/2,0)\oplus(0,1/2)$ representation space in the mathematical sense.* However, in this case we deal with the self/anti-self charge conjugate quantum field operator instead of the self/anti-self charge conjugate quantum states. Please remember that it is the latter that answers for neutral particles; the quantum field operator contains the information about more than one state, which may be either electrically neutral or charged.

As a discussion we observe that the origins and the consequences of the contradiction between (27) and (31) may be the following. In general, the QFT space reflection are performed by the unitary transformations in the Fock space. The time reflection is performed by the anti-unitary transformation. However, after writing the present paper I learnt from [15] about arguments of unitary time reversal on the first quantization level. What would be the influence of this proposition on the second quantization scheme and on the Majorana Anzatz should be the subject of future publications.

3 Conclusions

We conclude that something is missed in the foundations of the original Majorana theory and/or the Dirac "hole" theory. At the moment the above consideration points to the rotational symmetry breaking after application of the Majorana Anzatz in the $(1/2,0)\oplus(0,1/2)$ representation, for higher spins as well [16].

Acknowledgements

I acknowledge discussions with colleagues at recent conferences. I am grateful to the Zacatecas University for professorship.

Submitted on December 1, 2018

*Please note that the phase factors may have physical significance in quantum field theories as opposed to the textbook nonrelativistic quantum mechanics, as was discussed recently by several authors.

References

1. Majorana E. *Nuovo Cim.*, 1937, v. 14, 171.
2. Dirac P.A.M. *Proc. Roy. Soc. Lond. A*, 1928, v. 117, 610.
3. Sakurai J.J. Advanced Quantum Mechanics, Addison-Wesley, (1967).
4. Ryder L.H. Quantum Field Theory, Cambridge University Press, Cambridge, (1985).
5. Itzykson C. and Zuber J.-B. Quantum Field Theory, McGraw-Hill Book Co., (1980).
6. Bogoliubov N.N. and Shirkov D.V. Introduction to the Theory of Quantized Fields, 2nd Edition, Nauka, Moscow, (1973).
7. Schweber S.S. Introduction to Relativistic Quantum Field Theory, Harper & Row Publishers, New York, (1961).
8. Dvoeglazov V.V. *Hadronic J. Suppl.*, 2003, v. 18, 239.
9. Dvoeglazov V.V., *Int. J. Mod. Phys. B*, 2006, v. 20, 1317.
10. Varshalovich D.A., Moskalev A.N. and Khersonskiĭ V.K. Quantum Theory of Angular Momentum, World Scientific, Singapore, (1988), §6.2.5.
11. Dvoeglazov V.V., *Fizika B*, 1997, v. 6, 111.
12. Weinberg S. The Quantum Theory of Fields. Vol. I. Foundations, Cambridge University Press, Cambridge, (1995).
13. Greiner W. Field Quantization, Springer, (1996), Chapter 10.
14. Dvoeglazov V.V. *Int. J. Theor. Phys.*, 2004, v. 43, 1287.
15. Debergh N. *et al. J. Phys. Comm.*, 2018, v. 2, 115012.
16. Dvoeglazov V.V. *Int. J. Theor. Phys.*, 2019, v. 58, accepted manuscript.

Physical and Mathematical Consistency of the Janus Cosmological Model (JCM)

Jean-Pierre Petit[1], Gilles D'Agostini[2], and Nathalie Debergh[3]

Manaty Research Group

[1]jean-pierre.petit@manaty.net [2]gilles.dagostini@manaty.net [3]nathalie.debergh@manaty.net

The Janus Cosmological Model is based on a system of two coupled field equations. It explains the nature of dark matter and dark energy with negative mass and without the runaway paradox that arises in general relativity. We first recall how this system was built, from a simple Newtonian toy model to a relativistic bimetric theory, that is now improved in order to fulfill mathematical constraints and set up on a Lagrangian derivation.

1 The long genesis of the Janus Cosmological Model

Roots of the Janus Cosmological Model are like assembling different pieces of a puzzle. There are indeed several starting points for this bimetric approach. The first is the missing primordial antimatter, a problem solved in 1967 by Andrei Sakharov in [1] with the representation of the universe not as a single entity born from the beginning of time, but two spacetimes with opposite arrows of time communicating only through their common initial singularity, forming a "twin universe" in complete CPT symmetry, as represented in the didactic Figure 1.

Then, the first step is to consider that these two entities can interact gravitationally, which is equivalent to folding the object of Figure 1 on itself as in Figure 2.

In 1977, a first modeling using non relativistic theoretical tools is attempted in [2] and [3] with two Boltzmann equations coupled with Poisson's equation. We then realize Sakharov's seminal idea of a complete CPT symmetry between these two entities, an idea also independently used by other authors recently [4]. Such work suggests that a profound paradigm shift involving geometrical grounds should be performed.

Early 1990's, we explore, through computer simulations, what could emerge from interaction laws associated with a mix of positive and negative point masses, according to the following assumption. Interactions laws:

- Like masses attract, according to Newton's law.

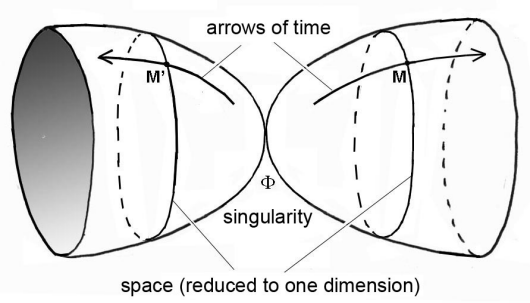

Fig. 1: 2D representation of Sakharov's twin universe model.

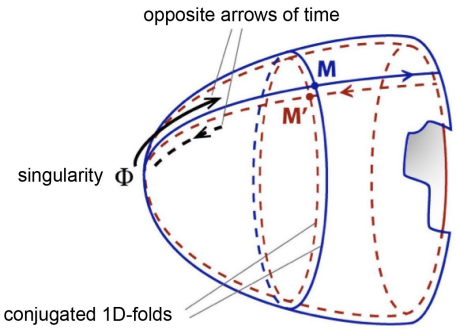

Fig. 2: Sakharov's model with "conjugate folds".

- Unlike masses repel, according to "anti-Newton".

At this stage, it is only a toy model. In 1992, first 2D simulations of two populations with opposite mass and same absolute value of density show a separation of the two entities, as shown in [5], a result reproduced below in Figure 3.

The purpose was to account for the large-scale structure of the universe, which admittedly wasn't a tight fit with these early experiments. But if we now introduce asymmetry in the two mass densities, taking a greater density for the negative mass species, then this population has a shorter Jeans time, hence it is the first to coalesce into conglomerates, by gravitational instability.

$$\text{if } |\rho^{(-)}| \gg \rho^{(+)} \quad \Rightarrow \quad t_{j^{(-)}} = \frac{1}{\sqrt{4\pi G\,|\rho^{(-)}|}} \ll t_{j^{(+)}} = \frac{1}{\sqrt{4\pi G\,\rho^{(+)}}} \tag{1}$$

Following simulations confirm this second hypothesis as they produce an evolution of the positive mass distribution into a large-scale structure with big negative mass conglomerates (optically invisible) repelling the positive mass matter in the remnant space around them as shown in [6], a decisive result reproduced below in Figure 4, this time in very good agreement with the observation of the lacunar, foam-

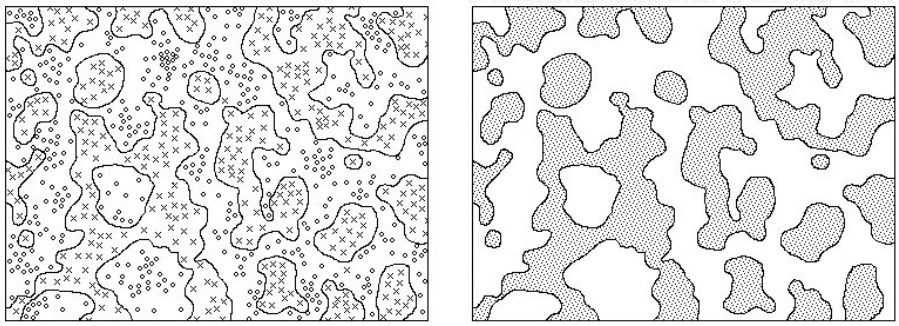

Fig. 3: Flocculation and percolation phenomena between two populations of opposite mass and same overall density. Right: Showing the optically-visible positive mass matter only.

like structure of the universe, where galaxies, clusters and superclusters are organized as a web of filaments, walls and nodes distributed around giant repulsive cosmic voids.

Same approach but different boundary conditions in [7], reproduced in Figure 5.

Such a scenario also produces, in 3D, a mechanism helping galaxy formation along. Indeed, after recombination, if large volumes of gas can coalesce into giant conglomerates, then a problem arises: how to dissipate such enormous gravitational energy transformed into heat? Considering an object of radius R, the amount of energy collected varies according to R^3 while the surface of the heatsink varies as R^2. Therefore, larger masses have a more important cooling time. But the constitution of the large-scale structure suggested by these simulations leads to a compression of the positive mass which distributes according to walls (as observed) that are actually sandwiched between two repulsive conglomerates of negative mass. A strong compression of the positive mass occurs in such planar structures, which are optimal for a quick radiative dissipation of energy, as explained in [6].

Besides 2D simulations, an effective confinement of galaxies despite their high peripheral velocity is analytically demonstrated using an exact solution of two Vlasov equations coupled with Poisson's equation, using the methodology exposed in [5]. The flat rotation curve obtained from such a solution, made possible by the repulsive effect of the surrounding negative mass, has been shown for the first time in [6], a curve reproduced in Figure 6. It is worth noting that such a typical rotation curve has been similarly obtained more recently using the same repulsive action of a negative mass distribution around galaxies, but from 3D computer simulations made by an independent researcher [8].

Using the exact solution of the analytical set of two Vlasov equations coupled with Poisson's equation (image of a 2D galaxy confined by a repulsive negative mass environment), we show in numerical simulations that the rotational motion of the galaxy generates a good-looking barred spiral structure in a few turns (1992 DESY results, published in [6] and [7]).

In order to progress beyond a simple toy model that opens up interesting prospects thanks to the various above-mentioned positive results, it was still necessary at that time to derive interaction laws from a coherent mathematical formalism. The introduction of negative mass in cosmology had been considered as soon as the 1950s, using general relativity, defined by the well-known Einstein field equations which may be written, with a zero cosmological constant:

$$R_{\mu\nu} - \frac{1}{2} R\, g_{\mu\nu} = +\chi T_{\mu\nu}. \qquad (2)$$

Let's notice that Einstein's equation describes the motion of point masses embedded in a given mass-energy field $T_{\mu\nu}$ along geodesics that derive from a single metric $g_{\mu\nu}$. Then, one gets Bondi's result from [9]. Interaction laws with a single metric:

- Positive masses attract everything.
- Negative masses repel everything.

Which inevitably produce the preposterous "runaway motion" paradox (see Figure 8), a term coined by Bonnor in [10].

Nonetheless, a few authors (Farnes [8], Chardin [11]) still consider that it is possible to introduce negative mass in cosmology keeping the general relativity framework, hence putting up with such phenomenon; despite the fact that the runaway motion has been associated with the possibility of perpetual motion machines since the 1950s, as discussed by Gold with Bondi, Bergmann and Pirani in [12].

On the contrary, from 1995 in [13] we propose a bimetric description of the universe with two coupled metrics and which produce trajectories along their own geodesics, for positive and negative mass particles, respectively. Then, the classical Schwarzschild solution allows, by simply reversing the integration constant, to get trajectories suggesting a gravitational repulsion of positive masses by a negative mass, and vice versa:

$$ds^2 = \left(1 - \frac{2GM}{rc^2}\right) c^2 dt^2 - \frac{dr^2}{1 - \dfrac{2GM}{rc^2}} - r^2 d\theta^2 - \sin^2\theta d\varphi^2, \quad (3)$$

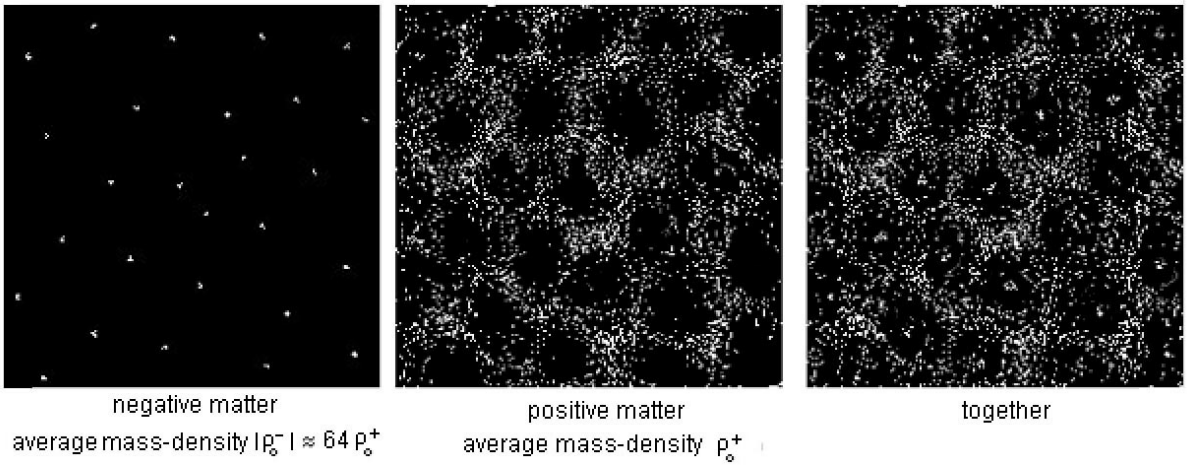

Fig. 4: Result of a 2D large-scale structure simulation [6].

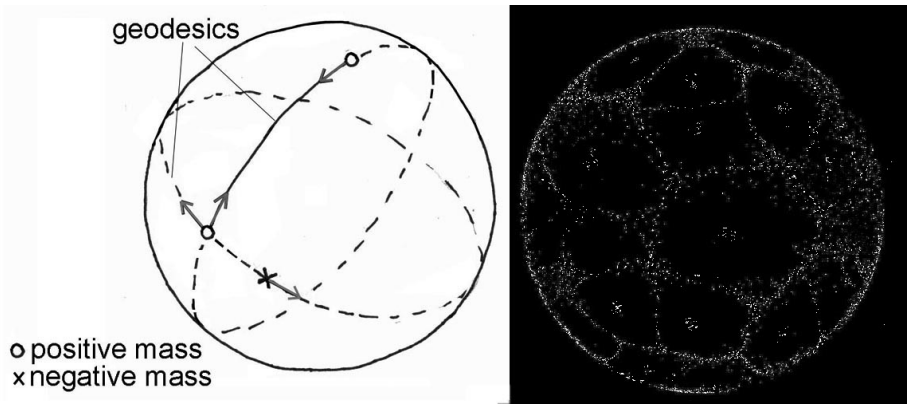

Fig. 5: Result of a 2D large-scale structure simulation on a 2-sphere [7].

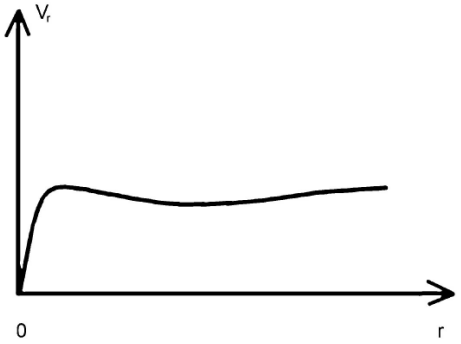

Fig. 6: Flat rotation curve of a galaxy surrounded by a negative mass distribution [6].

$$ds^2 = \left(1+\frac{2GM}{rc^2}\right)c^2dt^2 - \frac{dr^2}{1+\frac{2GM}{rc^2}} - r^2d\theta^2 - \sin^2\theta d\varphi^2. \quad (4)$$

Exploiting this idea, we introduce the concept of negative (diverging) gravitational lensing in the same paper [13]. Considering that a gap within a negative mass distribution is equivalent to a positive mass concentration, we suggest to attribute the strong gravitational lensing effects, observed in the vicinity of galaxies and galaxy clusters, not to a dark matter halo made of positive mass, but instead to their negative mass environment.

From 1994, we also suggest in [5] that such a bimetric description could result from the combination of two Lagrangian densities, due to two Ricci scalars $R^{(+)}$ and $R^{(-)}$. In 2001 [6], we proposed for the first time a system of two coupled field equations, which can be written as:

$$R^{(+)}_{\mu\nu} - \frac{1}{2}R^{(+)}g^{(+)}_{\mu\nu} = +\chi\left[T^{(+)}_{\mu\nu} + T^{(-)}_{\mu\nu}\right], \quad (5)$$

$$R^{(-)}_{\mu\nu} - \frac{1}{2}R^{(-)}g^{(-)}_{\mu\nu} = -\chi\left[T^{(+)}_{\mu\nu} + T^{(-)}_{\mu\nu}\right], \quad (6)$$

whose purpose was to account for the postulated interaction laws. Indeed, we make such laws emerge from a dual Newto-

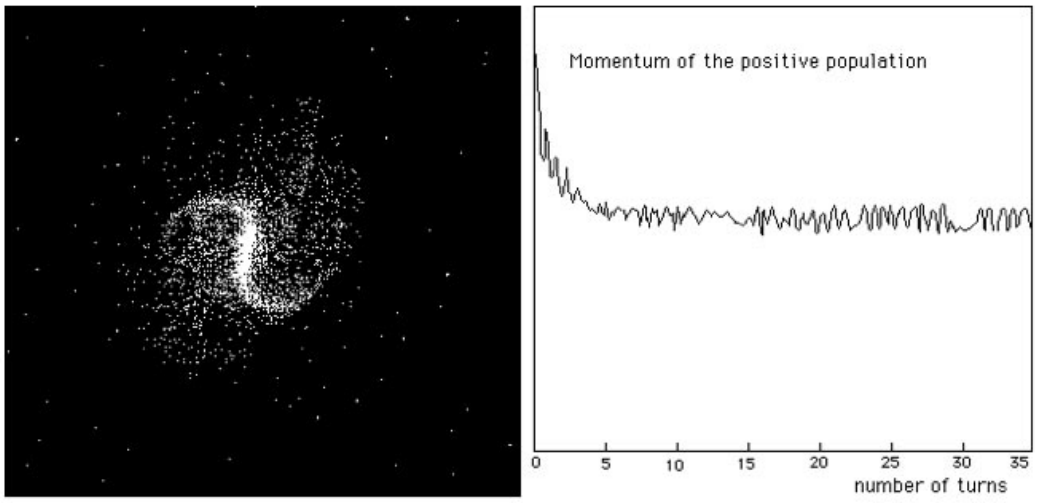

Fig. 7: 2D barred spiral structure [6, 7].

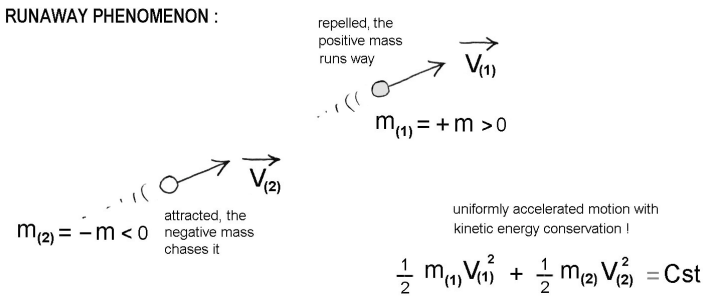

Fig. 8: Runaway motion in general relativity.

nian approximation of this system of two coupled equations. Depending locally on the type of dominant species in a given region of space, equations with no RHS produce solutions of type 36 or 37.

Aforementioned results of simulations showed that an asymmetry in the mass densities of the positive vs negative mass species is required to account for observations of the large-scale structure of the universe. Such density asymmetry can be caused, not because of a larger quantity of negative mass, but if the two space gauge factors $a^{(+)}$ and $a^{(-)}$ are different. Alas, at this level it is impossible to produce a time-dependent solution with $a^{(+)} \neq a^{(-)}$. Inconsistency becomes inevitable when FRLW metrics are introduced in the two field equations: similarly to Friedmann solutions, they produce a couple of differential equations in $a^{(+)}$, $a'^{(+)}$, $a''^{(+)}$ on one hand, and in $a^{(-)}$, $a'^{(-)}$, $a''^{(-)}$ on the other. In the calculation based on Einstein's equations, compatibility betweeen two equations leads to the relation $\rho a^3 = cst$ in the matter-dominated era, which expresses mass-energy conservation. In the bimetric framework of the Janus model based on the two coupled equations 5 and 6, such compatibility reduces the time-dependent solution to $a^{(+)} = a^{(-)}$.

Still in the same 2001 paper [6], we establish the connection between Sakharov's seminal work about two universes with opposite arrows of time, and negative gravity, using dynamical group theory from [14], which shows that time reversal goes with energy inversion, hence mass inversion as $-m = -E/c^2$. We then introduce the "Janus group" to handle the electric charge in a five-dimensional spacetime:

$$\begin{pmatrix} \lambda\mu & 0 & 0 \\ 0 & \lambda\,, L_0 & 0 \\ 0 & 0 & 1 \end{pmatrix} \qquad \text{with } \lambda = \pm 1 \quad \text{and } \mu = \pm 1, \quad (7)$$

where L_0 is the component of the orthochronous (forward in time) subset of the Lorentz group. It is the extension of the Poincaré group to five dimensions, which describes the existence of two different kinds of antimatter: one being C-symmetric with respect to normal matter, it has a positive mass; while the other antichronous (backward in time) antimatter is PT-symmetric and has a negative mass. Therefore,

the CPT theorem has to be reconsidered, since the exclusion of negative energy states follows on from an a priori axiom in quantum field theory, which postulates that the operator T has to be antiunitary and antilinear, a hypothesis not necessarily true as shown in [15].

Sakharov's conditions in [1] states that the baryon creation rate from an excess of quarks has been faster than the antibaryon creation rate from fewer antiquarks at $t > 0$, but such CP violation is opposite for $t < 0$ (the "initial singularity" triggering complete CPT reflections) thereby preserving the global symmetry of the whole universe. This allows to define the true nature of the invisible antichronous components of the universe: these are copies of antiparticles that are usually made in a lab, but with negative energy and mass, due to T-symmetry.

The invisibility of such objects is deduced from the idea that PT-symmetric antiparticles emit negative energy photons that follow null-geodesics of their own metric $g_{\mu\nu}^{(-)}$ hence escape detection by optical instruments that are made of positive mass matter.

In 2002, Damour and Kogan in [16] situate the issue with massive bigravity theories, where bimetry covers a different approach. In such models, two branes interact using various massive gravitons (hence the name) with a mass spectrum. The authors propose a Lagrangian derivation, based on an action, which leads to a system of two coupled field equations. But such a model, although mathematically consistent, does not stand up to scrutiny as it does not provide any solution able to be confronted with observations. As it has not been further pursued, it cannot answer this question.

On the other hand, in 2008 and 2009, Hossenfelder in [17] and [18] builds her own bimetric model involving negative mass, from a Lagrangian derivation where she produces a system of two coupled field equations. This time, LHS are identical to the system (5;6) which follows on from the presence of terms $R^{(+)}\sqrt{g^{(+)}}$ and $R^{(-)}\sqrt{g^{(-)}}$ in the Lagrangian densities considered. Exploiting her Lagrangian derivation, she reveals the determinant ratios of the two metrics $\sqrt{g^{(+)}/g^{(-)}}$ and $\sqrt{g^{(-)}/g^{(+)}}$ that had already been pointed out in previous work [19] and [20]. She finally tackles two Friedmann solutions, without confronting them to observational data. Actually, although sharing many similarities, having the same kind of coupled field equations regarding negative mass, a fundamental difference remains between Hossenfelder's bimetric theory and the Janus Cosmological Model.

Indeed, Hossenfelder doubts that the second entity can have an important effect on the distribution of standard matter, qualifying the gravitational coupling between the two species as "extremely weak". This is because "for symmetry reason" she considers that the absolute values of the mass density of the two populations should be of the same order of magnitude. Such hypothesis leads to a global zero field configuration, which does not fit with observations, as she notices. Then, examination of possible fluctuations seems to be her main concern. Not perceiving that a *profound dissymmetry* is on the contrary the key to the interpretation of many phenomena, including the acceleration of the cosmic expansion, she will not develop her model further during the following decade, focusing instead on other research topics.

Nonetheless, Hossenfelder points out a "smoking gun signal" that could highlight the existence of invisible negative mass in the universe, through the detection of diffracted light rays caused by diverging lensing, an effect previously predicted in [13]. We indeed showed from 1995 that photons emitted by high redshift galaxies ($z > 7$) are diffracted by the presence of invisible conglomerates of negative mass on their path. This reduces the apparent magnitude of such galaxies, making them appear as *dwarf*, which is consistent with observations.

In 2014 in [21] we take again the system (5;6) and attempt to modify it according to:

$$R_{\mu\nu}^{(+)} - \frac{1}{2} R^{(+)} g_{\mu\nu}^{(+)} = +\chi \left[T_{\mu\nu}^{(+)} + \varphi T_{\mu\nu}^{(-)} \right], \tag{8}$$

$$R_{\mu\nu}^{(-)} - \frac{1}{2} R^{(-)} g_{\mu\nu}^{(-)} = -\chi \left[\phi T_{\mu\nu}^{(+)} + T_{\mu\nu}^{(-)} \right]. \tag{9}$$

Introducing two functions $\varphi()$ and $\phi()$ that allow a time-dependent homogeneous and isotropic solution, so that $a^{(+)} \neq a^{(-)}$. This is possible by switching to the system:

$$R_{\mu\nu}^{(+)} - \frac{1}{2} R^{(+)} g_{\mu\nu}^{(+)} = +\chi \left[T_{\mu\nu}^{(+)} + \left(\frac{a^{(-)}}{a^{(+)}} \right)^3 T_{\mu\nu}^{(-)} \right], \tag{10}$$

$$R_{\mu\nu}^{(-)} - \frac{1}{2} R^{(-)} g_{\mu\nu}^{(-)} = -\chi \left[\left(\frac{a^{(+)}}{a^{(-)}} \right)^3 T_{\mu\nu}^{(+)} + T_{\mu\nu}^{(-)} \right]. \tag{11}$$

We obtained such a result by assuring energy conservation, not by deriving these equations from the system proposed in [18]. From (10;11) we then build an exact solution involving a large asymmetry, so that $|\rho^{(-)}| \gg \rho^{(+)}$, accounting fot the acceleration of the expansion of the universe. D'Agostini thereafter showed in 2018 in [22] that this exact solution is in very good agreement with latest observational data. In parallel we published in 2014 in [23] a Lagrangian derivation based on the functional relation:

$$\delta g^{(-)\mu\nu} = -\delta g^{(+)\mu\nu}, \tag{12}$$

giving the following system of two coupled field equations:

$$R_{\mu\nu}^{(+)} - \frac{1}{2} R^{(+)} g_{\mu\nu}^{(+)} = +\chi \left(T_{\mu\nu}^{(+)} + \sqrt{\frac{-\mathbf{g}^{(-)}}{-\mathbf{g}^{(+)}}}\, T_{\mu\nu}^{(-)} \right), \tag{13}$$

$$R_{\mu\nu}^{(-)} - \frac{1}{2} R^{(-)} g_{\mu\nu}^{(-)} = -\chi \left(T_{\mu\nu}^{(-)} + \sqrt{\frac{\mathbf{g}^{(+)}}{\mathbf{g}^{(-)}}}\, T_{\mu\nu}^{(+)} \right), \tag{14}$$

which is similar to Hossenfelder's system in her previous Lagrangian derivation [18], although both constructions are completely different. In our derivation, the square root in the determinant ratio of the metrics directly follows on from hypothesis (14). Let's recall that such a ratio always appears as soon as a bimetric approach is attempted, see for example [19] and [20]. Admittedly however, we cannot rule out that the system (15);(16), as well as the newer one exposed hereinbelow, can be considered as a particular case of Hossenfelder's own model.

In 2014 in [23] we extend the Janus framework to a class of solutions where the two speeds of light and, in the positive and negative sectors, are different. In 2018 in [25] we propose to evaluate the magnitude of their ratio, based on a study of the fluctuations in the CMB, which leads to the following conclusion:

$$\frac{a^{(-)}}{a^{(+)}} \simeq \frac{1}{100}, \qquad \frac{c^{(-)}}{c^{(+)}} \simeq \frac{1}{10}. \tag{15}$$

The combination of such different space scale factors and speeds of light would allow a gain factor of 1000 in travel time, regarding a hypothetical technology making apparent FTL interstellar travel by mass inversion possible, as evoked in [23] and [26].

The paper [23] then summarizes many observational data in good agreement with features of the Janus Cosmological Model.

2 The 2014 JCM and the Bianchi identities

From 2014, the Janus system of two coupled field equations (13; 14) satisfies the Bianchi identities, either trivially when the RHS are zero, or when one considers time-dependent homogeneous and isotropic solutions. However, inconsistency appears when one tries to describe with this system a time-independent situation with a spherical symmetry, modeling a star of constant density surrounded by a vacuum. Thus, a new modification of the equation system must be considered, as explained below.

Let's consider a portion of the universe where one of the two species is absent, e.g. the negative energy species, repelled away by a local concentration of positive mass. Let's limit our analysis to the search of a time-independent solution for a spherically symmetric system, and Newtonian approximation. The corresponding system is:

$$R^{(+)}_{\mu\nu} - \frac{1}{2} R^{(+)} g^{(+)}_{\mu\nu} = +\chi T^{(+)}_{\mu\nu}, \tag{16}$$

$$R^{(-)}_{\mu\nu} - \frac{1}{2} R^{(-)} g^{(-)}_{\mu\nu} = -\chi T^{(+)}_{\mu\nu}. \tag{17}$$

Then the two metrics have the form:

$$ds^{(+)2} = e^{\nu^{(+)}} c^2 dt^2 - e^{\lambda^{(+)}} dr^2 - r^2 d\theta^2 - r^2 \sin^2\theta\, d\phi^2, \tag{18}$$

$$ds^{(-)2} = e^{\nu^{(-)}} c^2 dt^2 - e^{\lambda^{(-)}} dr^2 - r^2 d\theta^2 - r^2 \sin^2\theta\, d\phi^2. \tag{19}$$

We consider a sphere whose radius r_s is filled by matter of constant density $\rho^{(+)}$ surrounded by vacuum. Outside of the sphere, the two metrics are:

$$ds^{(+)2} = \left(1-\frac{2m}{r}\right) c^2 dt^2 - \frac{dr^2}{1-\dfrac{2m}{r}} - r^2 d\theta^2 - r^2 \sin^2\theta\, d\phi^2, \tag{20}$$

$$ds^{(-)2} = \left(1+\frac{2m}{r}\right) c^2 dt^2 - \frac{dr^2}{1+\dfrac{2m}{r}} - r^2 d\theta^2 - r^2 \sin^2\theta\, d\phi^2, \tag{21}$$

with:

$$m = \frac{G}{c^2}\frac{4\pi r_s^3}{3}\rho^{(+)}. \tag{22}$$

We can write the stress-energy tensor as:

$$T^{(+)\nu}_{\ \ \mu} = \begin{pmatrix} \rho^{(+)} & 0 & 0 & 0 \\ 0 & -\frac{p^{(+)}}{c^2} & 0 & 0 \\ 0 & 0 & -\frac{p^{(+)}}{c^2} & 0 \\ 0 & 0 & 0 & -\frac{p^{(+)}}{c^2} \end{pmatrix}, \tag{23}$$

where $p^{(+)}$ is the pressure insides the star of radius r_s filled with constant density $\rho^{(+)}$. Equations (16) and (17) give the following differential equations:

$$p^{(+)\prime} = -\left(\rho^{(+)}c^2 + p^{(+)}\right)\frac{m(r) + 4\pi G p^{(+)} r^3/c^4}{r\,(r-2m(r))}, \tag{24}$$

$$p^{(+)\prime} = +\left(\rho^{(+)}c^2 + p^{(+)}\right)\frac{m(r) + 4\pi G p^{(+)} r^3/c^4}{r\,(r+2m(r))}, \tag{25}$$

where:

$$m(r) = \frac{G}{c^2}\frac{4\pi r^3}{3}\rho^{(+)}. \tag{26}$$

After Newtonian approximation:

$$p^{(+)} \ll \rho^{(+)}c^2 \quad , \quad r \gg 2m, \tag{27}$$

which gives:

$$p^{(+)\prime} = -\frac{\rho^{(+)}c^2 m(r)}{r^2}, \tag{28}$$

$$p^{(+)\prime} = +\frac{\rho^{(+)}c^2 m(r)}{r^2}. \tag{29}$$

So that we get a physical and mathematical contradiction, that must be cured.

3 Lagrangian derivation of a new JCM, as of 2019

Consider the two diagonal constant matrices:

$$I = \begin{pmatrix} 1 & 0 & 0 & 0 \\ 0 & 1 & 0 & 0 \\ 0 & 0 & 1 & 0 \\ 0 & 0 & 0 & 1 \end{pmatrix}, \quad \varphi = \begin{pmatrix} 1 & 0 & 0 & 0 \\ 0 & -1 & 0 & 0 \\ 0 & 0 & -1 & 0 \\ 0 & 0 & 0 & -1 \end{pmatrix}. \tag{30}$$

$$S = \int_{D4}\left[IR^{(+)}\sqrt{-g^{(+)}} + \varphi R^{(-)}\sqrt{-g^{(-)}} - \chi\,(I+\varphi)\,L^{(+)}\sqrt{-g^{(+)}} + \chi\,(I+\varphi)\,L^{(-)}\sqrt{-g^{(-)}}\right]\mathrm{d}^4x \tag{31}$$

$$\delta\int_{D4} R^{(+)}\sqrt{-g^{(+)}}\;\mathrm{d}^4x = \int_{D4}\left(R^{(+)}_{\mu\nu} - \frac{1}{2}R^{(+)}g^{(+)}_{\mu\nu}\right)\sqrt{-g^{(+)}}\;\delta g^{(+)\mu\nu}\;\mathrm{d}^4x \tag{32}$$

$$\delta\int_{D4} R^{(-)}\sqrt{-g^{(-)}}\;\mathrm{d}^4x = \int_{D4}\left(R^{(-)}_{\mu\nu} - \frac{1}{2}R^{(-)}g^{(-)}_{\mu\nu}\right)\sqrt{-g^{(-)}}\;\delta g^{(-)\mu\nu}\;\mathrm{d}^4x \tag{33}$$

$$\delta\int_{D4} L^{(+)}\sqrt{-g^{(+)}}\;\mathrm{d}^4x = \int_{D4} T^{(+)}_{\mu\nu}\sqrt{-g^{(+)}}\;\delta g^{(+)\mu\nu}\;\mathrm{d}^4x \tag{34}$$

$$\delta\int_{D4} L^{(-)}\sqrt{-g^{(-)}}\;\mathrm{d}^4x = \int_{D4} T^{(-)}_{\mu\nu}\sqrt{-g^{(-)}}\;\delta g^{(-)\mu\nu}\;\mathrm{d}^4x \tag{35}$$

$$ds^{(+)2} = \left(1 - \frac{8\pi G\,r_s^3\,\rho^{(+)}}{c^2}r\right)c^2dt^2 - \left(1 + \frac{8\pi G\,r_s^3\,\rho^{(+)}}{c^2}r\right)dr^2 - r^2d\theta^2 - \sin^2\theta d\varphi^2 \tag{36}$$

$$ds^{(-)2} = \left(1 + \frac{8\pi G\,r_s^3\,\rho^{(+)}}{c^2}r\right)c^2dt^2 - \left(1 - \frac{8\pi G\,r_s^3\,\rho^{(+)}}{c^2}r\right)dr^2 - r^2d\theta^2 - \sin^2\theta d\varphi^2 \tag{37}$$

$$\delta g^{(+)}_{00} = -\frac{8\pi G\,r_s^3\,\rho^{(+)}}{c^2}\,r\,\delta\rho^{(+)} = -\delta g^{(-)}_{00} \qquad \delta g^{(+)}_{11} = -\frac{8\pi G\,r_s^3\,\rho^{(+)}}{c^2}\,r\,\delta\rho^{(+)} = -\delta g^{(-)}_{11} \tag{38}$$

Introducing the action (eq. 31) and performing the following bivariation, taking account of $I\varphi = \varphi$ and $\varphi\varphi = I$, results in equations 32–35.

From a previous Lagrangian derivation [7] :

$$\delta g^{(-)\mu\nu} = -\delta g^{(+)\mu\nu} \tag{39}$$

Our goal: to set up a system of two coupled field equations providing joint solutions corresponding to Newtonian approximation. In such conditions the external metrics are given in equations (36) and (37).

We may consider that such metrics belong to subsets of Riemannian metrics with signature $(+---)$ which obey relationship (39) (see eqs. (38)). If we consider that (39) defines joint metrics, they obey:

$$R^{(+)}_{\mu\nu} - \frac{1}{2}R^{(+)}\,g^{(+)}_{\mu\nu} = +\chi\left(T^{(+)}_{\mu\nu} + \sqrt{\frac{-\mathbf{g}^{(-)}}{-\mathbf{g}^{(+)}}}\,\varphi\,T^{(-)}_{\mu\nu}\right), \tag{40}$$

$$R^{(-)}_{\mu\nu} - \frac{1}{2}R^{(-)}\,g^{(-)}_{\mu\nu} = -\chi\left(T^{(-)}_{\mu\nu} + \sqrt{\frac{\mathbf{g}^{(+)}}{\mathbf{g}^{(-)}}}\,\varphi\,T^{(+)}_{\mu\nu}\right). \tag{41}$$

4 Back to the star model

Starting from the new joint system (40);(41) we obtain the analogous of the system (16);(17) where, in the second equation, we would replace the tensor $T^{(+)}\,g^{(+)}_{\mu\nu}$ by $\hat{T}^{(+)}_{\mu\nu}$, so that:

$$\hat{T}^{(+)}_{00} = T^{(+)}_{00} = \rho^{(+)}, \tag{42}$$

$$\hat{T}^{(+)}_{ii} = -T^{(+)}_{ii} \qquad \text{with} \qquad \mathrm{j} = \{1,2,3\}, \tag{43}$$

$$R^{(-)}_{\mu\nu} - \frac{1}{2}\,R^{(-)}\,g^{(-)}_{\mu\nu} = -\chi\hat{T}^{(+)}_{\mu\nu}. \tag{44}$$

With the joint metrics (18) and (19), inside the star, plus compatibility conditions satisfying (20) and (21) at its border $r = r_s$ we get the following result:

$$p^{(+)\prime} = -\left(\rho^{(+)}c^2 + p^{(+)}\right)\frac{m(r) + 4\pi G p^{(+)}r^3/c^4}{r\,(r - 2m(r))}, \tag{45}$$

$$p^{(+)\prime} = -\left(\rho^{(+)}c^2 - p^{(+)}\right)\frac{m(r) - 4\pi G p^{(+)}r^3/c^4}{r\,(r + 2m(r))}, \tag{46}$$

with $m(r)$ given by (26).

Equation (45) is nothing but the famous Tolman-Oppenheimer-Volkoff equation.

Applying the Newtonian approximation, any inconsistency vanishes. Such equations mean that inside the star, the pressure counterbalances the gravitational pull. The geodesics are given by equations (48) and (49), with:

$$\hat{R}^2 = \frac{3c^2}{8\pi G\rho^{(+)}}. \tag{47}$$

Linearizing leads to equations (50) and (51). Notice that equation (52) fits (39).

$$ds^{(+)2} = \left[\frac{3}{2}\sqrt{1-\frac{r_s^2}{\hat{R}^2}} - \frac{1}{2}\sqrt{1-\frac{r^2}{\hat{R}^2}}\right]^2 c^2\mathrm{d}t^2 - \frac{\mathrm{d}r^2}{1-\dfrac{r^2}{\hat{R}^2}} - r^2\mathrm{d}\theta^2 - r^2\sin^2\theta\mathrm{d}\phi^2 \tag{48}$$

$$ds^{(-)2} = \left[\frac{3}{2}\sqrt{1+\frac{r_s^2}{\hat{R}^2}} - \frac{1}{2}\sqrt{1+\frac{r^2}{\hat{R}^2}}\right]^2 c^2\mathrm{d}t^2 - \frac{\mathrm{d}r^2}{1+\dfrac{r^2}{\hat{R}^2}} - r^2\mathrm{d}\theta^2 - r^2\sin^2\theta\mathrm{d}\phi^2 \tag{49}$$

$$ds^{(+)2} = \left(1 - \frac{3}{2}\frac{r_s^2}{\hat{R}^2} + \frac{1}{2}\frac{r^2}{\hat{R}^2}\right)c^2\mathrm{d}t^2 - \left(1 + \frac{3}{2}\frac{r_s^2}{\hat{R}^2} - \frac{1}{2}\frac{r^2}{\hat{R}^2}\right)\mathrm{d}r^2 - r^2\mathrm{d}\theta^2 - r^2\sin^2\theta\mathrm{d}\varphi^2 \tag{50}$$

$$ds^{(-)2} = \left(1 + \frac{3}{2}\frac{r_s^2}{\hat{R}^2} - \frac{1}{2}\frac{r^2}{\hat{R}^2}\right)c^2\mathrm{d}t^2 - \left(1 - \frac{3}{2}\frac{r_s^2}{\hat{R}^2} + \frac{1}{2}\frac{r^2}{\hat{R}^2}\right)\mathrm{d}r^2 - r^2\mathrm{d}\theta^2 - r^2\sin^2\theta\mathrm{d}\varphi^2 \tag{51}$$

$$\delta g_{00}^{(+)} = -\frac{4\pi G\left(3r_s^3 - r^2\right)}{3c^2}\,\delta\rho^{(+)} = -\delta g_{00}^{(-)} \qquad \delta g_{11}^{(+)} = -\frac{4\pi G\left(3r_s^3 - r^2\right)}{3c^2}\,r\,\delta\rho^{(+)} = -\delta g_{11}^{(-)} \tag{52}$$

5 Back to our basic assumption: $\delta g^{(-)\mu\nu} = -\delta g^{(+)\mu\nu}$

The time-dependent joint solutions presented in [21] correspond to the following FRLW metrics:

$$\mathrm{d}s^{(+)2} = \left(dx^0\right)^2 - a^{(+)^2}\frac{\mathrm{d}u^2 + u^2\,\mathrm{d}\theta^2 + u^2\,\sin^2\theta\,\mathrm{d}\varphi^2}{\left(1 + \dfrac{k^{(+)}\,u^2}{4}\right)^2}, \tag{53}$$

$$\mathrm{d}s^{(-)2} = \left(dx^0\right)^2 - a^{(-)^2}\frac{\mathrm{d}u^2 + u^2\,\mathrm{d}\theta^2 + u^2\,\sin^2\theta\,\mathrm{d}\varphi^2}{\left(1 + \dfrac{k^{(-)}\,u^2}{4}\right)^2}, \tag{54}$$

which give, with the single solution $k^{(+)} = k^{(-)} = -1$:

$$a^{(+)2}\frac{\mathrm{d}^2a^{(+)}}{(\mathrm{d}x^0)^2}, -\frac{8\pi G\rho_0}{3c_0^2} = 0 \tag{55}$$

$$a^{(-)2}\frac{\mathrm{d}^2a^{(-)}}{(\mathrm{d}x^0)^2}. + \frac{8\pi G\rho_0}{3c_0^2} = 0 \tag{56}$$

Whose exact parametric solutions are, for (55):

$$x^0 = \frac{4\pi G\rho_0}{3c_0^2}\left(1 + \frac{sh(2v)}{2} + v\right), \tag{57}$$

$$a^{(+)} = \frac{4\pi G\rho_0}{3c_0^2}ch^2(v), \tag{58}$$

and for (56):

$$x^0 = \frac{4\pi G\rho_0}{3c_0^2}\left(sh(2w) - 2\,w\right), \tag{59}$$

$$a^{(-)} = \frac{4\pi G\rho_0}{3c_0^2}\left(ch^2(w) - 1\right). \tag{60}$$

Let's compute the variations $\delta g_{\mu\nu}^{(+)}$ and $\delta g_{\mu\nu}^{(-)}$ under a variation $\delta\rho_0$ of their single parameter, the dominant matter density ρ_0. The variations $\delta g_{00}^{(+)}$, $\delta g_{00}^{(-)}$, $\delta g_{11}^{(+)}$, $\delta g_{11}^{(-)}$ depend on the factors $a^{(+)}\delta a^{(+)}$ and $a^{(-)}\delta a^{(-)}$. But we have:

$$\begin{aligned}&\frac{\mathrm{d}a^{(+)}}{\mathrm{d}x^0} = th(v),\\ &\frac{\mathrm{d}^2a^{(+)}}{(\mathrm{d}x^0)^2} = \frac{1}{\mathrm{d}x^0}\left(\frac{\mathrm{d}a^{(+)}}{\mathrm{d}x^0}\right) = \frac{3c_0^2}{4\pi G\rho_0}\frac{1}{2\,ch^4(v)},\end{aligned} \tag{61}$$

and similar equations for the second metric solution, so that $\delta a^{(+)}/\delta\rho_0 = \delta a^{(-)}/\delta\rho_0 = 0$ which fits our fundamental relationship (39).

6 Conclusion

A model is never definitively fixed in time. The set of two coupled field equations first established in [9] corresponded to a first step. The present paper proposes an updated system that has been mathematically enriched to give a precise description of the matter-dominated era. In its Newtonian approximation, it provides a new insight on astrophysics, especially in galactic dynamics which no longer depends on a set of a single Vlasov equation plus Poisson but on two Vlasov equations coupled with Poisson's equation. New results in that field will be published soon.

At the present time, JCM provides:

- joint solutions $\left(g_{\mu\nu}^{(+)}, g_{\mu\nu}^{(-)}\right)$ corresponding to the functional space of Riemannian metrics of signature $(+\,-\,-\,-)$, fitting fundamental relationship $g_{\mu\nu}^{(+)} = -g_{\mu\nu}^{(-)}$.
- with stationary and spherically symmetric conditions in the vacuum.
- time dependent homogeneous and isotropic solutions.

Which cover everything that can currently be confronted with observations.

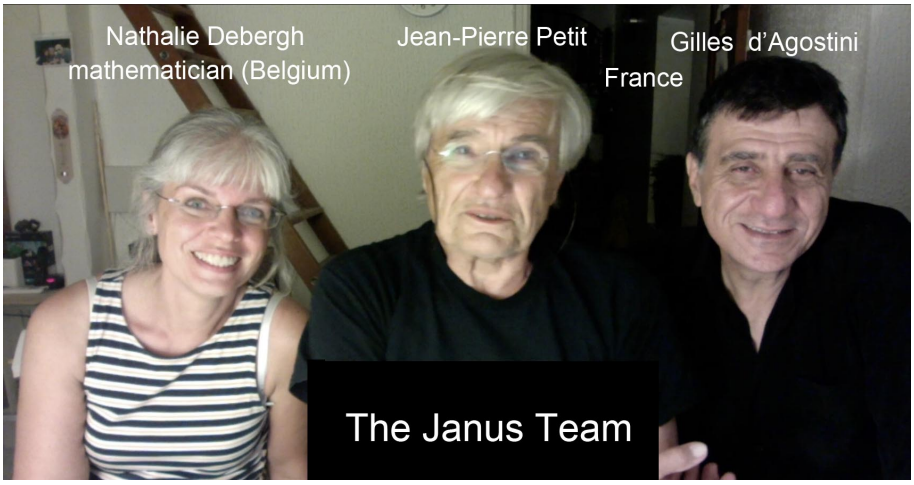

To a model already compliant with many observational data [22], a physically and mathematically coherent representation of joint geometries for positive energy and mass species, in the solar system and its neighborhood, has been added. Therefore, the Janus cosmological model agrees with classical verifications of general relativity.

By reversing this situation, considering instead a portion of space where negative mass largely dominates locally, i.e. where positive mass has been repelled away so its mass density can be taken equal to zero, we obtain the first coherent theoretical description of the *Great Repeller*, which has been exposed in [26].

When photons emitted by high redshift galaxies (z>7) cross negative mass conglomerates in the center of big cosmic voids, in the large-scale structure of the universe, negative gravitational lensing reduces their apparent magnitude, making them appear as dwarf galaxies, which is consistent with observations.

One may argue that the Janus theory exhibiting tow coupled metrics as a "natural" hypothesis with the confidence that subsequent results would eventually corroborate the postulate. However this bimetric model is formally sustained by a specific splitting of the Riemann Tensor which yields to 2nd rank tensor field equations, as shown in [27].

Submitted January 6, 2019

References

1. Sakharov A.D. Violation of CP invariance, C asymmetry, and baryon asymmetry of the universe. *JETP Letters*, 1967, v. 5(1), 24–26.
2. Petit J.-P. Univers jumeaux, énantiomorphes, à temps propre opposées. [Enantiomorphic twin universes with opposite proper times]. *Comptes Rendus de l'Académie des Sciences*, 1977, v. 263, 1315–1318.
3. Petit J.-P. Univers en interaction avec leurs images dans le miroir du temps. [Universes interacting with their opposite time-arrow fold]. *Comptes Rendus de l'Académie des Sciences*, 1977, v. 284, 1413–1416.
4. Boyle L., Finn K., Neil Turok N. CPT-Symmetric Universe. *Physical Review Letters*, 2018, v. 121, 251301. arXiv:1803.08928.
5. Petit J.-P. The missing-mass problem. *Il Nuovo Cimento B*, 1994, v. 109(7), 697–709.
6. Petit J.-P., Midy P., Landsheat F. Twin matter against dark matter. Marseille Cosmology Conference Where's the Matter? Tracing Dark and Bright Matter with the New Generation of Large Scale Surveys, Marseille, France, (2001).
7. Petit J.-P., d'Agostini G. Lagrangian derivation of the two coupled field equations in the Janus cosmological model. *Astrophysics and Space Science*, 2015, v. 357(67), 67.
8. Farnes J.S. A unifying theory of dark energy and dark matter: Negative masses and matter creation within a modified ΛCDM framework. *Astronomy & Astrophysics*, 2018, v. 620, A92. arXiv:1712.07962. doi:10.1051/0004–6361/201832898.
9. Bondi H. Negative Mass in General Relativity. *Reviews of Modern Physics*, 1957, v. 29(3), 423–428.
10. Bonnor W.B. Negative mass in general relativity. *General Relativity and Gravitation*, 1989, v. 21(11), 1143–1157.
11. Chardin G., Manfredi G. Gravity, antimatter and the Dirac-Milne universe. *General Relativity and Quantum Cosmology*, 2018, v. 239, 45. arXiv:1807.11198. doi:10.1007/s10751–018-1521–3.
12. Bondi H., Bergmann P., Gold T., Pirani F. Negative mass in general relativity in The Role of Gravitation in Physics: Report from the 1957 Chapel Hill Conference, Open Access Editions Epubli 2011. ISBN:978-3869319636.
13. Petit J.-P. Twin universes cosmology. *Astrophysics and Space Science*, 1995, v. 227(2), 273–307.
14. Souriau J.-M. "§14: A mechanistic description of elementary particles: Inversions of space and time" in Structure of Dynamical Systems. Progress in Mathematics. Boston: Birkhäuser, (1997). pp. 189–193. doi:10.1007/978–1–4612–0281–3_14. ISBN 978–1–4612–6692–1. Published originally in French in Structure des Systèmes Dynamiques, Dunod 1970.
15. Debergh N., Petit J.-P., d'Agostini G. On evidence for negative energies and masses in the Dirac equation through a unitary time-reversal operator. *Journal of Physics Communications*, 2018, v. 2(11), 115012. arXiv:1809.05046.
16. Damour T., Kogan I.I. Effective Lagrangians and universality classes of nonlinear bigravity. *Physical Review D*, 2002, v. 66, 104024. arXiv:hep-th/0206042.
17. Hossenfelder S. A Bi-Metric Theory with Exchange Symmetry. *Physical Review D*, 2008, v. 78(4), 044015. arXiv:0807.2838.
18. Hossenfelder S. Antigravitation. 17th International Conference on Supersymmetry and the Unification of Fundamental Interactions. Boston: American Institute of Physics, (2009). arXiv:0909.3456.

19. Lightman A.P., Lee D.L. New Two-Metric Theory of Gravity with Prior Geometry. *Physical Review D*, 1973, v. 8(10), 3293.

20. Rosen N. A bi-metric Theory of Gravitation. *General Relativity and Gravitation*, 1973, v. 4(6), 435–447.

21. Petit J.-P., d'Agostini G. Negative mass hypothesis in cosmology and the nature of dark energy. *Astrophysics and Space Science*, 2014, v. 354(2), 611.

22. D'Agostini G., Petit J.-P. Constraints on Janus Cosmological model from recent observations of supernovae type Ia. *Astrophysics and Space Science*, 2018, v. 363(7), 139.

23. Petit J.-P., d'Agostini G. Cosmological bimetric model with interacting positive and negative masses and two different speeds of light, in agreement with the observed acceleration of the Universe. *Modern Physics Letters A*, 2014, v. 29(34), 1450182.

24. Petit J.-P. Janus Cosmological Model and the Fluctuations of the CMB. *Progress in Physics*, 2018, v. 14(4), 226–229.

25. Petit J.-P., Debergh N., d'Agostini G. Negative energy states and interstellar travel. Advanced Propulsion Workshop. Estes Park, CO: Space Studies Institute, (September 2018).

26. Hoffman Y., Pomarède D., Tully R.B., Courtois H.M. The dipole repeller. *Nature Astronomy*, 2017, v. 1(2), 0036. arXiv:1702.02483.

27. Marquet P. On a 4th Tensor Gravitational Theory. *Progress in Physics*, 2017, v. 13(2), 106–110.

Non-commutativity: Unusual View

Valeriy V. Dvoeglazov

UAF, Universidad Autónoma de Zacatecas Apartado Postal 636, Suc. 3, C. P. 98061, Zacatecas, Zac., México. E-mail: valeri@fisica.uaz.edu.mx

Some ambiguities have recently been found in the definition of the partial derivative (in the case of presence of both explicit and implicit dependencies of the function subjected to differentiation). We investigate the possible influence of this subject on quantum mechanics and the classical/quantum field theory. Surprisingly, some commutators of operators of space-time 4-coordinates and those of 4-momenta are *not* equal to zero. We postulate the non-commutativity of 4-momenta and we derive mass splitting in the Dirac equation. Moreover, two iterated limits may not commute each other, in general. Thus, we present an example when the massless limit of the function of $E, \mathbf{p}, m$ does not exist in some calculations within quantum field theory.

1 Introduction

The assumption that the operators of coordinates do *not* commute $[\hat{x}_\mu, \hat{x}_\nu]_- \neq 0$ has been made by H. Snyder [1]. Therefore, the Lorentz symmetry may be broken. This idea [2, 3] received attention in the context of "brane theories". Moreover, the famous Feynman-Dyson proof of Maxwell equations [4] contains intrinsically the non-commutativity of velocities $[\dot{x}_i(t), \dot{x}_j(t)]_- \neq 0$ that also may be considered as a contradiction with the well-accepted theories (while there is no any contradiction therein).

On the other hand, it was recently discovered that the concept of partial derivative is *not* well defined in the case of both explicit and implicit dependence of the corresponding function, which the derivatives act upon [5]. The well-known example of such a situation is the field of an accelerated charge [6].* Škovrlj and Ivezić [7] call this partial derivative as '*complete* partial derivative'; Chubykalo and Vlayev, as '*total* derivative with respect to a given variable'. The terminology suggested by Brownstein [5] is 'the *whole*-partial derivative'.

2 Example 1

Let us study the case when we deal with explicite and implicite dependencies $f(\mathbf{p}, E(\mathbf{p}))$. It is well known that the energy in relativism is related to the 3-momentum as $E = \pm\sqrt{\mathbf{p}^2 + m^2}$; the unit system $c = \hbar = 1$ is used. In other words, we must choose the 3-dimensional mass hyperboloid in the Minkowski space, and the energy is *not* an independent quantity anymore. Let us calculate the commutator of the whole-partial derivatives $\hat{\partial}/\hat{\partial}E$ and $\hat{\partial}/\hat{\partial}p_i$. In order to make distinction between differentiating the explicit function and that which contains both explicit and implicit dependencies, the 'whole partial derivative' may be denoted as $\hat{\partial}$. In the general case one has

$$\frac{\hat{\partial} f(\mathbf{p}, E(\mathbf{p}))}{\hat{\partial} p_i} \equiv \frac{\partial f(\mathbf{p}, E(\mathbf{p}))}{\partial p_i} + \frac{\partial f(\mathbf{p}, E(\mathbf{p}))}{\partial E}\frac{\partial E}{\partial p_i}\,. \qquad (1)$$

Applying this rule, we find surprisingly

$$\begin{aligned}&\left[\frac{\hat{\partial}}{\hat{\partial} p_i}, \frac{\hat{\partial}}{\hat{\partial} E}\right]_- f(\mathbf{p}, E(\mathbf{p})) = \\ &\frac{\hat{\partial}}{\hat{\partial} p_i}\frac{\partial f}{\partial E} - \frac{\partial}{\partial E}\left(\frac{\partial f}{\partial p_i} + \frac{\partial f}{\partial E}\frac{\partial E}{\partial p_i}\right) = \\ &\frac{\partial^2 f}{\partial E \partial p_i} + \frac{\partial^2 f}{\partial E^2}\frac{\partial E}{\partial p_i} - \frac{\partial^2 f}{\partial p_i \partial E} - \frac{\partial^2 f}{\partial E^2}\frac{\partial E}{\partial p_i} - \frac{\partial f}{\partial E}\frac{\partial}{\partial E}\left(\frac{\partial E}{\partial p_i}\right).\end{aligned} \qquad (2)$$

So, if $E = \pm\sqrt{m^2 + \mathbf{p}^2}$ and one uses the generally-accepted representation form of $\partial E/\partial p_i = p_i/E$, one has that the expression (2) appears to be equal to $(p_i/E^2)\frac{\partial f(\mathbf{p}, E(\mathbf{p}))}{\partial E}$. Within the choice of the normalization the coefficient may be related to the longitudinal electric field in the helicity basis.† Next, the commutator is

$$\left[\frac{\hat{\partial}}{\hat{\partial} p_i}, \frac{\hat{\partial}}{\hat{\partial} p_j}\right]_- f(\mathbf{p}, E(\mathbf{p})) = \frac{1}{|E|^3}\frac{\partial f(\mathbf{p}, E(\mathbf{p}))}{\partial E}[p_i, p_j]_-\,. \qquad (3)$$

This should also not be zero according to Feynman and Dyson [4]. They postulated that the velocity (or, of course, the 3-momentum) commutator is equal to $[p_i, p_j] \sim i\hbar\epsilon_{ijk}B^k$, i.e., to the magnetic field. In fact, if we put in the coresponsdence to the momenta their quantum-mechanical operators (of course, with the appropriate clarification $\partial \to \hat{\partial}$), we obtain again that, in general, the derivatives do *not* commute $\left[\frac{\hat{\partial}}{\hat{\partial} x_\mu}, \frac{\hat{\partial}}{\hat{\partial} x_\nu}\right]_- \neq 0$.

Furthermore, since the energy derivative corresponds to the operator of time and the i-component momentum deriva-

*Firstly, Landau and Lifshitz wrote that the functions depended on t', and only through $t' + R(t')/c = t$ they depended implicitly on x, y, z, t. However, later (in calculating the formula (63.7)) they used the explicit dependence of R on the space coordinates of the observation point too. Jackson [8] agrees with [6] that one should find "a contribution to the spatial partial derivative for fixed time t from explicit spatial coordinate dependence (of the observation point)."

†The electric/magnetic fields can be derived from the 4-potentials which have been presented in [9].

tive, to $\hat{x}_i$, we put forward the following anzatz in the momentum representation:

$$[\hat{x}^\mu, \hat{x}^\nu]_- = \omega(\mathbf{p}, E(\mathbf{p}))\, F_\parallel^{\mu\nu}(\mathbf{p}) \frac{\partial}{\partial E}\,, \tag{4}$$

with some weight function ω being different for different choices of the antisymmetric tensor spin basis. The physical dimension of x^μ is $[energy]^{-1}$ in this unit system; $F_\parallel^{\mu\nu}(\mathbf{p})$ has the dimension $[energy]^0$, if we assume the mass shell condition in the definition of the field operators $\delta(p^2 - m^2)$, see [10]. Therefore, the weight function should have the dimension $[energy]^{-1}$. The commutator $[\hat{x}^\mu, \hat{p}^\nu]$ has the same form as in the textbook nonrelativistic quantum mechanics within the presented model.

In the modern literature, the idea of the broken Lorentz invariance by this method concurs with the idea of the *fundamental length*, first introduced by V. G. Kadyshevsky [11] on the basis of old papers by M. Markov. Both ideas and corresponding theories are extensively discussed. In my opinion, the main question is: what is the space scale, when the relativity theory becomes incorrect.

3 Example 2

In the previous Section (see also the paper [12]) we found some intrinsic contradictions related to the mathematical foundations of modern physics. It is well known that the partial derivatives commute in the Minkowski space (as well as in the 4-dimensional momentum space). However, if we consider that energy is an implicit function of the 3-momenta and mass (thus, approaching the mass hyperboloid formalism, $E^2 - \mathbf{p}^2c^2 = m^2c^4$) then we may be interested in the commutators of the whole-partial derivatives [5] instead. The whole-partial derivatives do not commute, as you see above. If they are associated with the corresponding physical operators, we would have the uncertainty relations in this case. This is an intrinsic contradiction of the SRT. While we start from the same postulates, on using two different ways of reasoning we arrive at the two different physical conclusions.

In this Section I would like to ask another question. Sometimes, when calculating dynamical invariants (and other physical quantities in quantum field theory), and when studying the corresponding massless limits we need to calculate iterated limits. We may encounter a rare situation when two iterated limits are not equal each other in physics. See, for example, Ref. [10]. We were puzzled calculating the iterated limits of the aggregate $\frac{E^2-\mathbf{p}^2}{m^2}$ (or the inverse one, $\frac{m^2}{E^2-\mathbf{p}^2}$, $c = \hbar = 1$):

$$\lim_{m\to 0} \lim_{E\to \pm\sqrt{\mathbf{p}^2+m^2}} \left(\frac{m^2}{E^2 - \mathbf{p}^2}\right) = 1\,, \tag{5}$$

$$\lim_{E\to \pm\sqrt{\mathbf{p}^2+m^2}} \lim_{m\to 0} \left(\frac{m^2}{E^2 - \mathbf{p}^2}\right) = 0\,. \tag{6}$$

Similar mathematical examples are presented in [13]. Physics should have well-defined dynamical invariants. Which iterated limit should be applied in the study of massless limits? The question of the iterated limits was studied in [14]. However, the answers leave room for misunderstandings and contradictions with the experiments. One can say: "The two limits are of very different sorts: the limit of $E \to \pm\sqrt{\mathbf{p}^2 + m^2}$ is a limit that subsumes the statement under the theory of Special Relativity. Such limits should be done first." However, cases exist when the limit $E \to \pm\sqrt{\mathbf{p}^2 + m^2}$ cannot be applied (or its application leads to the loss of the information). For example, we have for the causal Green's function used in the scalar field theory and in the $m \to 0$ quantum electrodynamics (QED), Ref. [15]:

$$D^c(x) = \frac{1}{(2\pi)^4}\int d^4p \frac{e^{-ip\cdot x}}{m^2 - p^2 - i\epsilon} \tag{7}$$
$$= \frac{1}{4\pi}\delta(\lambda) - \frac{m}{8\pi\sqrt{\lambda}}\theta(\lambda)\left[J_1(m\sqrt{\lambda}) - iN_1(m\sqrt{\lambda})\right] + \frac{im}{4\pi^2\sqrt{-\lambda}}\theta(-\lambda)K_1(m\sqrt{-\lambda}),$$

$\lambda = (x^0)^2 - \mathbf{x}^2$; J_1, N_1, K_1 are the Bessel functions of the first order. The application of $E \to \pm\sqrt{\mathbf{p}^2 + m^2} - i\delta$ results in non-existence of the integral. Meanwhile, the massless limit is made in the integrand in the Feynman gauge with no problems. Please remember that integrals are also the limits of the Riemann integral sums. The $m \to 0$ limits are made first sometimes.

Next, the application of the mass shell condition in the Weinberg-Tucker-Hammer $2(2S + 1)$-formalism leads to the fact that we would not be able to write the dynamical equation in the covariant form $[\gamma^{\mu\nu}\partial_\mu\partial_\nu - m^2]\Psi_{(6)}(x) = 0$. Apart, the information about the propagation of longitudinal modes would be lost (cf. formulas (19,20,27,28) of the first paper [10]). Moreover, the Weinberg equation and the mapping of the Tucker-Hammer equation to the antisymmetric tensor formalism have different physical contents on the interaction level [16, 17].*

Next, if we would always apply the mass shell condition first then we come to the derivative paradox of the previous Section. Finally, the condition $E^2 - \mathbf{p}^2 = m^2$ does not always imply the generally-accepted special relativity only. For instance, see the Kapuscik work, Ref. [18], who showed that similar expressions for energy and momentum exist for particles with $V > c$ and $m_\infty \in \mathfrak{R}e$.

Meanwhile, the case $m = 0$ appears to be equivalent to the light cone condition $r = ct$, which can be taken even without

*I take this opportunity to note that problems (frequently forgotten) may also exist with the direct application of $m \to 0$ in relativistic quantum equations. The case is: when the solutions are constructed on using the relativistic boosts in the momentum space the mass may appear in the denominator, $\sim 1/m^n$, which cancels the mass terms of the equation giving the non-zero corresponding result.

the mass shell condition to study the theories extending the special relativity. Not everybody realizes that it can be used to deduce the Lorentz transformations between two different reference frames. Just take squares and use the lineality: $r_1^2 - c^2t_1^2 = 0 = r_2^2 - c^2t_2^2$. Hence, in $d = 1 + 1$ we have $x_2 = \gamma(x_1 - vt_1)\,, \quad t_2 = \alpha(t_1 - \frac{\beta}{c}x_1)$ with $\alpha = \gamma = 1/\sqrt{1 - \frac{v^2}{c^2}}$, the Lorentz factor; $\beta = v/c$.

4 Example 3

The problem of explaining mass splitting of leptons (e, μ, τ) and quarks has a long history. See, for instance, a method suggested in Refs. [19], and some new insights in [20]. Non-commutativity [1] also exhibits interesting peculiarities in the Dirac case. Recently, we analyzed the Sakurai-van der Waerden method of deriving the Dirac (and higher-spin) equation [21]. We can start from

$$(EI^{(2)} - \boldsymbol{\sigma}\cdot\mathbf{p})(EI^{(2)} + \boldsymbol{\sigma}\cdot\mathbf{p})\Psi_{(2)} = m^2\Psi_{(2)}\,, \tag{8}$$

or

$$(EI^{(4)} + \boldsymbol{\alpha}\cdot\mathbf{p} + m\beta)(EI^{(4)} - \boldsymbol{\alpha}\cdot\mathbf{p} - m\beta)\Psi_{(4)} = 0\,. \tag{9}$$

E and $\mathbf{p}$ form the Lorentz 4-momentum. Obviously, the inverse operators of the Dirac operators exist in the non- commutative case. As in the original Dirac work, we have $\beta^2 = 1$, $\alpha^i\beta + \beta\alpha^i = 0$, $\alpha^i\alpha^j + \alpha^j\alpha^i = 2\delta^{ij}$.

We also postulate non-commutativity relations for the components of 4-momenta:

$$[E, \mathbf{p}^i]_- = \Theta^{0i} = \theta^i\,, \tag{10}$$

as usual. Therefore the equation (9) will *not* lead to the well-known equation $E^2 - \mathbf{p}^2 = m^2$. Instead, we have

$$\{E^2 - E(\boldsymbol{\alpha}\cdot\mathbf{p}) + (\boldsymbol{\alpha}\cdot\mathbf{p})E - \mathbf{p}^2 - m^2 \\ -i(\boldsymbol{\sigma}\otimes I_{(2)})[\mathbf{p}\times\mathbf{p}]\}\Psi_{(4)} = 0\,.$$

For the sake of simplicity, we may assume the last term to be zero. Thus, we arrive at

$$\left\{E^2 - \mathbf{p}^2 - m^2 - (\boldsymbol{\alpha}\cdot\boldsymbol{\theta})\right\}\Psi_{(4)} = 0\,. \tag{11}$$

We can apply the unitary transformation. It is known [22, 23] that one can* $U_1(\boldsymbol{\sigma}\cdot\mathbf{a})U_1^{-1} = \sigma_3|\mathbf{a}|$. For $\boldsymbol{\alpha}$ matrices we rewrite as

$$\mathcal{U}_1(\boldsymbol{\alpha}\cdot\boldsymbol{\theta})\mathcal{U}_1^{-1} = |\boldsymbol{\theta}|\begin{pmatrix}1&0&0&0\\0&-1&0&0\\0&0&-1&0\\0&0&0&1\end{pmatrix} = \alpha_3|\boldsymbol{\theta}|\,. \tag{12}$$

The explicit form of the U_1 matrix is ($a_{r,l} = a_1 \pm ia_2$):

$$U_1 = \frac{1}{\sqrt{2a(a+a_3)}}\begin{pmatrix}a+a_3 & a_l\\ -a_r & a+a_3\end{pmatrix} = \tag{13}$$
$$= \frac{1}{\sqrt{2a(a+a_3)}}[a + a_3 + i\sigma_2 a_1 - i\sigma_1 a_2]\,,$$
$$\mathcal{U}_1 = \begin{pmatrix}U_1 & 0\\ 0 & U_1\end{pmatrix}. \tag{14}$$

We now apply the second unitary transformation:

$$\mathcal{U}_2\alpha_3\mathcal{U}_2^\dagger = \begin{pmatrix}1&0&0&0\\0&0&0&1\\0&0&1&0\\0&1&0&0\end{pmatrix}\alpha_3\begin{pmatrix}1&0&0&0\\0&0&0&1\\0&0&1&0\\0&1&0&0\end{pmatrix} = \\ = \begin{pmatrix}1&0&0&0\\0&1&0&0\\0&0&-1&0\\0&0&0&-1\end{pmatrix}. \tag{15}$$

The final equation is then

$$\left[E^2 - \mathbf{p}^2 - m^2 - \gamma^5_{chiral}|\boldsymbol{\theta}|\right]\Psi'_{(4)} = 0\,. \tag{16}$$

In physical terms this implies mass splitting for a Dirac particle over the non-commutative space, $m_{1,2} = \pm\sqrt{m^2 \pm \theta}$. This procedure may be attractive as explanation of mass creation and mass splitting in fermions.

5 Conclusions

We found that the commutator of two derivatives may be *not* equal to zero. As a consequence, for instance, the question arises, if the derivative $\hat\partial^2 f/\hat\partial p^\nu\hat\partial p^\mu$ is equal to the derivative $\hat\partial^2 f/\hat\partial p^\mu\hat\partial p^\nu$ in all cases?† The presented consideration permits us to provide some bases for non-commutative field theories and induces us to look for further development of the classical analysis in order to provide a rigorous mathematical basis for operations with functions which have both explicit and implicit dependencies. Several other examples are presented. Thus, while for physicists everything is obvious in the solutions of the paradoxes, this is not so for mathematicians.

Acknowledgements

I am grateful to participants of conferences where this idea has been discussed.

Submitted on February 18, 2019

*Some relations for the components $\mathbf{a}$ must be assumed. Moreover, in our case $\boldsymbol{\theta}$ must not depend on E and $\mathbf{p}$. Otherwise, we must take the non-commutativity $[E, \mathbf{p}^i]_-$ into account again.

†The same question can be put forward when we have differentiation with respect to the coordinates too, that may have impact on the correct calculations of the problem of accelerated charge in classical electrodynamics.

References

1. Snyder H. *Phys. Rev.*, 1947, v. 71, 38; ibid., v. 72, 68.
2. Seiberg N. and Witten E. *JHEP*, 1999, v. 9909, 032, hep-th/9908142
3. Kruglov S.I. *Ann. Fond. Broglie*, 2002, v. 27, 343, hep-th/0110059; Sidharth, B.G. *Ann. Fond. Broglie*, 2002, v. 27, 333, physics/0110040.
4. Dyson F. *Am. J. Phys.*, 1990, v. 58, 209; Tanimura S. *Ann. Phys.*, 1992, v. 220, 229; Land M., Shnerb N. and Horwitz L. hep-th/9308003.
5. Brownstein K.R., *Am. J. Phys.*, 1999, v. 67, 639.
6. Landau L.D. and Lifshitz E.M. The Classical Theory of Fields. 4th revised English ed. [Translated from the 6th Russian edition], Pergamon Press, (1979). 402p., §63.
7. Škovrlj L. and Ivezić T. hep-ph/0203116.
8. Jackson J.D. hep-ph/0203076.
9. Jacob M. and Wick G.C. *Ann. Phys.*, 1959, v. 7, 404; Ruck H.M. and Greiner W. *J. Phys. G: Nucl. Phys.*, 1977, v. 3, 657.
10. Dvoeglazov V.V. *Int. J. Theor. Phys.* 1998, v. 37, 1915; idem., *Czech. J. Phys.*, 2000, v. 50, 225.
11. Kadyshevsky V.G. *Nucl. Phys.* v. B141, 477 (1978); Kadyshevsky V.G., Mateev M.D., Mir-Kasimov R.M. and Volobuev I.P. *Theor. Math. Phys.*, 1979, v. 40, 800 [*Teor. Mat. Fiz.*, 1979, v. 40, 363]; Kadyshevsky V.G. and Mateev M.D. *Phys. Lett.*, 1981, v. B106, 139; Kadyshevsky V.G. and Mateev M.D. *Nuovo Cim.*, 1985, v. A87, 324.
12. Dvoeglazov V.V. *Phys. Essays*, 2018, v. 31, 340.
13. https://en.wikipedia.org/wiki/Iterated Limit .
14. Ilyin V.A, Sadovnichii V.A. and Sendov B.Kh. Mathematical Analysis. Continuation, MSU, Moscow, (1987), in Russian; Ilyin V.A. and Poznyak E.G., Fundamentals of Mathematical Analysis. Vol. 1. Ch. 14. Functions of Several Variables, Fizmatlit, Moscow, (2002), in Russian.
15. Bogoliubov N.N. and Shirkov D.V. Introduction to the Theory of Quantized Fields. 2nd Edition, Nauka, Moscow, (1973), in Russian.
16. Weinberg S. *Phys. Rev.*, 1964, v. B133, 1318.
17. Tucker R.H. and Hammer C.L. *Phys. Rev.*, 1971, v. D3, 2448.
18. Kapuścik E. In: Relativity, Gravitation, Cosmology: Beyond Foundations. Ed. by Dvoeglazov V.V., Nova Science Pubs., Hauppauge, NY, USA, (2018).
19. Barut A.O. *Phys. Lett.*, 1978, v. B73, 310; idem., *Phys. Rev. Lett.*, 1979, v. 42, 1251; Wilson R., *Nucl. Phys.*, 1974, v. B68, 157.
20. Dvoeglazov V.V. *Int. J. Theor. Phys.*, 1998, v. 37, 1909; idem., *Adv. Appl. Cliff. Alg.*, 2008, v. 18, 579.
21. Dvoeglazov V.V. *Rev. Mex. Fis. Supl.* , 2003, v. 49, 99. (*Proceedings of the DGFM-SMF School, Huatulco, 2000*).
22. Berg R.A. *Nuovo Cimento*, 1966, v. 42A, 148.
23. Dvoeglazov V.V. *Nuovo Cimento*, 1995, v. A108, 1467.

Progress in Physics is an American scientific journal on advanced studies in physics, registered with the Library of Congress (DC, USA): ISSN 1555-5534 (print version) and ISSN 1555-5615 (online version). The journal is peer reviewed and listed in the abstracting and indexing coverage of: Mathematical Reviews of the AMS (USA), DOAJ of Lund University (Sweden), Scientific Commons of the University of St.Gallen (Switzerland), Open-J-Gate (India), Referential Journal of VINITI (Russia), etc. Progress in Physics is an open-access journal published and distributed in accordance with the Budapest Open Initiative: this means that the electronic copies of both full-size version of the journal and the individual papers published therein will always be accessed for reading, download, and copying for any user free of charge.
The journal is issued quarterly (four volumes per year).

Electronic version of this journal: http://www.ptep-online.com

Postal address:
Department of Mathematics and Science, University of New Mexico,
705 Gurley Avenue, Gallup, NM 87301, USA